Fluid biomarkers of extracellular matrix remodelling across neurological diseases

Karolina Minta

Department of Psychiatry and Neurochemistry
Institute of Neuroscience and Physiology
Sahlgrenska Academy at the University of Gothenburg
Gothenburg, Sweden

UNIVERSITY OF GOTHENBURG

Gothenburg 2021

Cover illustration by Anna Marszałek and Karolina Minta

Fluid biomarkers of extracellular matrix remodelling across neurological diseases

karolina.minta@neuro.gu.se
ISBN 978-91-8009-162-6 (PRINT)
ISBN 978-91-8009-163-3 (PDF)

Printed in Borås, Sweden 2021
Printed by Stema Specialtryck AB

Don’t underestimate the beauty of your mind,
you never know when it will fly away…

Fluid biomarkers of extracellular matrix remodelling across neurological diseases

Karolina Minta

Department of Psychiatry and Neurochemistry
Institute of Neuroscience and Physiology
Sahlgrenska Academy at the University of Gothenburg

ABSTRACT

Fluid biomarkers of neuropathological features are important tools for clinical assessment of various neurological diseases. This thesis focuses on two inflicted brain injuries (traumatic brain injury; TBI, and radiation-induced brain injury; RIBI), as well as three neurodegenerative disorders (idiopathic normal pressure hydrocephalus; iNPH, Alzheimer's disease; AD, and vascular dementia; VaD). Common neuropathological features for these diseases include neuronal and synaptic damage. Yet, there is an emerging need to find biomarkers of other pathologies to contribute to further understanding of the underlying mechanisms, ideally specific to a particular condition. The brain extracellular matrix (ECM) mediates many aspects of neuronal and glial function. Under physiological conditions, ECM constantly undergoes controlled remodelling. However, under pathological conditions, ECM homeostasis becomes dysregulated. The changes induced in the ECM composition and structure could thus provide insights into various neurological diseases. Brevican and neurocan are the major proteoglycans in the ECM of the brain. Together with tenascins and hyaluronic acid they form ECM structures called perineuronal nets that are mainly responsible for regulating synaptic plasticity and neuronal growth. The two major families of extracellular proteases, matrix metalloproteinase (MMP) and "a disintegrin and metallo-proteinase with thrombospondin motifs" (ADAMTS), together with their inhibitors (tissue inhibitor of metalloproteinase, TIMP), are contributors to ECM remodelling during both physiological and pathological conditions. In the latter, ECM becomes extensively degraded leading to the disrupted communication between the brain cells. The overall aim of this thesis is to examine various ECM proteins and their proteolytic processing in the context of inflicted brain injuries and neurodegenerative disorders. ECM proteins have been identified and quantified in human body fluids using various immuno-techniques and liquid chromatography-mass spectrometry analysis. The main results were that increased cerebrospinal fluid (CSF) levels of brevican, tenascins, and MMP-2 and -10 were associated with unfavourable outcome following TBI and could serve as novel biomarkers for TBI outcome prediction. The increased concentrations of ECM proteins in iNPH might indicate even more severe disease stages of the brain ECM than TBI. The analysis of brevican fragment patterns revealed that there are three sets of brevican in CSF, representing three different parts of the protein, all differentially modulated in TBI. CSF levels of brevican and neurocan peptides were decreased in the VaD group compared with AD patients, showing a novel diagnostic biomarker potential to differentiate VaD from AD. However, ECM proteins do not reflect AD pathology in CSF. In addition, the progressive decline of brevican and neurocan in CSF might represent long-term structural remodelling of the ECM after cranial radiotherapy. In conclusion, identification and quantification of ECM proteins in human body fluids serve a promising tool to increase our understanding of the role of ECM remodelling across neurological diseases.

Keywords: Alzheimer's disease, biomarker, extracellular matrix, idiopathic normal pressure hydrocephalus, immunoassay, mass spectrometry, radiation-induced brain injury, traumatic brain injury, vascular dementia.

SAMMANFATTNING PÅ SVENSKA

Vätskebaserade biomarkörer för neuropatologiska tillstånd är viktiga verktyg i klinisk bedömning av olika neurologiska sjukdomar. Denna avhandling fokuserar på två tillfogade hjärnskador (traumatisk hjärnskada; TBI, och strålningsinducerad hjärnskada) samt på tre neurodegenerativa sjukdomar (idiopatisk normaltrycks-hydrocefalus; iNPH, Alzheimers sjukdom; AD, och vaskulär demens; VaD). Neuronal och synaptisk skada är vanliga neuropatologiska kännetecken för dessa sjukdomar. Det finns ett växande behov av att hitta biomarkörer för andra patologier för att bidra till ökad förståelse för de bakomliggande mekanismerna, i synnerhet biomarkörer som är specifika för ett visst tillstånd. Hjärnans extracellulära matris (ECM) speglar många aspekter av nervcellernas och gliacellernas funktion. Under fysiologiska förhållanden genomgår ECM en ständig, kontrollerad omstrukturering medans under patologiska förhållanden blir istället ECM-homeostasen felreglerad. De förändringar som då uppstår i dess sammansättning och struktur kan ge insikter i olika neurologiska sjukdomar. Brevican och neurocan är de två viktigaste proteoglykanerna i hjärnans ECM. Tillsammans med tenasciner och hyaluronsyra bildar de ECM-strukturer som kallas perineuronala nät, vars huvuduppgift är att reglera synaptisk plasticitet och neuronal tillväxt. De två huvudsakliga familjerna av extracellulära proteaser, matris-metalloproteinas (MMP) och ”ett disintegrin och metalloproteinas med trombospondin-motiv” (ADAMTS), samt deras hämmare (vävnadsinhibitor av metalloproteinas, TIMP) bidrar till omstrukturering av ECM under både fysiologiska och patologiska tillstånd. I det sistnämnda skadas ECM i stor utsträckning vilket leder till störd kommunikation mellan hjärncellerna. Huvudsyftet med denna avhandling är att undersöka olika ECM-proteiner och deras proteolytiska bearbetning i samband med påförda hjärnskador och neurodegenerativa störningar. ECM-proteinerna har identifierats och kvantifierats i mänskliga kroppsvätskor med hjälp av olika immuntekniker och vätskekromatografi kombinerad med masspektrometrisk-analys. De viktigaste resultaten var ökande nivåer av brevican, tenasciner och MMP-2 och -10 i cerebrospinalvätska (CSV) - vilka associerades med ett ogynnsamt utfall efter TBI och skulle kunna fungera som nya biomarkörer för att förutspå återhämtningen efter TBI. De ökade koncentrationerna av ECM-proteiner i iNPH kan tyda på att ECM är kraftigare påverkad vid iNPH än vid TBI. Analysen av fragmentsmönstret från brevican visade att det finns tre uppsättningar brevican i CSV och att uppsättningarna påverkades olika i TBI. Nivåerna av brevican- och neurocan-peptiderna i CSV minskade i VaD-gruppen jämfört med AD-patienterna, vilket visar på en ny diagnostisk biomarkörspotential för att skilja VaD från AD. ECM-proteiner återspeglar dock inte AD-patologi i CSV. Dessutom skulle nedreglering av brevican och neurocan i CSV kunna bero på långvarig strukturomvandling av ECM efter kraniell strålbehandling. Sammanfattningsvis är identifiering och kvantifiering av ECM-proteiner i kroppsvätskor lovande verktyg för att öka vår förståelse för vilken roll ECM-skada och -omsättning spelar vid olika neurologiska sjukdomar.

STRESZCZENIE PO POLSKU

Płynne biochemiczne markery zmian neuropatologicznych są ważnymi narzędziami do oceny klinicznej chorób neurologicznych. W pracy uwzględniono nie tylko uszkodzenie mózgu w wyniku urazów głowy bądź wywołanym przez promienionanie, ale również w przebiegu trzech chorób neurodegeneracyjnych: wodogłowia normotensyjnego, choroby Alzheimera i otępienia naczyniowego. Do typowych zmian neuropatologicznych tych chorób zalicza się uszkodzenie neuronów i synaps. Wówczas istnieje możliwość znalezienia swoistych biomarkerów w celu zrozumienia różnorodnych mechanizmów. Mózgowa macierz pozakomórkowa bierze udział w wielu aspektach funkcjonowania komórek nerwowych i glejowych. W warunkach fizjologicznych macierz pozakomórkowa nieustannie podlega kontrolowanej przebudowie. Jednakże w warunkach patologicznych homeostaza tej macierzy ulega rozregulowaniu. Zmiany wywołane w składzie i strukturze mózgowej macierzy pozakomórkowej mogą zapewnić wgląd w różne choroby neurologiczne. Brevican i neurocan są głównymi proteoglikanami tej macierzy i wraz z tenascynami i kwasem hialuronowym tworzą one ustrukturalizowane formy zwane sieciami perineuronalnymi, które są przede wszystkim odpowiedzialne za regulację plastyczności synaps i wzrostu neuronów. Dwie główne rodziny enzymów proteolitycznych macierzy pozakomórkowej, zwane metaloproteinazy macierzy pozakomórkowej (MMP) i “białka zawierające domenę dezintegryny i metaloproteinazy z motywem trombospondyny”, wraz z ich inhibitorami (tkankowe inhibitory metaloproteinaz), uczestniczą w przebudowie macierzy pozakomórkowej zarówno podczas fizjologicznych, jak i patologicznych stanów. W tym drugim przypadku macierz pozakomórkowa ulega znacznej degradacji, co prowadzi do zakłócenia komunikacji pomiędzy komórkami nerwowymi. Głównym celem tej pracy jest analiza białek macierzy pozakomórkowej i ich proteolitycznego fragmentowania w kontekście patomechanizmu omawianych w tej pracy przyczyn uszkodzenia mózgowia. Białka te zostały zidentyfikowane i określone ilościowo w płynach ustrojowych człowieka przy użyciu technik immunologicznych oraz analizy metodą chromatografii cieczowej w połączeniu ze spektrometrią mas. Wykazano, że podwyższone poziomy brevicana, tenascyn, MMP-2 i MMP-10 w płynie mózgowo-rdzeniowym były związane z niekorzystnym rokowaniem po urazowym uszkodzeniu mózgu i mogą one służyć jako innowacyjne biomarkery do oceny klinicznej pacjentów. Zwiększone poziomy białek macierzy pozakomórkowej u pacjentów z wodogłowiem normotensyjnym mogą wskazywać na jeszcze cięższe stadia choroby niż po urazowym uszkodzeniu mózgu. Analiza fragmentacji brevicana wykazała, że występuje on w płynie mózgowo-rdzeniowym w trzech podzbiorach, gdzie każdy z nich jest modulowany w różny sposób w przypadku urazowego uszkodzenia mózgu. Poziomy peptydów brevicana i neurocana w płynie mózgowo-rdzeniowym były obniżone u pacjentów z otępieniem naczyniowym w porównaniu z chorobą Alzheimera, co wskazuje na nowy potencjał diagnostyczny tych markerów do różnicowania dwóch powszechnych chorób neuro-degeneracyjnych. Jednakże białka macierzy pozakomórkowej nie odzwierciedlają patologii choroby Alzheimera w płynie mózgowo-rdzeniowym. Ponadto, obniżenie poziomów brevicana i neurocana w tym płynie ustrojowym może odpowiadać długoterminowej przebudowie struktury macierzy pozakomórkowej podczas uszkodzenia mózgu wywołanym promieniowaniem mózgowia. Podsumowując, identyfikacja i oznaczenie ilościowe białek macierzy pozakomórkowej w płynach ustrojowych człowieka są doskonałymi narzędziami do poszerzenia wiedzy na temat regulacji tej macierzy w chorobach neurologicznych.

LIST OF PAPERS

This thesis is based on the following studies, referred to in the text by their Roman numerals.

I. **Minta K**, Cullen NC, Al Nimer F, Thelin EP, Piehl F, Clarin M, Tullberg M, Jeppsson A, Portelius E, Zetterberg H, Blennow K, and Andreasson U. *Dynamics of extracellular matrix proteins in cerebrospinal fluid and serum and their relation to clinical outcome in human traumatic brain injury.*
Clinical Chemistry and Laboratory Medicine 2019; 57:1565-1573

II. **Minta K**, Brinkmalm G, Thelin EP, Al Nimer F, Piehl F, Tullberg M, Jeppsson A, Portelius E, Zetterberg H, Blennow K, and Andreasson U. *Cerebrospinal fluid brevican and neurocan fragment patterns in human traumatic brain injury.*
Clinica Chimica Acta 2020; 512(2021):74-83

III. **Minta K**, Brinkmalm G, Al Nimer F, Thelin EP, Piehl F, Tullberg M, Jeppsson A, Portelius E, Zetterberg H, Blennow K, and Andreasson U. *Dynamics of cerebrospinal fluid levels of matrix metalloproteinases in human traumatic brain injury.*
Scientific Reports 2020; 10(1):18075

IV. **Minta K**, Jeppsson A, Brinkmalm G, Portelius E, Zetterberg H, Blennow K, Tullberg M, and Andreasson U. *Lumbar and ventricular CSF concentrations of extracellular matrix proteins before and after shunt surgery in idiopathic normal pressure hydrocephalus.*
Manuscript.

V. **Minta K**, Brinkmalm G, Portelius E, Johansson P, Svensson J, Kettunen P, Wallin A, Zetterberg H, Blennow K, and Andreasson U. *Brevican and neurocan peptides as potential cerebrospinal fluid biomarkers for differentiation between vascular dementia and Alzheimer's disease.*
Journal of Alzheimer's Disease 2021; doi: 10.3233/JAD-201039, in press

VI. **Minta K**, Portelius E, Janelidze S, Hansson O, Zetterberg H, Blennow K, and Andreasson U. *Cerebrospinal fluid concentrations of extracellular matrix proteins in Alzheimer's disease.*
Journal of Alzheimer's Disease 2019; 69(4):1213-1220

VII. Fernström E*, **Minta K***, Andreasson U, Sandelius Å, Wasling P, Brinkmalm A, Höglund K, Blennow K, Nyman J, Zetterberg H, and Kalm M. *Cerebrospinal fluid markers of extracellular matrix remodelling, synaptic plasticity and neuroinflammation before and after cranial radiotherapy.*
Journal of Internal Medicine 2018; 284:211-225

* Equal contribution

Additional studies carried out during the PhD period, but not included in this thesis:

I. **Minta K**, Brinkmalm G, Janelidze S, Sjödin S, Portelius E, Stomrud E, Zetterberg H, Blennow K, Hansson O, and Andreasson U. *Quantification of total apolipoprotein E and its isoforms in cerebrospinal fluid from patients with neurodegenerative diseases.* Alzheimer's Research and Therapy 2020; 12(1):19.

II. **Minta K***, Vrillon A*, Brinkmalm G, Dumurgier J, Cognat E, Portelius E, Zetterberg H, Blennow K, Andreasson U, and Paquet C. *Cerebrospinal fluid apolipoprotein E glycosylation in relation to APOE genotypes and amyloid status.* Manuscript.

III. Moore E, Schimmel S, Khan O, **Minta K**, Meier S, Pechman K, Acosta L, Bell S, Liu D, Gifford K, Davis T, Anderson A, Landman B, Blennow K, Zetterberg H, Hohman T, and Jefferson A. *Cerebrospinal fluid matrix-metalloproteinases are associated with compromised white matter microstructure among older adults.* Manuscript.

IV. **Minta K**, Brinkmalm G, Thelin EP, Al Nimer F, Piehl F, Johansson P, Svensson J, Portelius E, Zetterberg H, Blennow K, and Andreasson U. *Cerebrospinal fluid levels of cathepsin S in Alzheimer's disease, vascular dementia and traumatic brain injury.* Manuscript.

* Equal contribution

CONTENT

ABBREVIATIONS

ABZ	2-aminobenzoyl
Aβ	Amyloid-β
ACH	Amyloid cascade hypothesis
AD	Alzheimer's disease
ADAMTS	A disintegrin and metalloproteinase with thrombospondin motifs
AIC	Akaike information criterion
AUC	Area under the curve
APOE	Apolipoprotein E
APP	Amyloid precursor protein
BBB	Blood-brain barrier
BCSFB	Blood-CSF barrier
BSA	Bovine serum albumin
CAA	Cerebral amyloid angiopathy
CBF	Cerebral blood flow
CNS	Central nervous system
CS	Chondroitin sulfate
CSF	Cerebrospinal fluid
CSPG	Chondroitin sulfate proteoglycan
CT	Computed tomography
CTE	Chronic traumatic encephalopathy
CTRL	Controls
CVD	Cardiovascular disease
DNP	2,4-dinitrophenyl
ECL	Electrochemiluminescence
ECM	Extracellular matrix
EGF	Epidermal-growth factor
ELISA	Enzyme-linked immunosorbent assay
EOAD	Early-onset Alzheimer's disease
ESI	Electrospray ionisation
EVD	External ventricular drainage
FAD	Familial Alzheimer's disease
FDG	Fluorodeoxyglucose
fMRI	Functional magnetic resonance imaging

FRET	Fluorescence/Förster resonance energy transfer
GCS	Glasgow coma scale
GFAP	Glial fibrillary acidic protein
GOS	Glasgow outcome scale
HC	Healthy control
HCD	Higher-energy collisional dissociation
HLB	Hydrophilic-lipophilic balance
HPLC	High-performance liquid chromatography
HRP	Horseradish peroxidase
ICP	Intracranial pressure
IgG	Immunoglobulin G
iNPH	Idiopathic normal pressure hydrocephalus
IP	Immunoprecipitation
LC	Liquid chromatography
LED	Light-emitting diode
LOAD	Late-onset Alzheimer's disease
LCSF	Lumbar CSF
LVD	Large vessel dementia
MCI	Mild cognitive impairment
MID	Multi-infarct dementia
MMP	Matrix metalloproteinase
MMSE	Mini-mental status examination
MRI	Magnetic resonance imaging
MS	Mass spectrometry
m/z	Mass-to-charge
NFL	Neurofilament light
NFT	Neurofibrillary tangles
NPH	Normal pressure hydrocephalus
NSE	Neuron-specific enolase
PCI	Prophylactic cranial irradiation
PET	Positron emission tomography
PE	Phycoerythrin
PNN	Perineuronal net
PSEN	Presenilin
RIBI	Radiation-induced brain injury

PBS	Phosphate-buffered saline
PBS-T	Phosphate-buffered saline/Tween 20
PRM	Parallel reaction monitoring
p-TAU	Phosphorylated tau
S100B	S100 calcium-binding protein B
SAD	Sporadic Alzheimer's disease
SAH	Subarachnoid haemorrhage
SCD	Subjective cognitive decline
SCLC	Small cell lung cancer
SPE	Solid phase extraction
SVD	Small vessel disease
TA	Tenascin assembly
TIMP	Tissue inhibitor of metalloproteinase
TBI	Traumatic brain injury
TMB	3,3′,5,5′-tetramethylbenzidine
TNC	Tenascin-C
TNR	Tenascin-R
TP	Time point
TSP	Thrombospondin
t-TAU	Total tau
UHPLC	Ultra-high -performance liquid chromatography
VaD	Vascular dementia
VCSF	Ventricular CSF

1 INTRODUCTION

Neuroscience is one of the most fascinating branches of science due to the complexity of the brain, the grandest biological frontier. Our entire understanding of reality depends on it, who we are, how our thoughts and memories work. I hope this book will encourage you to find neurology just as an exciting aspect of medicine as I believe it to be.

After all, the brain is the most intriguing organ in the body

...according to the brain.

1.1 Human body fluids

1.1.1 Cerebrospinal fluid

Cerebrospinal fluid (CSF) is a colourless body fluid that occupies the subarachnoid space and ventricular system of the brain, as well as the subarachnoid cavity of the spinal cord and its central canal. CSF assists the brain by providing nourishment and waste removal of the brain's metabolism products [1]. In addition, it acts as a shock absorber protecting the brain from the damage that results from a sudden movement of the skull and it provides buoyancy to support the weight of the brain by reducing it approximately 30 times [1]. CSF is produced by choroid plexus cells located in the four ventricles of the brain, with the lateral ventricles being the primary producers [1]. From there, CSF circulates into the subarachnoid space of the cerebral hemispheres and down to the central canal and subarachnoid space of the spinal cord [1]. In arachnoid mater, one of the three brain's meninges, the small protrusions called arachnoid villi allow CSF to exit the subarachnoid space and enter the venous system. The total CSF volume in an adult is estimated to be 150 mL, of which 25 mL are present within the ventricles [1].

The central nervous system (CNS) is separated from the periphery by the blood-brain barrier (BBB) and the blood-CSF barrier (BCSFB) [2]. Their function is to restrict the passage of noxious blood-borne substances from the bloodstream to the CNS, while simultaneously allowing for the motion of essential substances needed for metabolic function of the brain and facilitating the removal of metabolic waste into the blood. The key elements of these barriers are tight junctions that interconnect endothelial cells of the CNS's microvessels (BBB) or epithelial cells of the choroid plexus (BCSFB) [2]. Approximately 80% of the CSF proteins are blood-derived, while only 20% originate from the CNS [3].

CSF can be used for a variety of diagnostic and therapeutic purposes [4]. For instance, discoloured CSF could be a sign of cerebral haemorrhage, bacterial or viral infection might be a result of meningitis or encephalitis, while a high level of immunoglobulin in CSF could indicate multiple sclerosis. An example of therapeutic use of CSF is its drainage in order to relieve intracranial pressure (ICP).

CSF can be sampled through a lumbar puncture, also known as a spinal tap. During this procedure, a sterile needle is inserted into the subarachnoid space between the L3/L4 or L4/L5 vertebrae (Fig. 1) [1]. There are established standardised procedures to follow with regard to CSF sampling [5]. The lumbar puncture procedure is considered to be fairly invasive and post-lumbar puncture headache may occur, mainly in young patients. However, severe side effects are very rare.

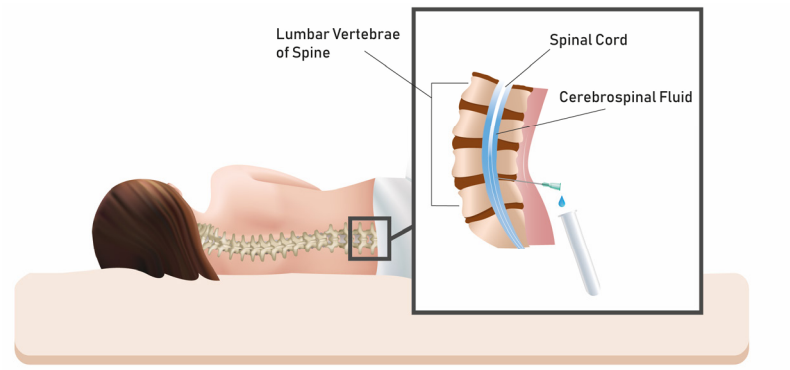

Fig. 1. Lumbar puncture. A spinal needle is inserted into the lumbar region between two vertebrae to collect cerebrospinal fluid.

CSF sampling can also be performed through a ventricular catheter, *e.g.*, in traumatic brain injury (TBI) or hydrocephalus patients who are in need of ICP monitoring. In this surgical intervention, called external ventricular drainage (EVD), a flexible plastic catheter is inserted into one of the ventricles (usually lateral) and the excess CSF is drained into an external collection bag (Fig. 2). However, EVD is an invasive procedure and might lead to brain infection or haemorrhage.

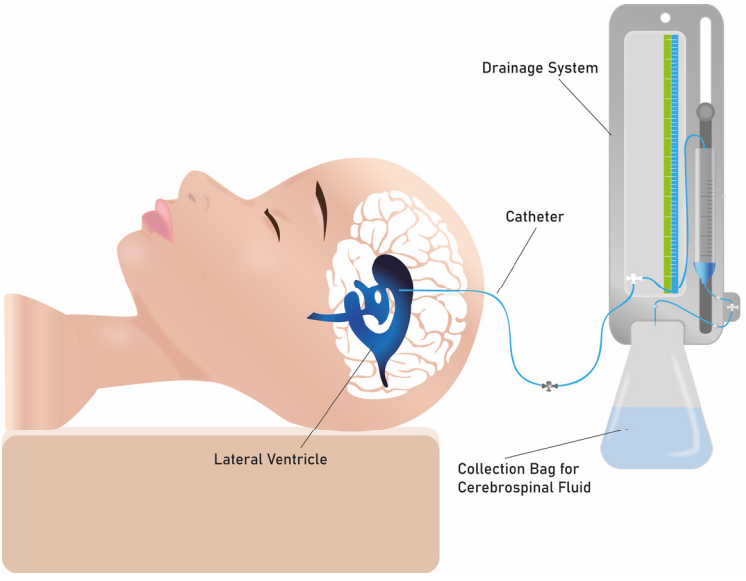

Fig. 2. External ventricular drainage. A plastic catheter is inserted into the lateral ventricle of the brain to drain cerebrospinal fluid and to monitor intracranial pressure.

The total protein concentration in lumbar CSF is 2.5 times higher than in ventricular CSF. This is caused by the gradual influx of proteins on the way from the ventricles to the lumbar spinal channel [3]. However, the amount of brain-derived proteins is either similar between the two sampling sites, or may even be decreased in lumbar CSF compared with ventricular [3].

1.1.2 Blood

Blood accounts for 7-8% of the body mass and its main function is to transport oxygen and nutrients to, and remove metabolic waste products from, the body cells. Most laboratory testing for clinical purposes is performed using either plasma or serum. Plasma is a cell-free aqueous matrix of blood that mainly consist of water with a suspension of proteins, lipids, hormones, enzymes, antibodies, electrolytes and clotting factors. Serum is plasma without clotting factors.

1.1.3 Fluid biomarkers

Biomarkers are objectively measured and are evaluated as indicators of physiological or pathogenic processes [6]. They can be used to record the very early stages of a disease, increase the confidence in disease diagnosis, predict the clinical outcome in patients, monitor the progression of pathology, monitor the drug activity or other therapeutic interventions and discriminate between diseases with an overlapping pathology. Depending on the main objective, biomarkers are commonly divided into five categories: screening, diagnostic, prognostic, predictive and monitoring biomarkers (Table 1) [7].

Table 1. Objectives for the use of biomarkers.

Biomarker type	Objective to use
Screening	To get a first indication of whether an individual may have a disease or not
Diagnostic	To establish the presence of a disease
Prognostic	To portend the disease outcome (with no reference to a specific therapy)
Predictive	To predict outcome of a particular therapy
Monitoring	To monitor progression of pathology or response to treatment

Blood is an easily assessable body fluid for biomarker evaluation and, in comparison with CSF, the blood sample collection is more affordable, less invasive and allows for easily repeated sampling. However, blood lacks direct contact with the brain, as opposed to CSF, which surrounds this organ and is believed to more closely mirror CNS metabolism. Moreover, very high levels of plasma proteins, such as albumin or immunoglobulin, might interfere with the small amounts of brain proteins entering the blood. In addition, brain proteins released into the blood might undergo proteolytic degradation or might be cleared by the liver or in the kidneys.

1.2 Neurological diseases

The neurological diseases investigated in this thesis include inflicted brain injuries (TBI and radiation-induced brain injury; RIBI) as well as neurodegenerative disorders (idiopathic normal pressure hydrocephalus; iNPH, Alzheimer's disease; AD and vascular dementia; VaD) (Fig. 3).

Inflicted brain injuries are characterised by damage to the brain tissue and an alteration in brain function caused by external force (TBI) or radiation (RIBI).

Dementia (from the Latin *de mens*, without mind) refers to cognitive symptoms, severe enough to interfere with social and occupational functioning [8]. It covers a wide range of diseases, characterised by progressive loss of neurons, and is the leading cause of disability and dependency among the elderly. In 2019, there were over 50 million people living with dementia worldwide and this number is predicted to raise to over 150 million by 2050 [9]. Dementia is caused by damage of the nerve cells in the brain. Depending on the area that is affected by the damage, dementia can cause different symptoms that affect memory, thinking, orientation, language and behaviour. Yet, there is no single test for diagnosing dementia and the diagnosis is mainly based on mental ability tests. Neurodegenerative diseases are classified into two groups, reversible, including iNPH, and irreversible, of which AD and VaD are the most common.

Mild cognitive impairment (MCI) is a transitional state between normal ageing and dementia [10], where the patient's cognitive decline is worse than expected for a healthy person, but not severe enough to interfere with daily activities. MCI is clinically defined by a deficit in at least one cognitive domain, in the absence of dementia or impaired daily activities [11]. Although MCI is often a preclinical stage of dementia, MCI patients might remain clinically stable (stable MCI) and not become cognitively worse or develop dementia [12].

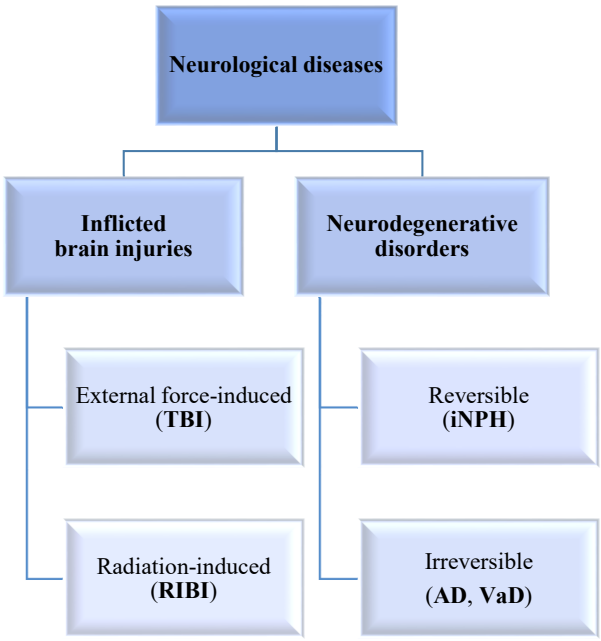

Fig. 3. Division of the neurological diseases investigated in this thesis.

1.2.1 Traumatic brain injury

TBI is a head injury induced by external mechanical forces damaging the brain tissue and it affects almost 70 million people annually [13]. It is the highest contributor to trauma-related mortality [14]. The most common causes of TBI are falls, traffic accidents, firearms and high-impact sports [15]. Head injuries can be closed-head or penetrating, where the skull and dura mater either remain intact or damaged, respectively [16]. TBI is clinically grouped by severity into mild, moderate or severe, depending on structural brain imaging characteristics, duration of the loss of consciousness and amnesia [16]. The vast majority of all TBI cases are mild (around 80%), synonymous with concussion, where the injuries are closed-head [17]. Symptoms of TBI are highly variable and they greatly depend on trauma severity. Mild TBI might involve nausea, dizziness, headache, poor concentration, short-term amnesia, temporal loss of consciousness and behavioural changes, while severe TBI may lead to death [16].

Repeated head injuries can lead to the neurodegenerative condition called chronic traumatic encephalopathy (CTE) [16]. This disease often occurs in contact sports athletes, such as ice hockey, American football and rugby players, or in military veterans [16]. Common symptoms include depression, sleep disturbances, aggression, confusion, memory loss and eventually progressive dementia, and they usually do not appear until years after the onset of head impacts. Moderate and severe TBI as well as CTE have been observed to increase the risk of developing AD [16, 18].

1.2.1.1 Pathology

TBI is also divided into focal or diffuse. The first injury subgroup occurs in a specific location and may involve intraventricular, subdural and epidural hematomas, cerebral contusions and cerebral lacerations. The diffuse injuries, such as diffuse axonal injury, occur over a more widespread area.

Axonal injury is an important pathologic feature of TBI, where the head trauma stretches, tears and damages axons [16]. This leads to microtubule disruption and consequently impaired axonal transport [16]. The microtubule disassembly can be caused by their mechanical breakage and by ionic disturbances. In the latter, axonal cell membrane leakage leads to increased influx of calcium ions that in turn triggers the proteolysis of neuronal cytoskeleton by calpain, a calcium-activated protease [16, 19].

Other pathological features of some of the TBI cases include amyloid-β (Aβ) and tau aggregations, described in detail in the AD section (1.2.3.). In addition, microglial activation, myelin disruption, soluble cytokine response, oxidative and nitrosative stress, BBB damage and mitochondrial dysfunction are commonly observed pathologies in TBI [16]. The injury of the pituitary gland is a common issue in TBI patients, giving rise to several endocrine complications such as growth hormone deficiency, hypogonadism, hypothyroidism, hypocoticolism and diabetes insipidus [20]. TBI can lead to increased ICP, where the normal pressure inside the skull rises due to brain swelling. An increase of ICP can impede cerebral blood flow (CBF) leading to ischemia [21].

However, the TBI pathology highly depends on the severity and extent of the injury. Mild TBI involves mild multifocal axonal and astrocyte injury, activation of microglia, microhaemorrhages, synaptic dysfunction and impaired axonal transport [16]. Severe TBI might result in much more acute neuronal, glial or microvascular injury and brain oedema. Often, several different types of injuries are simultaneously present in TBI patients, raising a heterogenous challenge for clinicians.

CTE disease is strongly associated with the irregular distribution of hyperphosphorylated tau deposits, known as neurofibrillary tangles (NFTs), throughout the brain [22], while Aβ aggregation occur in 50% of CTE cases at the later stage of the disease [23]. Another pathological abnormality present in CTE involves deposits of TAR DNA-binding protein 43 (TDP43) that occur in 80% of CTE cases [24].

1.2.1.2 Genetics and risk factors

Different genetic factors influence neurological and functional outcome following TBI. The most known genetic risk factor for poor outcome after TBI is the ε4 allele of the apolipoprotein E (*APOE)* gene [25]. *APOE*-ε4 is associated with more severe symptoms of chronic TBI [26] and worse cognitive performance after trauma [27].

A significant risk factor for CTE is occurrence of a previous brain injury. Contact sports athletes or military veterans are thus at increased risk of developing CTE.

1.2.1.3 Diagnosis

The Glasgow Coma Scale (GCS) is the most widely used classification to describe the level of consciousness in a person following a brain injury [28]. This scale (3-15) consists of subscale scores that rate eye opening, verbal and motor responses, grouping TBI patients into mild (13-15), moderate (9-12) and severe (3-8) head trauma (Table 2). The minimum score of three indicates total unresponsiveness (deep coma) while the highest possible score of 15 indicates the best response and a fully awake person. In addition to the GCS score, to make a proper severity assessment of trauma, other clinical factors are taken into consideration, such as structural brain imaging characteristics as well as duration of amnesia and of consciousness [16, 29]. Mild TBI is characterised by normal structural brain image, post-traumatic amnesia for less than one day and lack of consciousness for less than 30 minutes [16, 18]. The abbreviated injury scale is an anatomically-based classification system of TBI severity that classifies each injury by body region, ranging from 1 (minor injury) to 6 (unsurvivable) [30].

Table 2. Score system of the Glasgow Coma Scale.

Score	Eye opening	Verbal response	Motor response
1	No eye opening	No speech	No movement
2	Eyes open to pain	Incoherent speech	Extension response to pain
3	Eyes open to voice	Inappropriate words	Abnormal flexion
4	Eyes open spontaneously	Confused	Normal flexion
5		Oriented	Moves to localized pain
6			Obeys commands
3-8		Severe head trauma	
9-12		Moderate head trauma	
13-15		Mild head trauma	

Brain imaging plays a crucial role in the assessment of TBI. Computed tomography (CT) scans are commonly used to detect brain shift, collapsed ventricles or subarachnoid haemorrhage (SAH). Compared with CT, magnetic resonance imaging (MRI) has better resolution and contrast between the different types of brain matter, and thus, provides greater anatomical details including the detection of smaller haemorrhages. However, MRI is more expensive (and less available) and slower compared with CT. Additionally, functional MRI (fMRI) can reveal reduced or increased activation of specific brain areas. However, CT or MRI scans can only detect macroscopic injuries, while mild TBI occurs at the microscopic level. Therefore, the abnormal findings in mild TBI might not be seen in neither CT nor MRI scans and its diagnosis is only defined clinically. Radiological grading of injury can be performed using different scoring systems based on CT scans (Marshall CT classification [31], Rotterdam CT score [32], Helsinki CT score [33] and Stockholm CT score [34]) or MRI scans (*e.g.*, Firsching MRI score [35]). Due to the high costs of neuroimaging, not all

TBI patients undergo this procedure and clinicians follow several criteria, including the New Orleans Criteria [36] and the Canadian CT Head Rule [37], required for the need of imaging use. Usually, all TBI patients with GCS below 15 or 13 (depending on the clinics), headache, nausea, amnesia, age >60 years are imaged.

Good outcome measurements are essential for the accurate estimation of medical care and treatment. Prognosis of outcome after TBI primarily involves clinical predictors such as age, CT characteristics, pupillary reactivity or motor response. However, the sensitivity and specificity of these factors are moderate. The most common tool to measure functional outcome following TBI is Glasgow Outcome Scale (GOS) [38]. It is five-score scale, where 1 indicates death and 5 good recovery (Table 3). However, a more sensitive prediction of outcome would be very beneficiary in the clinic.

Table 3. Score system of the Glasgow Outcome Scale.

Score	Functional status	Description
1	Death	Self-explanatory
2	Persistent vegetative state	Coma/unresponsive
3	Severe disability	Dependent for daily support
4	Moderate disability	Independent in daily life
5	Good recovery	Resumption of normal life

1.2.1.4 Biomarkers

Biomarkers in TBI are mainly used to identify and quantify the extent of brain injury, but also to predict the possible functional outcome. Early prognostication for the patient's outcome after TBI is of importance to guide in treatment decisions and to provide patients and relatives with realistic long-term outlooks. To date, there is no TBI marker that entirely fulfils the criteria for a biomarker of brain injury [39]. However, there are several TBI biomarker candidates.

In CSF, the biomarker candidates for brain tissue injury can reflect neuronal damage (total tau, t-tau [40-44]; neurofilament light, NFL [43, 44]; neuron-specific enolase, NSE [45]), astroglial damage (S100 calcium-binding protein B; S100B [44-47]), BBB integrity and immune response [16]. The CSF concentrations of t-tau, NFL, NSE and S100B acutely increase in TBI patients and progressively decrease over time [40-47]. Since NSE is present in erythrocytes and its levels are highly sensitive to haemolysis and t-tau levels are more a consequence of repeated trauma, NFL is considered to be the most reliable and sensitive marker for neuronal damage. CSF NFL levels increase with severity of trauma and with increasing number of hits to the head [43, 44].

The candidate blood biomarkers for brain tissue injury following TBI include NFL, NSE and S100B [48-51]. For the outcome prediction, serum NFL and S100B have previously been shown to be important clinical outcome predictors in TBI patients [48, 49, 52, 53].

Imaging facilitates the structural classification of TBI. However, CSF biomarkers have shown higher sensitivity by detecting minor brain damage that is not visible in MRI/CT scans [16].

There is no biomarker available to detect the neuronal damage in mild TBI, to identify CTE or to differentiate this disease from other neurodegenerative disorders, such as AD.

1.2.1.5 Management

It is important to initiate the pre-hospital care of TBI patients already at the scene of the accident, immediately after the trauma, to prevent further brain injury. The most common pre-hospital clinical features involve hypotension, hypoxia and hypothermia, all associated with increased mortality and poor outcome [54].

The clinical care of TBI patients mainly involves monitoring of ICP and CBF [21]. Depending on the severity of the brain damage, surgical procedures might be involved to repair skull fractures, remove pieces of skull in the brain or to remove large blood clots. In order to limit secondary damage to the brain, medications to treat symptoms and secondary conditions are prescribed, *e.g.*, antiseizure drugs, antidepressants, anticoagulants or antibiotics.

1.2.2 Idiopathic normal pressure hydrocephalus

Hydrocephalus (from the Greek *hydro*, water and *cephalus*, head) is characterised by abnormal accumulation of CSF in the ventricles of the brain, usually caused by a disturbed CSF circulation. There are two types of hydrocephalus: obstructive and communicating. The obstructive form results from blockage of the CSF flow within the ventricular system. The aqueduct of Sylvius, a narrow channel connecting the third and the fourth ventricles, is the most common site of obstruction, leading to dilatation of the lateral and the third ventricles [55]. Communicating hydrocephalus can be caused either by impaired reabsorption of CSF into the blood or, more seldom by overproduction of CSF. This results in the enlargement of all four ventricles.

The term normal pressure hydrocephalus (NPH) was introduced in 1965 by the neurologist Salomón Hakim, who noted that a state of symptomatic hydrocephalus may exist in the presence of normal CSF pressure [56]. NPH, recognised as the dominant form of hydrocephalus in adults, occurs as either a secondary or an idiopathic (iNPH) condition, each accounting for around 50% of the cases [57]. The secondary form mainly results from SAH, head trauma, meningitis or CNS tumours, and might occur at any age. In contrast, iNPH, where the cause is largely unknown, is primarily observed in individuals over 60 years [57]. The most prominent and usually first clinical feature of iNPH is gait abnormality, characterised by slow, short-stepped and "glued to the floor" gait [58]. Other symptoms of iNPH involve problems with balance, involuntary micturition with incontinence and cognitive deterioration or dementia [59]. iNPH is a common disorder affecting up to 3% of all persons over the age of 65 [60-62] and it is estimated that 10% of all dementia patients may suffer from iNPH [63].

1.2.2.1 Pathology

The most evident pathology of iNPH are enlarged ventricles (ventriculomegaly) defined as an Evans' index ≥0.3 (determined by ratio of the maximal width of the frontal horns divided by the diameter of the internal skull) [64], with no macroscopic obstruction of CSF flow. Other supporting neuroimaging features involve a sharp callosal angle, periventricular white matter lesions and a marked flow void in the Sylvian aqueduct [57, 58]. iNPH implies multiple vascular anomalies such as white matter lesions resulting from microvascular disturbances and small vessel disease (SVD), and it has been suggested that iNPH is a possible subtype of VaD [65]. Cerebral hypometabolism including both reduced oxygen metabolism and reduced blood flow in the periventricular white matter, basal ganglia and other regions have been observed in iNPH patients [66]. Additionally, the pathologic hallmarks of AD, Aβ plaques and tau tangles, have been reported in brain biopsies from iNPH patients [67], making iNPH diagnosis even more challenging.

1.2.2.2 Genetics and risk factors

Although iNPH is considered sporadic, occurrences of familial cases have been reported, with a potential autosomal dominant inheritance [68, 69]. The dementia seems to be more frequent with more severe symptoms in the familial subgroup of iNPH patients compared with the sporadic cases [69]. The familial form of iNPH more frequently shows the presence of venous thrombosis and hypertension [69]. However, still, very little is known about the familial characteristics of iNPH.

The frequency of *APOE*-ε4 allele in iNPH patients is the same as in the control population [70] and to date, there is no specific genetic risk factor identified for iNPH.

iNPH has been shown to be associated with vascular risk factors such as diabetes mellitus [65], hyperlipidemia [65] and arterial hypertension [71] further supporting a vascular cause. Thus, it is believed that early intervention against vascular risk factors can reduce the iNPH development. In addition, decreased renal function, chronic kidney disease and abdominal obesity have also shown a strong association with iNPH [65].

1.2.2.3 Diagnosis

There is no single diagnostic test for iNPH. Evidence-based guidelines for clinical diagnosis of iNPH have been proposed and are now used worldwide [59]. The documentation of ventriculomegaly (Evans' index ≥0.3) without signs of CSF blockage by brain imaging techniques is critical but not sufficient for iNPH diagnosis [59]. Apart from neuroimaging, other clinical evaluations showing typical symptoms and signs are necessary to confirm the iNPH diagnosis. These evaluations include the following: clinical history, neurological examination, neuropsychological testing, and differentiation from other disorders [59]. Additionally, grading scales for assessment of symptom severity and treatment outcome for iNPH patients has been developed including the iNPH scale [72]. This scale covers the four symptom domains affected by iNPH: gait, balance, neuropsychology and continence, and it ranges from 0 to 100, where lower scores correspond to more symptoms [72]. However, the clinical symptoms of iNPH widely overlap those of neurodegenerative diseases, *e.g.,* progressive dementia and gait disturbances can be misinterpreted for AD or Parkinson's disease, which makes the differential diagnosis very challenging [73]. In addition, CSF tap test and temporary external CSF drainage help to confirm suspected cases of iNPH and are applied as prognostic tests to decide whether ventricular shunt surgery would be beneficial for the patient.

1.2.2.4 Biomarkers

To date, there are no reliable biomarkers to diagnose iNPH or predict its outcome following shunt surgery. The CSF biomarker profile of iNPH is shown to be characterised by the decreased concentrations of products derived from amyloid precursor protein (APP) such as sAPPα, sAPPβ and Aβ peptides, possibly explaining the reduced brain metabolism in the periventricular zone, normal or reduced levels of t-tau and phosphorylated tau (p-tau), elevated NFL indicating damage to large myelinated axons as well as increased glial fibrillary acidic protein (GFAP) indicating astrogliosis [74-76].

1.2.2.5 Management

iNPH is a potentially treatable disease. Treatment comprises the surgical placement of a CSF diverting shunt catheter draining CSF from the brain ventricles to the peritoneal cavity (ventriculo-peritoneal shunt) or sometimes to the right atrium of the heart (ventriculo-artial shunt) [58]. A CSF removal tests can aid in predicting the response to shunting [58]. To date, shunt surgery is considered to be a definite therapy and it improves outcome in around 80% of the iNPH patients [77]. It increases CBF and reduces periventricular white matter lesions [78, 79]. In addition, neuronal dysfunction was observed to be reversed by a shunt surgery [80].

1.2.3 Alzheimer's disease

AD is the most prevalent cause of dementia, accounting for 60-80% of all dementia cases [81]. It is a slowly progressive neurodegenerative disease characterised by the impairment of episodic memory and a deterioration of various other cognitive abilities including language, orientation, recognition and learning. Although the average duration of the disease is 8-10 years, AD is characterised by a long preclinical stage, where the brain changes preceding AD may occur already 20 years before the symptoms of brain dysfunction become apparent [82]. The incidence rate of AD increases with age and doubles every fifth year after the age of 65 [83]. There are two forms of AD based on the age of onset: early-onset AD (EOAD), which gives symptoms between 30 and 60-65 years, and late-onset AD (LOAD), which is the most common form of AD, where the symptoms begin after the age of 60-65 [84].

The first case of AD was described in 1906 by the German psychiatrist Alois Alzheimer. His patient was a 51-year old woman named Auguste Deter, who developed rapid memory loss, disorientation and hallucinations [85]. After her death, the post-mortem examination showed an atrophic brain with depositions of extracellular bodies (plaques) and intracellular dense bundles of neurofibrils (tangles) [85], which today are known as the hallmarks of AD. Emil Kraepelin, a colleague of Alois, named the disease after Alzheimer.

1.2.3.1 Pathology

The main pathological hallmarks of AD include neuronal loss together with the presence of plaques, composed of Aβ peptides, and tangles, composed of abnormally hyperphosphorylated tau protein. Neuronal loss in AD primarily affects the medial temporal lobe, *e.i.*, the hippocampus and the entorhinal cortex.

APP, a transmembrane glycoprotein concentrated in the synapses, plays a central role in AD pathogenesis and is processed by two major pathways (Fig. 4). In the non-amyloidogenic pathway, α-secretase cleaves APP within the Aβ domain, releasing a soluble form of APP (sAPPα), thus precluding the formation of longer Aβ peptides, such as $A\beta_{1-42}$. The remaining C83 fragment of APP is further cleaved by the γ-secretase complex (incl. presenilin 1 (PSEN1) and presenilin 2 (PSEN2)) forming the p3 peptide. Amyloidogenic processing of APP involves β-secretase that cleaves APP just before the Aβ domain releasing sAPPβ, and the γ-secretase complex that cleaves the remaining C99 fragment of APP producing several Aβ peptides, including $A\beta_{1-42}$, which is prone to aggregate and form neurotoxic fibrillary assemblies in the brain [82].

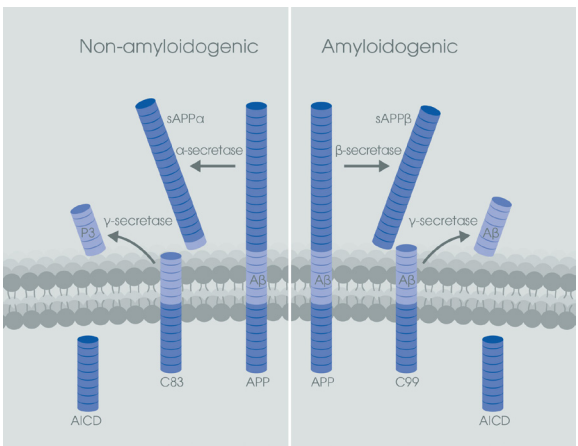

Fig. 4. The non-amyloidogenic and amyloidogenic pathways of APP processing (courtesy of Abcam).

Amyloid pathology starts in neocortex and spreads to subcortical regions [86]. Thal phasing, a scoring system (0-5), is used to determine the distribution of amyloid plaques throughout the brain [86].

Tau is an axonal protein that binds to microtubules and promotes their stability. There are six different isoforms of tau in the CNS, all containing several serine and threonine residues that can be phosphorylated. The degree of phosphorylation of tau regulates its affinity to bind to the microtubules. Hyperphosphorylation of tau causes disassembly of microtubules and impaired axonal transport, leading to neuronal and synaptic dysfunction. Moreover, hyperphosphorylated tau becomes prone to aggregate into insoluble fibrils, known as paired helical filaments (PHFs), followed by the formation of NFTs (Fig. 5). Tau pathology starts in subcortical regions, hippocampus and amygdala, followed by neocortical areas [87]. Braak staging, a scoring system (0-VI), is used to determine the spread of tau pathology throughout the brain [87].

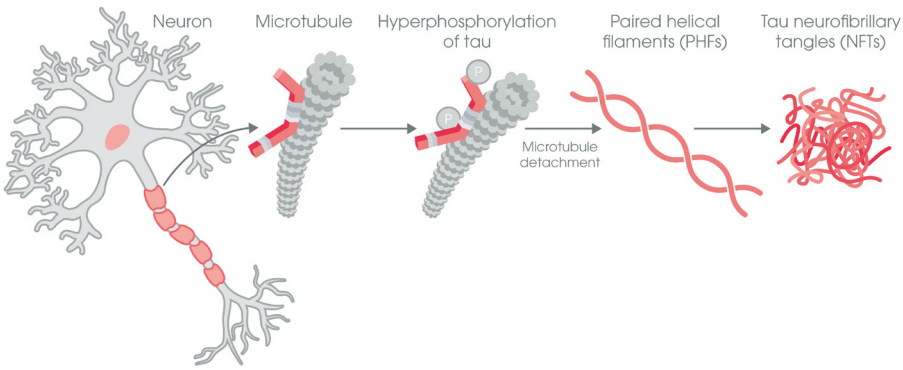

Fig. 5. Formation of neurofibrillary tangles (courtesy of Abcam).

It is believed that extracellular Aβ aggregates interfere with synaptic connections between neurons, while intracellular accumulations of NFTs inhibit the cargo transport inside neurons. AD also involves neuroinflammation and brain atrophy (affecting primarily hippocampus), as well as degeneration and loss of synapses. The severity of synaptic loss is more associated with degree of cognitive impairment rather than plaque or tangle counts [88]. Thus, synaptic degeneration is believed to be the best anatomical correlate of cognitive deficits in AD.

1.2.3.2 The amyloid cascade hypothesis

According to the amyloid cascade hypothesis (ACH), the increased production (or decreased degradation) and aggregation of $A\beta_{1-42}$ is the causative agent of a series of events resulting in deposition of NFTs and neuronal death, ultimately leading to AD [89]. There is a substantial evidence supporting ACH. Firstly, genes implicated in the hereditary form of AD (*APP*, *PSEN1*, *PSEN2*) are linked to Aβ metabolism. Secondly, people with Down's syndrome, who carries an extra copy of the *APP* gene, develop Aβ plaques early in life, by 35 years of age [90]. However, ACH has been extensively criticized [91] pointing at the evidence that amyloid plaques and NFTs may develop independently and that these deposits might rather be a consequence of neurodegeneration than the cause. In response to this, alternative hypotheses for the underlying cause of AD have been developed, *e.g.,* inflammation [92] and oxidative stress [93].

1.2.3.3 Genetics and risk factors

AD is genetically divided into familial (FAD) and sporadic (SAD) forms. FAD is a rare (<1%) autosomal dominant disease with early onset (EOAD), with a mean onset age of 45 years [82]. It is caused by single mutations in one of three different genes: *APP*, *PSEN1* or *PSEN2* [94]. These mutations generate more aggregation-prone Aβ peptides. SAD is the more widespread form of AD, with mean age of onset of 80 years (classifies as LOAD) [82]. The cause of SAD is unknown, however this form of the disease has strong association with *APOE* [95, 96] - a genetic risk factor for AD. There are three major forms of the *APOE* gene: ε2, ε3 and ε4, which cause the protein to differ with single amino acid substitutions at two positions (amino acids 112 and 158) resulting in apoE2 (Cys112, Cys158), apoE3 (Cys112, Arg158) and apoE4 (Arg112, Arg158) [97]. Therefore, there are six possible genotypes: ε2/ε2, ε2/ε3, ε2/ε4, ε3/ε3, ε3/ε4 and ε4/ε4. The ε3 allele is the most common (77%), while ε2 is the least frequent (8%) [98]. The amino acid changes in the apoE isoforms alter the protein's structure as well as its lipid- and receptor-binding properties [99]. There is a differential effect of each apoE isoform on AD risk. The ε4 allele of *APOE* increases the risk of developing AD by 3 or 15 times for one or two copies of the allele, respectively [100], and lowers the mean age of onset by almost 10 years [96]. The ε2 allele of *APOE* is known to be protective compared with ε3 [18]. ApoE binds to Aβ in an isoform-dependent pattern (E4<E3<E2) [97] and affects Aβ uptake by neurons and glia (Aβ clearance) differently [99]. Lower efficiency in Aβ clearance by apoE4 compared with other isoforms may explain larger amyloid depositions in *APOE*-ε4 carriers. Moreover, apoE4 is also less efficient than apoE3 and apoE2 in the transport of cholesterol in the brain [98], which leads to a loss of synaptic integrity. ApoE isoforms also regulate synaptic plasticity and repair differently, where apoE4 is the least effective in synaptic repair [98]. ApoE4 promotes proinflammatory responses and reduces anti-inflammatory functions [99]. The intramolecular interaction between N- and C-terminal domains, a structural property only observed in apoE4, is suspected to be responsible for apoE4-associated neuropathology [98]. There are several possible strategies for AD therapy targeting apoE, which include restoration of the physiological functions of apoE, increased lipidation levels of apolipoproteins, disruption of apoE4 domain connection, conversion of the apoE4 structure to apoE3-like molecule or upregulation of apoE receptors expression [98, 99].

Besides aging and *APOE* status, other risk factors for developing AD include reduced mental and physical activity, low education attainment, head injury, diabetes, hypertension, obesity, depression and smoking [101].

1.2.3.4 Diagnosis

Diagnosis of AD involves clinical history, neuropsychological testing, brain imaging and body fluid analysis. However, the definite diagnosis of AD can only be made post-mortem.

The first criteria proposed for AD diagnosis were launched in 1984 by the National Institute of Neurological and Communicative Disorders and Stroke and the Alzheimer's Disease and Related Disorders Association (NINCDS-ADRDA) and was based exclusively on clinical symptoms [102]. These criteria classify patients into possible, probable and definite AD.

The biological definition of AD was introduced for the first time in 2007 by the International Working Group (IWG) and required episodic memory disturbances and at least one abnormal biomarker (CSF $A\beta_{42}$, CSF t-tau or p-tau, amyloid positron emission tomography (PET) or hippocampal volumetric MRI) [103]. Seven years later, an update of the IWG criteria was presented, IWG-2, which includes only CSF biomarkers together with amyloid PET, but not volumetric MRI, as supporting evidence of AD pathology [104].

From 2016, tau pathology and markers of neurodegeneration are considered separately since individuals can have brain atrophy, but no tau deposits in the brain. Therefore, the A/T/N classification was introduced, where biomarkers are grouped based into brain amyloidosis (amyloid

PET or CSF $A\beta_{42}$), tau pathology (tau PET or CSF p-tau) and neuronal degeneration (hippocampal atrophy measured by MRI, temporoparietal hypometabolism indicated by ^{18}F-fluorodeoxyglucose (FDG) PET, or CSF t-tau) [105].

In 2018, the National Institute on Aging and the Alzheimer's Association (NIA-AA) presented criteria that defines AD as a pathologic process, which is identified primarily by biomarkers, while clinical phenotype is used for deciding the stage of the patient [106].

The assessment of cognitive dysfunction can be performed using screening tests, such as Mini-Mental State Examination (MMSE). It is a 30-point questionnaire measuring memory, language, orientation and concentration [107]. It divides patients into three categories: cognitively intact (27-30), mild AD (21-26) and moderate AD (12-20) [108].

Unfortunately, co-morbidities such as cerebrovascular disease and hippocampal sclerosis amongst people with AD are common features making the clinical evaluation very challenging.

1.2.3.5 Biomarkers

The core AD CSF biomarkers ($A\beta_{42}$, t-tau and p-tau) reflect key elements of AD pathophysiology. They show 85-90% sensitivity and specificity for AD [109] and their abnormalities can be detected 15-20 years before the onset of clinical symptoms [82].

Low CSF $A\beta_{42}$ levels in AD patients are believed to reflect the aggregation of this hydrophobic peptide in amyloid plaques, with reduced amounts remaining to be secreted into the CSF [110]. However, the $A\beta_{42}$ level in CSF depends not only on its deposition in amyloid plaques, but also on the patient's total amount of Aβ peptides, which varies between individuals. $A\beta_{40}$, the most abundant Aβ peptide in CSF, is less prone to aggregation compared with $A\beta_{42}$ [111]. Thus, it is believed that $A\beta_{40}$ is a measure of the total Aβ production. Therefore, the $A\beta_{42/40}$ ratio is considered to compensate for individual variations in the total Aβ production [112], resulting in a higher performance to identify AD than CSF $A\beta_{42}$ alone [113-116].

A high CSF level of t-tau reflects the intensity of neuronal degeneration or severity of neuronal damage [117], while a high CSF level of p-tau reflects tangle formation in AD in the brain [118]. Measurements of t-tau in CSF reflect tau protein independent of phosphorylation state, while p-tau only measures tau that is phosphorylated at the threonine amino acid residue 181 (p-tau 181). While, increased levels of t-tau in CSF are also found in other neurodegenerative disorders, a p-tau increase is specific for AD [119].

Moreover, biomarkers for synaptic dysfunction and degeneration, including neurogranin, reflect additional aspects of AD pathophysiology. High CSF neurogranin level is a promising novel biomarker candidate for synaptic loss and is specific to AD [120].

There is no well-established and validated blood-based biomarker for AD, although lower $A\beta_{42/40}$ [121-123] and higher p-tau 181 [124-126] plasma levels were reported to be associated with AD.

Imaging biomarkers are used to monitor pathophysiological changes in the brain. MRI determines the degree of brain atrophy (enlarged ventricles and shrinkage of cerebral cortex). In AD, the entorhinal cortex followed by hippocampus and amygdala are the earliest areas affected by atrophy. PET scans measure emission from radiolabelled tracer molecules, thus the uptake of radioactive ligand in the brain. The ^{18}F-FDG PET measures the uptake of radiolabelled glucose and consequently estimates the temporoparietal hypometabolism in AD brain. Additionally, PET tracers that bind to Aβ plaques (*e.g.,* ^{11}C-Pittsburgh compound B (PiB), ^{18}F-florbetapir, ^{18}F-flutemetamol) and to NFTs (*e.g.,* ^{18}F-Genentech Tau Probe 1 (GTP1)) are gaining traction in the clinic.

1.2.3.6 Management

There are symptomatic treatments for AD, which prevent the breakdown of acetylcholine (acetylcholinesterase inhibitors) or regulate the activity of glutamate (NMDA receptor antagonists) [94]. The first therapeutic approach, involving donepezil, rivastigmine and galantamine, is directed to enhance cholinergic neurotransmission by inhibiting the degradation of acetylcholine, a chemical messenger important for learning and memory. Acetylcholinesterase inhibitors are usually prescribed to treat early to moderate stages of AD. The second therapeutic approach, involving memantine, protects neurons from glutamate-mediated excitotoxicity. Drugs containing memantine and a combination of memantine and donepezil are frequently prescribed for more advanced symptoms (moderate-severe AD). Additionally, antipsychotic drugs may be used to treat behavioural changes in AD patients. However, all these treatments only temporarily mitigate AD symptoms and do not change the natural course of AD. To date, there is still no cure for AD.

1.2.4 Vascular dementia

VaD is the second most common cause of dementia [127], accounting for around 15% of all dementia cases [128]. It is characterised by reduced cerebral blood supply to the brain due to the damage of blood vessels within this organ. Blood carries oxygen and nutrients to the brain and the lack of their supply causes the death of brain cells, leading to the deterioration of cognitive abilities, including attention, executive function, memory, thinking, language and reasoning. When the blood flow to the brain is blocked, a stroke, also known as brain infarct, occurs. Although the damage from a stroke may cause cognitive impairment, strokes do not always lead to the progression of VaD. There are two main types of strokes, caused by the blockage of a blood vessel (ischemic type, 87% of all strokes) or rupture of a blood vessel supplying blood to the brain (haemorrhagic stroke) [129]. If the blood flow is interrupted only for a short time, it is known as a mini stroke or a transient ischemic attack.

The incidence rate of VaD increases exponentially with age and doubles every fifth year after the age of 70 [130]. The mean survival of patients diagnosed with VaD is 3-5 years [131].

The first case of cerebrovascular disease as a cause of dementia was described in 1672 by Thomas Willis under the name post-apoplectic dementia [132]. For many years, it was incorrectly believed that only multiple brain infarcts are responsible for dementia and the term multi-infarct dementia (MID) became synonymous with VaD [133]. However, from 1991 VaD is recognised as a group of many syndromes related to various vascular mechanisms, where MID is only one of them [132]. The subtypes of VaD are defined based on the blood vessel size, origin of vascular occlusion, size and anatomical location of lesions and genetic background [134]. Depending on the size of affected blood vessels, VaD is divided into large vessel disease (LVD) and small vessel disease (SVD; subcortical VaD) (Fig. 6). In addition, other subtypes of VaD include strategic infarct dementia (infarcts in strategic locations), haemorrhagic dementia (multiple microbleeds), hypoperfusive dementia (hippocampal or laminar cortical sclerosis) and hereditary VaD [134, 135]. However, SVD accounts for most of the VaD cases [128]. The severity of cognitive impairment of VaD patients depends on the nature and location of the lesions, and a number of other factors, including age [135].

The use of the term “vascular dementia” is controversial, due to its highly heterogenous nature. Thus, the broader term of vascular cognitive impairment, which refers to any degree of cognitive dysfunction that is associated with vascular pathology, is believed to be more applicable [136].

1.2.4.1 Pathology

The pathology of VaD includes either small (microangiopathy; SVD) or large (macroangiopathy; LVD) vessel damage. Both types can trigger ischemic or haemorrhagic strokes (Fig. 6) and contribute to neurological dysfunction and degeneration [137]. Although they share common features, they also have unique characteristics.

SVD is an umbrella term covering abnormalities related to small blood vessels in the brain. These include arteriosclerosis, lacunar infarcts, white matter lesions and microbleeds [134]. Cerebral arteriosclerosis is characterised by thickening and hardening of the walls of cerebral arteries, restricting the blood flow to the brain (Fig. 6). Lacunes are small (3-15 mm) ischaemic infarcts caused by the blockage of tiny arteries in a deep cerebral white matter [138-140]. Most of the lacunar infarcts are clinically silent, where no symptoms are observed. Extensive and confluent white matter lesions incorporating myelin loss correspond to hyperintensities on MRI. Additionally, haemorrhages resulting in microbleeds are the other features of SVD [135]. Cerebral amyloid angiopathy (CAA), characterised by amyloid deposition in the small blood vessels in the brain (Fig. 6), and Binswanger’s disease, involving white matter damage and lacunar infarcts, both fall into the category of SVD [134].

LVD involves cerebrovascular abnormalities related to larger blood vessels. Atherosclerosis is characterised by a build-up of fats, cholesterol and other substances in large arteries [137] (Fig. 6) and is strongly associated with hypercholesterolemia and cardiac disease [141].

Brain atrophy is commonly observed in patients with SVD and LVD [141].

VaD pathology overlaps to a great extent with other neurodegenerative diseases. For example, most of the VaD patients have AD-type pathologies such as amyloid plaques and NFTs, and pure VaD (cerebrovascular disease without other pathologies) accounts for only 10% of all cases [142].

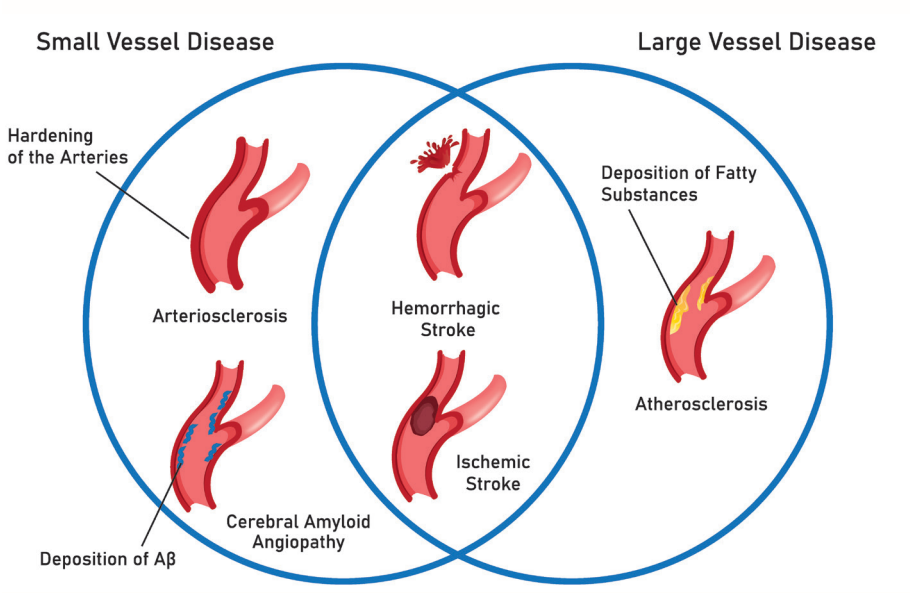

Fig. 6. Schematic picture of examples of SVD and LVD subtypes.

1.2.4.2 Genetics and risk factors

Cerebral autosomal dominant arteriopathy with subcortical infarcts and leukoencephalopathy (CADASIL) is the most frequent heritable form of VaD caused by mutations of the *NOTCH3* gene on chromosome 19 [143]. It is a small artery disease with extensive white matter changes [144]. The common manifestations of CADASIL include migraine with aura, recurrent strokes, motor deficits and psychiatric disturbances leading to disability and dementia in mid-life [134].

Fabry disease (FD) is another monogenic disorder caused by mutations in the *GLA* gene on chromosome X. It is characterised by the absence or reduction of α-galactosidase activity that leads to the accumulation of glycosphingolipid (globotriaosylceramide) in the vascular endothelium. Stroke, renal disease or cardiomyopathy are often present in FD [145].

Another inherited form of VaD is familial CAA and it is characterised by deposits of Aβ peptides into the walls of vessels resulting in leukoaraiosis, small cortical infarcts and microbleeds. The clinical features of CAA include cognitive impairment, spasticity, ataxia, facial paralysis and seizures [134].

There is a significant association between the *APOE*-ε4 allele and increased risk of VaD [145]. Apart from age and *APOE* status, the main vascular risk factors include hypertension [146] and diabetes [147]. Other factors are reduced physical and mental activities, alcohol intake, smoking and obesity [135].

1.2.4.3 Diagnosis

The definite diagnosis of VaD can only be done post-mortem and, to date, antemortem VaD diagnosis is mainly based on imaging criteria to visualize the presence of vascular lesions. CT or MRI scans are used to rule out brain tumour or NPH since these diseases can give similar symptoms to those of VaD. A CT scan is sufficient to detect stroke and white matter damage, while MRI, the more sensitive imaging, can give more details on the degree, location and extent of the cerebrovascular disease. The imaging techniques are also used to detect brain atrophy, mainly in the hippocampal area. Several diagnostic criteria focusing on neuroimaging have been developed to diagnose VaD. For instance, the commonly used Alzheimer's Disease Diagnostic and Treatment Centers (ADDTC) criteria [148], also known as California Criteria, for VaD diagnosis requires two or more ischemic strokes, where at least one infarct is observed outside the cerebellum.

Although the demonstration of abnormalities using neuroimaging is the most apparent evidence of vascular pathology, the medical history, and physical and mental examination may provide additional information. The assessment of cognitive impairments is performed using screening tests. Apart from MMSE examination, tests prioritising attention and executive function, the two most affected cognitive abilities in VaD, are more applicable for VaD diagnosis. These include the Montreal Cognitive Assessment scale (MoCA) [149] and the Vascular Dementia Assessment Scale-cognitive subscale (VADAS-cog) [150]. There is substantial overlap between the clinical symptoms of AD and VaD patients. However, depression and apathy are more prominent, while delusions and hallucinations are rare in VaD compared with AD [151, 152].

There is a lack of well-defined standardised diagnostic criteria. The reason lies in the fact that VaD is not a single pathological entity, but more of an umbrella term covering a large group of highly heterogenous lesions with multifactorial pathogenesis [153]. Moreover, the pure VaD diagnosis become more challenging in elderly patients who have additional degenerative pathology (amyloid plaques, NFTs). The substantial overlap between AD and VaD pathologies makes it challenging to estimate the degree of contribution of each disease to the cognitive decline [153].

In the early 1990s, four sets of diagnostic criteria for VaD were published: the National Institute of Neurological Disorders and Stroke-Association Internationale pour la Recherche et l'Enseignement en Neurosciences (NINDS-AIREN) [154], the Diagnostic and Statistical Manual of Mental Disorders-IV (DSM-IV) [155], ADDTC [148] and the International Classification of Diseases-10 (ICD-10) [156]. However, these criteria are highly criticised since they use the definition of dementia based on clinical features of AD while the predominant VaD characteristics involve disturbances in frontal-executive functions rather than episodic memory [157]. In 2009, a new set of clinical and neuroimaging criteria specific for VaD was proposed to address some of the limitations in VaD diagnostics [135].

1.2.4.4 Biomarkers

The highly heterogenous nature of VaD has made the development of reliable fluid biomarkers very challenging. The potential candidates for fluid biomarkers for VaD include extensively used CSF/serum albumin ratio or novel platelet-derived growth factor receptor-β (PDGFRβ) [158] as markers for BBB damage, CSF matrix metalloproteinases (MMPs) and tissue inhibitor of metalloproteinase-1 (TIMP-1) for extracellular matrix (ECM) remodelling [159], CSF myelin basic protein and sulfatide for white matter degradation, CSF NFL and t-tau for neural degeneration, serum C reactive protein and interleukins for inflammation, and CSF YKL-40 for glial activation [160, 161]. However, none of the above fluid biomarkers are specific to VaD. Thus, they are not recommended for diagnostic purposes to be used in isolation. As opposed to fluid biomarkers, imaging biomarkers such as CT and MRI are more established and widely used to determine the rate of brain atrophy or vascular changes.

1.2.4.5 Management

There are no approved drugs for preventing or treating VaD. The lack of treatment success is largely due to the heterogeneity of the disease. Most of the medications used to treat cognitive symptoms in AD patients, also find a use for VaD. Both acetylcholinesterase inhibitors and NMDA receptor antagonists appear to be effective alternative for patients with VaD [162]. Management of VaD risk factors, *e.g.*, high blood pressure, high cholesterol levels, obesity, and the treatment of underlying conditions of heart and blood vessel diseases, *e.g.*, coronary heart disease or peripheral artery disease, could prevent further cognitive decline. Antithrombotic medication, including antiplatelet drugs, is commonly used to prevent recurrent stroke [163].

1.2.5 Radiation-induced brain injury

Prophylactic cranial irradiation (PCI) of the entire brain is a treatment used to prevent or delay the spread of cancer in the brain, usually given to patients with small cell lung cancer (SCLC), accounting for approximately 20% of all lung tumours [164]. SCLC has a clinically aggressive nature with a high potential for metastasis. Approximately 10% of the patients with SCLC present brain metastases at the time of diagnosis [165] and in more than 50% of the cases brain metastases are found at autopsy [166]. Even though PCI reduces the risk of brain metastasis incidence, various neurological and neuropsychological side effects can be observed after PCI.

RIBI occurs in 50-90% of patients who survive six months post-irradiation [167]. RIBI is divided into: acute (occurs within days-weeks after irradiation), early delayed (1-6 months after) and late delayed injury (more than 6 months after PCI) [167]. Acute and early delayed brain injuries are both reversible, while late delayed injury is permanent. The cognitive impairment following RIBI is mainly characterised by deterioration in verbal and spatial memory, attention and problem solving, eventually leading to dementia [167].

1.2.5.1 Pathology

The exact underlying pathological mechanisms following PCI are largely unknown. However, vascular abnormalities and demyelination belong to the predominant histological changes seen in RIBI [168].

The CNS changes develop already within hours following PCI. Early delayed brain injury involves mainly microvascular damage and neuroinflammation [167]. It is believed that early delayed reactions are primarily due to the effects of radiation on oligodendrocytes, the myelinating cells of the CNS [168]. Oligodendrocytes are very sensitive to irradiation and their numbers decrease already within a few hours following PCI [169] leading to demyelination [170].

Late delayed injury is not only characterised by vascular abnormalities, neuroinflammation and demyelination, but also involves ischemia, downregulated neurogenesis (mainly hippocampal), cerebral atrophy and white matter necrosis [167]. Radiation-induced vascular changes include thickening of vessel walls, vasodilation, perivascular astrocyte hypertrophy, vascular endothelial loss and reduction in blood vessel number and length [167]. These changes can trigger ischemic strokes [168]. Moreover, the brain irradiation induces the degradation of collagen type IV, a major ECM component of the BBB basement membrane, leading to BBB impairment [171]. It is observed that irradiated microglia activate astrocytes which in turn become hypertrophic and begin a reactive gliosis process [172]. This results in the expression of proinflammatory cytokines [173]. Radiation-induced neuroinflammation, a strong inhibitor of neurogenesis, might explain the failure of irradiated hippocampus to generate neurons [168]. Vascular endothelial and glial loss are presumed to cause white matter damage leading to cognitive impairment [174].

1.2.5.2 Diagnosis

The diagnosis of brain metastases is based on patient's medical history, mental ability tests and neuroimaging. The metastases originating from SCLC occur at multiple sites of the brain, but they tend to be located in the posterior cranial fossa [175], with lesions that can be visualized with MRI scans. However, this technique is not sensitive enough to detect more subtle radiation-induced changes in the brain. Therefore, other measures of the brain function should be applied. Of these, fMRI is used to estimate the blood flow, diffusion tensor imaging to detect early changes in white matter integrity and ^{18}F-FDG PET to measure the brain tissue metabolism [167]. The assessment of radiation-induced cognitive impairment mainly involves MMSE examination.

1.2.5.3 Biomarkers

Fluid biomarkers are of great clinical interest to evaluate the adverse effects during and after cranial radiotherapy. Even though there is no well-established biomarker to evaluate the neurotoxic side effects after PCI, there are several promising candidates, *e.g.*, elevated CSF NFL levels reflecting neuronal injury, and decreased CSF sAPPα levels reflecting cognitive decline and memory dysfunction [176].

1.2.5.4 Management

Up to now, there is no established effective treatment to reverse or terminate RIBI pathogenesis.

However, prior to PCI, there are several clinical aspects of CNS radiation tolerance that should be carefully considered for each patient individually to avoid RIBI progression. These include volume of treated brain tissue, radiation quality, total time of radiation, radiation dose per fraction and the total radiation dose [168]. Additionally, age and medical history of the patient are also associated with the radiation tolerance of the brain tissue.

1.3 Extracellular matrix proteins

An extracellular space surrounds neurons and glial cells in the brain and it is filled with ECM-like material, including proteoglycans and glycoproteins, that strongly interact with each other [177]. They play important roles in regulating cell migration, neurite elongation, synaptogenesis and synaptic stabilization [177, 178].

Chondroitin sulfate proteoglycans (CSPGs) belong to the most abundant proteoglycan family in the CNS [179]. Brevican and neurocan are CNS-specific CSPGs [178, 180, 181], while tenascin-R (TNR) and tenascin-C (TNC) are ECM glycoproteins. The principal differences between proteoglycans and glycoproteins are structure-based and are summarized in Table 4.

Table 4. Summary of differences between proteoglycans and glycoproteins.

PROTEOGLYCANS (brevican/neurocan)	**GLYCOPROTEINS** (TNR/TNC)
higher carbohydrate content	lower carbohydrate content
lower protein content	higher protein content
long glycosaminoglycan side chains	short oligosaccharide side chains
elongated core protein	globular core protein

1.3.1 Brevican and neurocan

Brevican is mostly expressed by astrocytes, while neurocan is predominantly expressed by neurons [182]. However, reactive astrocytes rapidly upregulate both these proteoglycans in the tissue surrounding a lesion site [183, 184]. The two proteins are widely distributed in many parts of the brain [178, 185, 186]. While brevican is expressed relatively late during the brain development, neurocan is instead characteristic for the more immature brain [178].

Brevican and neurocan contain two globular domains: the N-terminal G1 and the C-terminal G3, which are connected by a central domain, where chondroitin sulfate (CS) glycosaminoglycan side chains are covalently attached [179, 180] (Fig. 7). These two structural elements have different functions. While the CS chains act as the main inhibitory structures of axonal outgrowth, the core protein has instead a promoting effect [180]. However, a great contribution of inhibitory effects from CS chains makes CS-bearing proteoglycans the major inhibitors of plasticity and neural regeneration in the adult CNS [187]. Brevican (from the Latin *brevis*, short) has a shorter central domain compared with neurocan, with fewer (1-3 [188]) or no [189] CS chains. Since brevican can occur without CS chains, this protein is known to be a bifunctional regulator of neurite outgrowth: both inhibitor and promoter [178, 180]. CS-free neurocan on the other hand does not exist [190].

There are two isoforms of brevican which originate from the same gene via alternative splicing: a major form that is secreted into the extracellular space and a minor form that lacks the C-terminal globular interacting domain, making it tightly attached to the cell membrane via a glycosyl-phosphatidylinositol (GPI)-anchor at Ala^{646} [191]. The latter isoform accounts for less than 1% of the brevican transcripts [178]. The size of the secreted brevican core protein corresponds to 145 kDa [181]. Brevican is a substrate for multiple MMPs that all cleave at its central domain producing several fragments [192]. In humans, the characteristic site for MMP cleavage in brevican has been assigned to the $^{361}A/I^{362}$ bond producing a 53 kDa N-terminal and a ~90 kDa C-terminal brevican fragment [193]. However, the best described protease to cleave brevican is ADAMTS [185]. In humans, it cleaves brevican at a single specific site at the $^{400}E/S^{401}$ bond, producing a 55 kDa N-terminal and a ~90 kDa C-terminal brevican fragment [193].

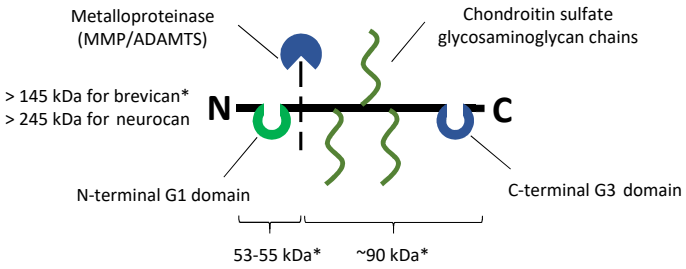

Fig. 7. Schematic picture of the brevican/neurocan structure. Indicated masses correspond to observed molecular masses using immunoblotting techniques (* for secreted brevican isoform). The actual mass of the unmodified core protein (calculated from the sum of masses of all amino acids in the target protein using the UniProt database) is 99 kDa for brevican and 143 kDa for neurocan.

Neurocan has no isoforms and is expressed mainly in juvenile brain giving a full-length protein of approximately 300 kDa, containing a 245 kDa core protein and about three CS chains [190, 194]. In the mature brain, proteolytic processing produces two neurocan fragments that become its major forms [194], an N-terminal part of 130 kDa and a C-terminal part of 150 kDa [195]. Neurocan is a substrate for both ADAMTS [196] and MMPs [197]. However, its ADAMTS and MMP-specific cleavage sites have not yet been determined in human. All variants of neurocan are secreted into the extracellular space.

There are conflicting results regarding the functional relevance of brevican and neurocan in the brain. It is widely known that these proteins are involved in important developmental processes of neuronal tissue, *e.g.*, cell migration, neurite outgrowth and synaptic plasticity. However, both proteoglycans were also reported to be dispensable for formation and maintenance of brain ECM since brevican- or neurocan-deficient mice showed no obvious defects in brain morphology [186, 198]. Nevertheless, the same animal models displayed a similar impairment of hippocampal long-term potentiation [186, 198]. Thus, brevican and neurocan must play an important role in synaptic strengthening after all [179].

The two proteins are upregulated in several rodent injury models of entorhinal cortex lesions [184, 199] and spinal cord injury [200]. Following a CNS injury, the amounts of these proteins in the brain are increased around the lesion and CS-bearing proteoglycans are associated with inhibitory effects of glial scars on axon regeneration [179, 201]. To my knowledge, brevican and neurocan levels in human body fluids and human brain tissue have previously not been studied in relation to inflicted brain injuries.

Brevican and neurocan may also be implicated in the pathogenesis of neurodegenerative disorders such as AD. Brevican is believed to have a neuroprotective function in AD, as neurites surrounded by a brevican-based perisynaptic matrix are spared from tau pathology [202]. In mouse models of AD brevican also appeared with shorter and fewer CS chains while the holoprotein variant was increased [188], with the possible role to promote axonal sprouting and functional recovery. Although the brevican levels were elevated in mice and human AD brain tissues compared with controls [203-205], its serum levels could not separate the two groups [206]. To my knowledge, brevican levels in CSF in relation to AD have not been reported. The expression of neurocan was increased in mouse model of AD [205]. However, neurocan levels in CSF did not differ between AD and controls [207, 208].

Brevican and neurocan interact with a number of ECM proteins, predominantly with tenascins. Both are major interaction partners of TNR and TNC, although TNR appears to be the best partner for brevican, while TNC is the best for neurocan [177, 178, 190, 209, 210].

1.3.2 Tenascins

In vertebrates, the tenascin family consists of four members: TNC, TNR, tenascin-W and tenascin-X [211] of which the two first are the most studied. Although TNC and TNR belong to same family, there are not fully homologous. The “C” in the TNC name represents “cytotactin”, while the “R” in TNR stands for “restrictin” as this glycoprotein is restricted to the CNS [212]. TNC on the other hand is present in many different tissues, such as brain, bone marrow, muscles, endocrine tissues, etc. [213]. TNR is produced by oligodendrocytes and neurons, but not by astrocytes, which in turn are the main producers of TNC [182]. While TNR shows its highest expression in the adult brain, TNC is most prominently expressed during the CNS development and is downregulated after maturation of the adult brain [214]. However, the expression can be increased in tissue undergoing remodelling processes, *e.g.*, wound repair, or in pathological states such as inflammation, tumorigenesis or CNS injuries [214].

TNC is a homohexamer assembled from six subunits that vary in size (200-300 kDa) due to the variability in glycosylation [214]. The six monomers are connected to each other via a tenascin assembly (TA) domain located at the N-terminal part of TNC, thus forming a hexabrachion [215] (Fig. 8 A). Following the TA domain, the TNC monomer consists of a cysteine-rich domain, 14.5 epidermal-growth factor (EGF)-like domains, eight constitutive fibronectin-type III repeats and a fibrinogen-like globe [215] (Fig. 8 C). The two latter are main ligands for CS proteoglycans [216]. In addition, TNC can have up to nine extra alternatively spliced fibronectin-type III domains. Hence, there are numerous isoforms of TNC, theoretically even up to 512 variants in humans [211], produced via alternative splicing within the fibronectin-type III repeats [214].

TNR is a homotrimeric glycoprotein assembled from three identical monomers (Fig. 8 B) of similar modular structure to TNC. The TNR monomer consists of a TA domain, a cysteine-rich domain, 4.5 EGF-like domains, eight constitutive fibronectin-type III repeats and a fibrinogen-like globe [215] (Fig. 8 C). In addition, TNR can have one more extra fibronectin-type III domain, as a result of an alternative splicing. Thus, TNR has two major isoforms in humans: the main form (180 kDa) and a smaller more rare form (160 kDa), which is produced either by alternative splicing [217] or proteolytic cleavage [218].

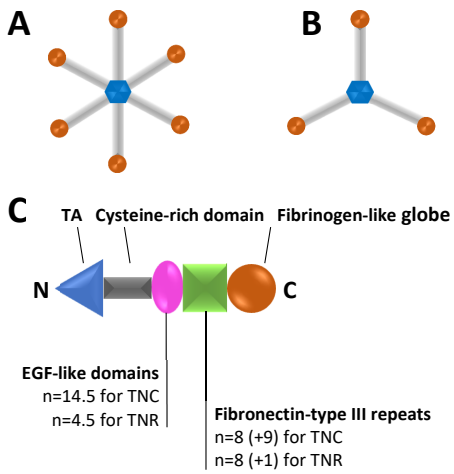

Fig. 8. Schematic structure of TNC hexamer (A), TNR trimer (B) and individual domains within a monomer (C). Spliced fibronectin-type III repeats are indicated in parenthesis.

Tenascins regulate the cell adhesiveness and play important roles in communication between neurons and glial cells [214, 219]. They can exhibit both adhesive and non-adhesive effects on various cell types, depending on the domain being involved [220]. For instance, most fibronectin-type III repeats have adhesive effects, while the EGF-like domains exhibit anti-adhesive properties [220]. Although the intact TNC promotes neurite outgrowth overall, some of its individual domains have inhibitory effects on neurite growth [220]. Similarly to TNC, TNR can either promote or inhibit neurite outgrowth, depending on the domain being involved [221].

Tenascins are also involved in inflammation processes. TNC is a broad inducer of inflammation as its presence switches the microglial phenotype from an anti-inflammatory M2 to pro-inflammatory M1 [222]. TNR is less well investigated in inflammation processes, but it is known to stimulate microglia to generate cytokines [223].

Comparably to proteoglycans, knock-out of *TNC/TNR* genes in mice models does not cause profound abnormalities [224, 225]. Nevertheless, a lack of tenascins revealed subtle changes [214]. For example, *TNC* knock-out mice show an increased migration and a decreased proliferation of oligodendrocyte precursors [226], while *TNR* knock-out mice show behavioural deficits [227, 228].

An increased expression of TNC was observed in several rodent models of cerebral cortex injury [229], entorhinal cortex lesion [230] and spinal cord injury [231]. Beside animal models, the enhanced TNC expression has been seen in human brain tissues following TBI [232, 233]. This increase of TNC is mainly localized around the lesion site in the brain and is associated with reactive astrocytes [232]. Furthermore, TNC levels were observed to be increased in serum of TBI patients and were associated with both trauma severity and unfavourable outcome [234]. In addition, TNC levels in CSF were positively correlated with SAH severity [235]. TNR also shows increased expression in rodent models of spinal cord injury [231] and it restricts post-traumatic synaptic plasticity [236]. To my knowledge, TNR levels have not previously been studied in human body fluids.

Transcription of the *TNC* gene increases in microglia exposed to Aβ and TNC expression rises in AD mice models, while the Aβ plaque burden is reduced in *TNC* knock-out mice [237]. TNC deposits colocalize with and selectively surround dense core, but not diffuse, Aβ plaques [238], where the dense core is more closely associated with neuronal and synaptic loss in AD [239]. However, it is unknown if TNC is a part of the progression or the clearance processes of amyloid plaques. The relation between TNR and AD is largely unexplored, and previous results showed either increased expression of TNR in AD mice models [205] or decreased TNR levels in post-mortem human brain tissues of AD patients [240].

Table 5. Changes of ECM protein concentrations in relation to healthy controls. # indicates an additional increase with TBI severity and unfavourable outcome.

			Brevican	Neurocan	TNC	TNR
Traumatic brain injury	Rodent	brain	↑ [199, 201, 241]	↑ [184, 241-244]	↑ [229, 230]	
	Human	brain			↑ [232, 233]	
		CSF				
		blood			↑ [234]#	
Alzheimer's disease	Rodent	brain	↑ [205]	↑ [205]	↑ [237]	↑ [205]
	Human	brain	↑ [203, 204]			↓ [240]
		CSF		↔ [207, 208]		
		blood	↔ [206]			

1.3.3 Perineuronal nets

The components of the ECM in the mature CNS form dense, lattice-like structures called perineuronal nets (PNNs), which surround neuronal bodies, dendrites and often axon initial segments [245]. Abundant constituents of PNNs are proteoglycans, glycoproteins and hyaluronic acid, which is the central polysaccharide of the neural ECM [178]. Formation of PNNs starts at embryonal development by the accumulation of an early type ECM, including neurocan, TNC and hyaluronic acid [246] and reaches its mature form around the preadolescent period [247]. Brevican, neurocan and TNR are highly enriched in PNN structures [182]. While the two proteoglycans and TNC are not essential for PNN formation [186, 198, 248], TNR-deficient PNNs become abnormal [249]. All elements of PNNs tightly interact with each other. CSPGs bind to hyaluronic acid via their N-terminal domain and to tenascins via the C-terminal domain, forming the structure of the lattice (Fig. 9).

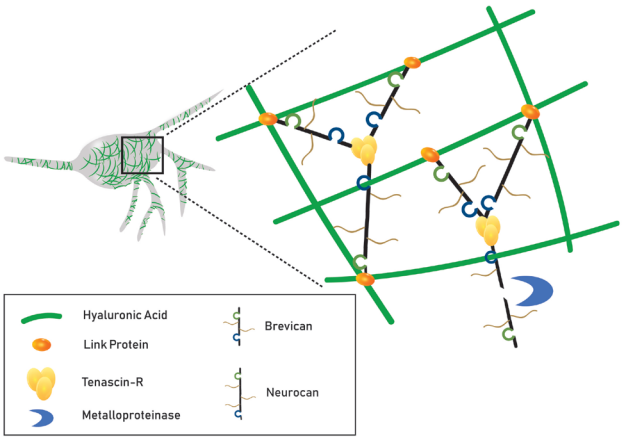

Fig. 9. Schematic picture of PNNs.

Studies with knock-out mice lacking all four *BCAN*, *NCAN*, *TNR* and *TNC* genes have revealed significant changes of synapse development [250-252]. For example, the model shows an increase of excitatory, but decrease of inhibitory, synaptic molecules [252]. Such an imbalance between the excitation and inhibition in neural networks can result in structural changes at synapses and consequently neurodevelopmental abnormalities.

Before the first report of PNN in 1989 [253], this structure was misinterpreted as a trivial histological artifact over 60-70 years [246]. Today, we know that PNNs are essential for normal brain function [246]. PNNs regulate the size of the extracellular space [254]. For example, involvement of brevican, which has a shorter central domain, makes the matrix tighter [180]. This compact structure is a repulsive barrier for approaching axons and inhibits cell migration. However, when the interactions between proteoglycans and other components of PNNs are disrupted, the matrix becomes loose, which facilitates axonal growth and cell movements [180]. PNNs are also important regulators of brain plasticity [179]. This structure keeps the balance between plasticity and tenacity in neuronal circuits by eliminating unused synapses and stabilizing synaptic contacts between neurons [185]. PNN deposition typically increases with brain maturation, leading to increased suppression of brain plasticity. These inhibitory effects may be involved in memory dysfunction. On the other hand, PNNs show protective properties for the neurons they surround. As an example, neurons ensheathed by PNNs are protected from oxidative stress [255], amyloid toxicity [256] and tangle pathology in AD brain [202, 257]. Although the PNN scaffold is disrupted following brain injury, its distribution and structure remain unchanged in AD [202].

1.3.4 Metalloproteinases

Proteolysis of the ECM has both beneficial and deleterious effects. In physiological conditions, a tight control of ECM remodelling is crucial to ensure homeostasis and normal functions of the CNS [258]. However, when ECM proteolysis becomes excessive and uncontrolled, it may lead to disrupted cell-cell and cell-matrix communications, which in turn contributes to pathological conditions [258]. The remodelling processes of the ECM are mediated by specific enzymes, belonging to groups such as "a disintegrin and metalloproteinase with thrombospondin motifs" (ADAMTS) and MMP families. These two zinc-dependent endopeptidase families share the metalloproteinase domain and are expressed throughout the CNS [259]. They are both main regulators of ECM abundance, composition and structure, and there is an accumulating evidence of their pivotal role in brain injury-induced pathology and neurodegeneration [260].

1.3.4.1 MMP

The MMPs are considered to be a major class of enzymes involved in ECM degradation [261]. They are produced as either soluble or membrane-anchored enzymes [262]. However, the soluble forms can also localize to the cell surface through their binding to other cell surface-associated proteins [260]. In humans, there are 23 known members of MMPs, historically grouped based on domain organization and substrate preference into the following sub-families: collagenases (MMP-1, -8, -13), gelatinases (MMP-2, -9), stromelysins (MMP-3, -10), matrilysins (MMP-7, -26), membrane-type MMPs (MT-MMPs) and other MMPs [261, 263]. MMPs are composed of four common domains: signal peptide, propeptide, catalytic and hemopexin domains (the latter of which is absent in matrilysins) (Fig. 10). However, the MMPs differ in the occurrence of additional unique domains within the C-terminus of the MMPs, *e.g.*, transmembrane domain, cytosolic tail, EGF-like factor, immunoglobulin domain and many more [262].

Both glial cells and neurons secrete MMPs to the ECM as inactive proenzymes that only become active when the propeptide domain (containing the Cys-switch motif) is separated from the catalytic domain (containing the zinc-binding motif) by the disruption of Cys-zinc interaction under oxidizing conditions followed by autocatalytic cleavage (Fig. 10) [264]. Various MMPs can also activate each other, *e.g.*, MMP-3 and -10 activate MMP-1, -7, -8 and -9 [265], MMP-2 and -13 activate MMP-9 [260], while MMP-12 activates MMP-2 and -3 [266]. This complex network of cross-activations between MMPs might be the leading cause of abnormal excessive ECM degradation, resulting in pathological conditions [260]. In addition, MMPs can be also activated by other enzymes, *e.g.*, serine proteases that directly cleave off the propeptide domain in the inactive proenzymes [260, 262].

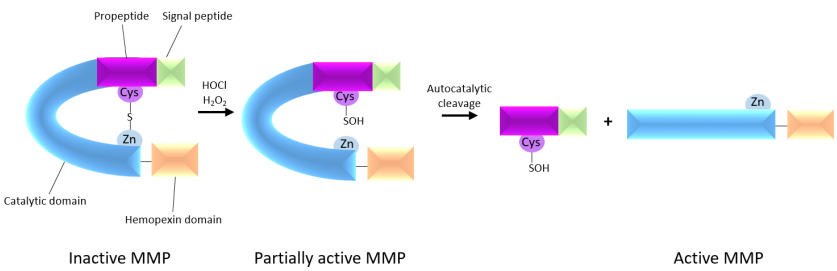

Fig. 10. The structural domains of MMPs and schematic representation of the proteolytic activation of the MMP proenzymes.

The C-terminal hemopexin domain facilitates protein-protein interactions and is involved in substrate specificity of MMPs [262]. However, the mechanism by which MMPs select their substrate is largely unknown. Brevican and neurocan are substrates for different MMPs*, e.g.,* MMP-2 and -3 [192, 197]. However, some of them, *e.g.,* MMP-9, have not shown any ability to degrade these proteoglycans [192, 267]. TNC can also be processed by MMPs, *e.g.*, MMP-1, -3 and -7 [268, 269], while the ability of MMPs to degrade TNR has not been investigated.

Among MMPs, MMP-2, -3 and -9 are the most extensively studied MMPs in the brain [260]. MMPs are critical for neuronal network remodelling [263]. MMPs play a crucial role in many physiological processes including cell proliferation and migration, axonal growth and regeneration, and myelinogenesis [263]. Following a brain injury, MMP activity is increased and an excessive proteolysis may have a detrimental contribution to BBB leakage (by digesting the tight junction proteins of the BBB), neuroinflammation, synaptic dysfunction, demyelination and neuronal death [263]. The concentrations of MMP-2, -3 and -9 have been shown to be either increased or unchanged in human body fluids following TBI [270-273]. Furthermore, the CSF MMP-9, but not MMP-2, concentrations increased with TBI severity [271].

MMPs exert multiple effects in neurodegenerative diseases. As an example, MMP-9 plays a diversified role in AD that is difficult to understand. It is upregulated in the brain tissues of AD patients and localized in close proximity to Aβ plaques [274]. It has also shown ability to cleave Aβ peptides at several sites and degrade Aβ plaques, pointing at its beneficial role in AD where it possibly contributes to the clearance of Aβ plaques [275]. However, Aβ can induce production of MMP-9 and inhibition of Aβ-induced MMP-9 activity improves the cognitive performance in mice [276]. The observed discrepancy of MMP-9 in AD is difficult to explain. It has been suggested that a latent form of MMP-9 might accumulate in the AD brain and in turn contribute to the aggregation of insoluble Aβ peptides in plaques, while the activated form exhibits more beneficial effects in AD [274]. However, the functional role of MMP-9 in AD pathogenesis needs to be further evaluated to draw any firm conclusion.

As mentioned, MMP-2, -3, and -9 are the most extensively studied MMPs in the brain while the other MMPs stay in their shadow, largely unexplored, though many of them are also present in the CNS [277]. Some even showed a potential to serve as targets for therapeutic interventions in neurological diseases, *e.g.*, CSF levels of MMP-10, but not MMP-2, -3, -9, are increased in AD compared with healthy controls [159]. In addition, CSF levels of MMP-9 and -10 are higher in VaD patients compared with the control group [159, 278].

1.3.4.2 ADAMTS

The ADAMTS enzymes are secreted proteases consisting of 19 members that differ in structure and substrate specificity. Individual members of this family differ in the number of thrombospondin (TSP) motifs or additional domains at the C-terminal region [189] (Fig. 11). Based on the substrate preference, ADAMTSs are classified into those that cleave proteoglycans (ADAMTS -1, -4, -5, -8, -9, -15, -20), pro-collagens (ADAMTS-2, -3, -14) and the von Willebrand factor (ADAMTS-13) [279]. The substrates of the remaining ADAMTSs have not yet been fully identified [280].

ADAMTSs consist of several domains: signal peptide, propeptide, catalytic domain (with a zinc-binding motif), central TSP-1 domain, cysteine-rich region and a variable number of TSP repeats [280] (Fig. 11). ADAMTS is initially synthesized as a proenzyme and can be activated intracellularly by furin that removes the propeptide domain from the catalytic domain [259] (Fig. 11), while in their active forms they can be secreted into the ECM mainly by astrocytes, but also by microglia or neurons [193, 280]. None of the ADAMTSs are located in the cell membrane [281].

ADAMTSs are expressed in many CNS structures [281]. Their expression is increased in response to CNS damage and is believed to be an effect of post-injury repair mechanisms, rather than having a harmful contribution [193]. They have a great impact on neurite growth through the degradation of CSPGs, with better efficacy than MMPs [282]. ADAMTS also promotes neuroplasticity and functional recovery after CNS injury [279]. The functions of ADAMTS enzymes, in addition to ECM remodelling and thus neuroplasticity, include regulation of inflammatory processes [280].

The levels of ADAMTS in human AD brain tissues were either increased (ADAMTS-1) or unchanged (ADAMTS-5) [283], while its levels in CSF or blood are largely unexplored.

ADAMTS-4 (aggrecanase-1, the first cloned and identified ADAMTS [193]) is the shortest and the only non-glycosylated ADAMTS [193]. Although it is present in many different tissues, it is the most abundant proteoglycanase in the brain [193, 279]. Both ADAMTS-4 and -5 cleave brevican in an identical pattern [192, 284], while ADAMTS-1 did not show this capability [284]. Neurocan can be cleaved by both ADAMTS-4 [285] and -12 [196], while TNC by ADAMTS-5 [286]. However, whether any ADAMTS is able to cleave TNR remains unknown.

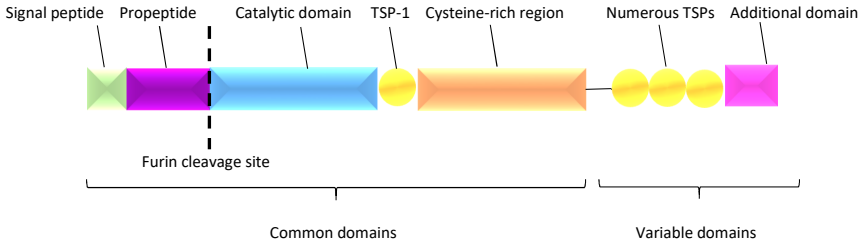

Fig. 11. The structural domains of ADAMTS.

1.3.5 Metalloproteinase inhibitors

ECM proteolysis needs to be tightly regulated to avoid excessive and detrimental tissue degradation, and the inhibitors that deactivate metalloproteinases are crucial to maintain the normal tissue integrity. Hence, the ratios of protease-to-inhibitor determine the overall ECM proteolytic activity. However, an imbalance between the proteolytic activation and inhibition can lead to the progression of various pathologies. This dysregulation can result from either an overexpression of metalloproteinases or from an insufficient control of their endogenous inhibitors [260].

Tissue inhibitors of metalloproteinase (TIMP) is a major inhibitor family for both MMPs and ADAMTSs, though its impeding mechanisms towards MMPs have been much more extensively studied. In humans, there are four subtypes of TIMPs (TIMP-1, -2, -3 and -4) with sizes in the 22-29 kDa range [261]. TIMP-1 and -3 are glycoproteins, while TIMP-2 and -4 do not contain carbohydrates [261]. TIMP-1, -2 and -4 are all secreted, while TIMP-3 is anchored to the ECM [287]. All consist of two domains stabilized by internal disulphide bonds, where the N-terminal domain plays the major inhibitory function as it can interact with the zinc ion in the catalytic domain of MMPs [260, 288]. Both the isolated N-terminal TIMP domain and the full-length TIMP show inhibitory properties; to a stronger degree for the latter form [260]. In addition, the C-terminal domain of TIMPs can bind to the hemopexin domains of MMPs [260, 288]. TIMPs inhibit ADAMTS enzymes through similar interactions as with MMPs [260], although this mechanism is largely unexplored.

The four types of TIMPs have inhibiting properties towards all MMPs, with slightly different affinities [261]. For example, TIMP-1 is more efficient in inhibiting the activity of MMP-3 and -9, while TIMP-2 mainly regulates MMP-2 [289-291]. Whereas MMPs can be inhibited by all four TIMPs, the majority of ADAMTS, including ADAMTS-4 and -5, are inhibited only by TIMP-3 [292]. The reason why the four TIMPs vary in inhibitory efficacy for the different metalloproteinases is not fully resolved.

Similarly to metalloproteinases, the expression of TIMPs is highly controlled during physiological conditions to maintain a balance in the metabolism of the ECM [287]. Under pathological conditions, this balance is disrupted, resulting in an uncontrolled turnover of the ECM [287]. TIMPs are multifunctional proteins and apart from inhibiting metalloproteinases, they also have several other biological functions, such as cell growth promotion, matrix binding and inhibition of apoptosis [287]. Some of these activities might be partially attributed to the inhibition of metalloproteinases, while some others are independent of metalloproteinase-inhibitory activity (such as cell growth activity or apoptosis suppression).

Expression levels of TIMP-1 are elevated in rodent models of TBI [293] and its higher concentrations in serum are associated with TBI severity and mortality [294]. In addition, both TIMP-1 and -2 concentrations in CSF and serum are increased in TBI compared with healthy controls [271].

TIMPs also localize around plaques and NFTs in the AD brain [295]. However, CSF and serum levels of neither TIMP-1 nor -2 were reported to separate AD from healthy controls [159, 278, 296].

Table 6. Changes of ECM protein concentrations in relation to healthy controls or hydrocephalus patients (*). # indicates an additional increase with TBI severity. The + indicates an increase compared with both healthy controls and with AD patients.

			MMP	ADAMTS	TIMP
Traumatic brain injury	Rodent	brain	**-2**: ↑ [297] **-9**: ↑ [297-301]		**-1**: ↑ [293]
	Human	brain	**-1**: ↔ [302] **-2**: ↑ [303] or ↔ [302] **-7**: ↔ [302] **-9**: ↑ [302, 303] **-10**: ↔ [302]		
		CSF	**-2**: ↑ [271] or ↔ [270]* **-3**: ↑ [270]* **-9**: ↑# [271] and [270, 272]*		**-1**: ↑ [271] **-2**: ↑ [271]
		blood	**-2**: ↑ [271, 273] **-9**: ↔ [270] or ↑ [271, 273]		**-1**: ↑ [271] and [294]# **-2**: ↑ [271]
Alzheimer's disease	Rodent	brain			
	Human	brain	**-9**: ↑ [274]	**-1:** ↑ [283] **-5:** ↔ [283]	
		CSF	**-1**: ↔ [304] **-2**: ↔ [159, 278] or ↓ [305] **-3**: ↔ [159, 304] **-9**: ↔ [159, 278, 304] **-10**: ↑ [159]		**-1**: ↔ [159, 278] or ↓ [304] **-2**: ↔ [159, 278]
		blood	**-1**: ↑ [306] **-2**: ↔ [296, 305] **-3**: ↑ [305] **-9**: ↑ [296] or ↓ [305] **-10:** ↔ [305]		**-1**: ↔ [296] **-2**: ↔ [296]
Vascular dementia	Rodent	brain			
	Human	brain			
		CSF	**-2**: ↔ [159, 278] **-3**: ↔ [159] **-9**: ↑+ [159, 278] **-10**: ↑ [159]		**-1**: ↑+ [159] or ↔ [278] **-2**: ↔ [159, 278]
		blood			

Table 7. Matrix metalloproteinases and their substrates. Grey indicates that no digestion was observed.

	BCN	NCN	TNC	TNR
MMP-1	[192]		[269]	
MMP-2	[192]; [267]	[197, 267]	[268]; [269]	
MMP-3	[192, 267]	[267]	[268, 269]	
MMP-7	[192]		[268, 269]	
MMP-8	[192]			
MMP-9	[192, 267]	[267]	[268, 269]	
MMP-10	[192]			
MMP-13	[192]			
ADAMTS-1	[284]			
ADAMTS-4	[192]	[285]		
ADAMTS-5	[284]		[286]	
ADAMTS-12		[196]		

1.4 Methodology

1.4.1 Immunoassays

Immunoassays are used to quantify the target analytes, *e.g.*, peptides and proteins in a biological sample, using antibody-antigen interactions. There are several classes of antibodies, depending on their structure and immune function. The immunoglobulin G (IgG) is the most abundant type and consists of two light and two heavy polypeptide chains, connected through disulphide bonds to form a Y-shaped molecule (Fig. 12). Each IgG has two antigen-binding sites (paratopes) and each antigen potentially has multiple epitopes. A monoclonal antibody binds to a specific epitope, while a polyclonal antibody is actually a collection of several antibodies, potentially recognising different epitopes on the same antigen.

Immunoassays are considered relatively fast and straightforward methods. Equipment is rather inexpensive and widely available. However, the use of antibodies involves some pitfalls that should be acknowledged. Firstly, the sample properties can affect the binding affinity of the antibody to the target analyte (matrix effect) and antibodies might cross-react with other components present in the sample. However, this can be investigated and mitigated during method development. The standards used for the production of calibration curves are analysed in separate wells, usually not in the same matrix where the target analyte is present. Additionally, it is challenging to generate selective antibodies to distinguish between different isoforms or other modified target molecules. Moreover, the epitope can be hidden in the protein structure, and thus not accessible for the antibody.

Immunoassays can employ a variety of different labels, which allow for the detection of target analytes. The typical labels are enzymes, fluorophores and electrochemiluminescent tags.

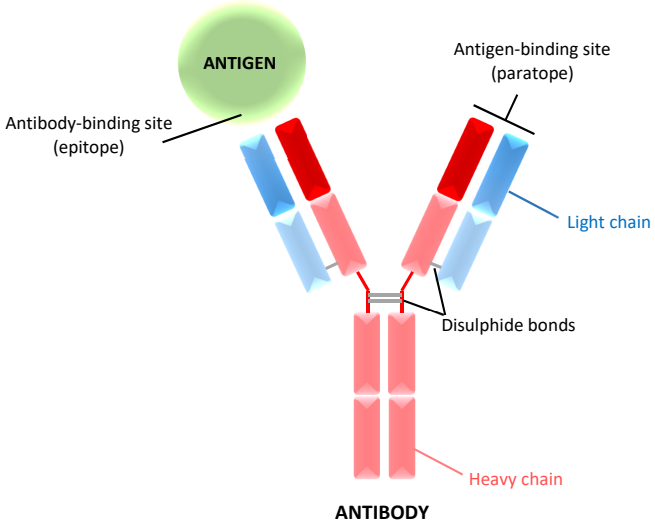

Fig. 12. IgG antibody structure and its binding site to an antigen. The variable regions of antibody are marked in dark blue and dark red for light and heavy chains, respectively.

1.4.1.1 Enzyme immunoassay

Enzyme-linked immunosorbent assay (ELISA) is based on enzymatic reactions, where the enzyme is the detectable label. There are several types of ELISA techniques such as direct, indirect, sandwich, and competitive ELISA.

The sandwich ELISA (Fig. 13) is the most common approach. It uses two antibodies (capture and detection) to target and quantify an antigen. In short, samples are added to pre-coated wells containing capture antibodies, which are specific to the target antigen. After sample addition, a biotinylated detection antibody is added to "sandwich" the analyte, followed by horseradish peroxidase (HRP)-conjugated streptavidin. The final step consists of the application of a 3,3′,5,5′-tetramethylbenzidine (TMB) substrate solution, which is a visualising reagent that reacts with the HRP enzyme. In this reaction, TMB is oxidized. Consequently, a blue by-product is produced, which colour intensity is proportional to the amount of HRP, and thus to the target analyte concentration. This reaction is stopped using a stop solution (sulphuric acid), which inactivates the HRP enzyme by changing the pH and at the same time the colour changes from blue to yellow. The results are viewed and quantified using a spectrophotometric plate reader.

With the ELISA technique, the amount of light absorbed by the sample is measured, *i.e.*, the absorbance. A spectrophotometer consists of three major components: a light source, a monochromator and a detector. The light source emits light with a broad range of wavelengths, which is filtered by the monochromator to a narrower wavelength range. The sample, placed between the monochromator and the detector, absorbs a fraction of the light and the signal, expressed in unit-less absorbance, is calculated from this fraction.

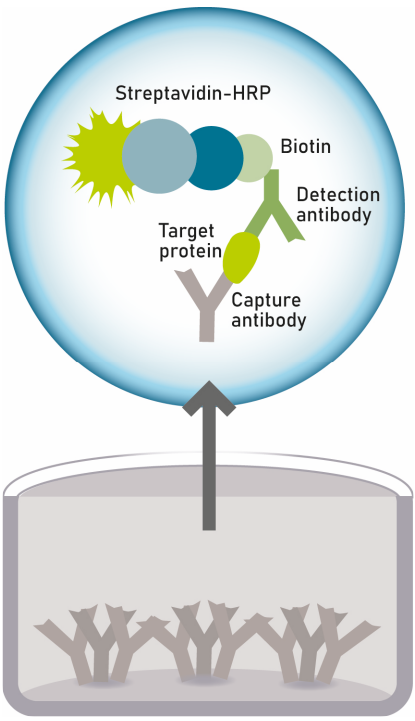

Fig. 13. Sandwich ELISA.

1.4.1.2 Fluorescent immunoassay

The fluorescent xMAP technology is a bead-based immunoassay (Fig. 14) and a multiplex alternative to ELISA, although it can also be used for singleplex analysis. Instead of an enzyme, it uses a fluorophore as a detectable label that absorbs and re-emits absorbed light at specific wavelengths.

In this method the capture antibodies are attached to magnetic beads (6.5 μm in size), which in turn are colour coded to enable their differentiation from each other, which is needed for multiplexing. The combinations of different concentrations of red and infrared fluorophores can create up to 500 distinct beads (FLEXMAP 3D), each recognising a different analyte. However, the maximal reading capacity for fluorescent MAGPIX imager is limited to 50 bead sets, meaning that 50 different analytes can be detected within a single sample.

In the multiplex format, a sample containing the target analyte is added to the mixture of antibody-coated beads. Next, a cocktail of biotinylated detection antibodies is added, followed by phycoerythrin (PE)-conjugated streptavidin. The final step consists of the application of a delivery medium prior to reading. A magnet in the fluorescent imager captures and holds the magnetic beads in a monolayer, where two light-emitting diodes (LEDs) illuminate the beads. The red LED (635 nm) excites the inner fluorescent dyes of the beads and thus identifies the bead region and in turn determines the analyte that is being detected. If the target analyte is present, the green LED (525 nm) recognises the fluorophore and determines the magnitude of the PE-derived signal, which is in proportion to the amount of the captured analyte. The image is recorded with a charge-coupled device camera and the results are viewed and quantified using a fluorescence imager.

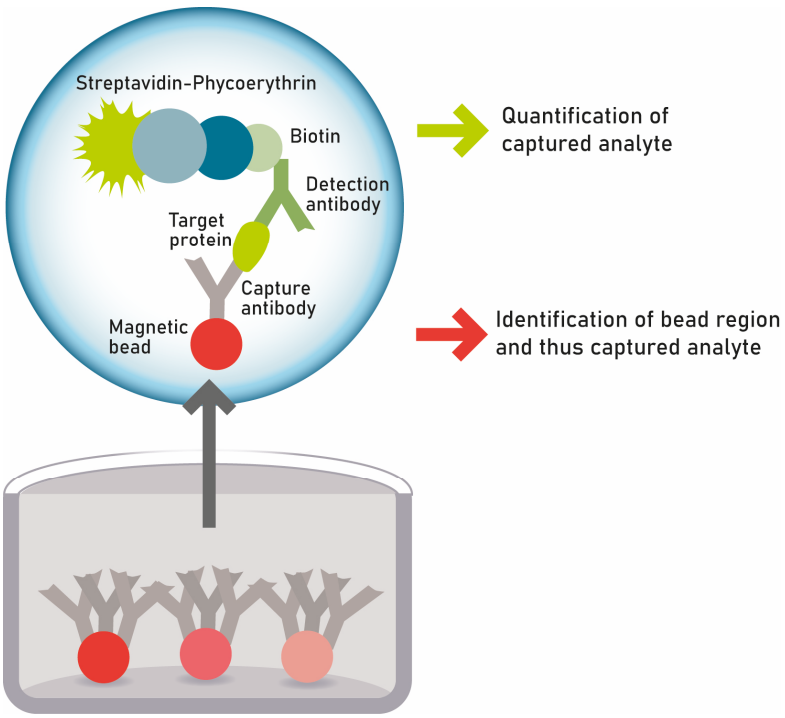

Fig. 14. Bead-based multiplex fluorescent immunoassay.

1.4.1.3 Electrochemiluminescence immunoassay

Electrochemiluminescence (ECL) immunoassays (Fig. 15) use luminescence produced during electrochemical reactions to quantify the target analytes. Here, the detectable label is an electrochemiluminescent tag.

Capture antibodies are immobilized on the working carbon electrodes, placed at the bottom of the assay plate. Sample containing the target analyte is added followed by detection antibodies labelled with an electrochemiluminescent label (called sulfo-tag, a ruthenium complex). Next, a Tris-based buffer containing tripropylamine (TPA) is added to provide an appropriate chemical environment for ECL.

In the detection imager instrument system, a voltage is applied to the plate's electrodes oxidizing both TPA and ruthenium. During the ECL reaction, TPA serves as a reductant and transfers an electron to ruthenium. When the excited ruthenium returns to the ground state, it emits a photon. The intensity of the emitted light is measured to quantify analytes in the sample.

ECL immunoassays can be used in both singleplex and multiplex formats (up to 10-plex in each well), where capture antibodies against specific target analytes are either coated on one or several different electrodes in a single well, respectively.

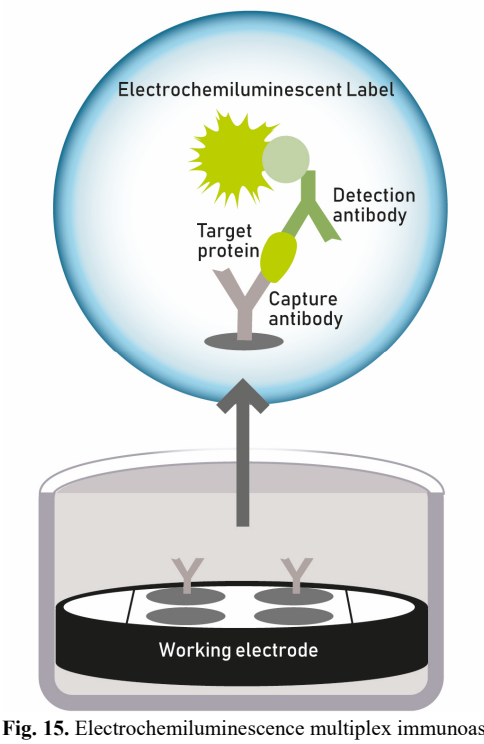

Fig. 15. Electrochemiluminescence multiplex immunoassay.

1.4.2 Fluorescence/Förster resonance energy transfer

Fluorescence or Förster resonance energy transfer (FRET) is a distance-dependent physical process, where a light source excites a donor fluorophore and the exited state of energy is transferred from the donor molecule to an acceptor molecule (quencher chromophore) (Fig. 16). The excited fluorophore then returns to the ground state without emitting light. This energy transfer is only possible when both the donor and acceptor molecules are close to each other (1-10 nm) and when the emission spectrum of the excited fluorophore overlaps with the absorption spectrum of the acceptor. However, if donor and acceptor are separated from each other, *e.g.*, after enzymatic cleavage, the excited fluorophore is no longer quenched and a fluorescent signal is produced.

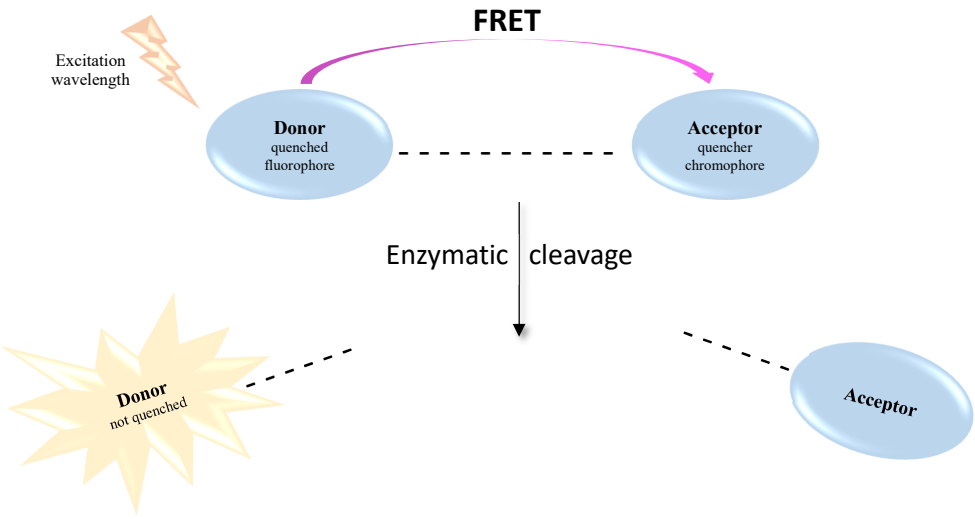

Fig. 16. Schematic representation of the FRET mechanism.

1.4.3 Mass spectrometry-based proteomics

Proteomics is the large-scale study of proteins in biological samples. MS is the main technique utilised in proteomics. The analysis involves detection, identification and quantification of a large diversity of proteins and protein variants. Characterisation of these biomolecules may contribute to the further comprehension of their dynamics, interactions and functions. Sample preparation combined with chromatographic separation techniques and MS analysis provide highly sensitive measurements for investigation of proteins and protein variants in biological samples.

1.4.3.1 Sample preparation

Sample preparation prior to MS-based analysis is essential to detect and quantify proteins and protein variants of interest in a complex mixture of other biomolecules. It is a crucial step in the protein analysis workflow to reduce the sample complexity as the more abundant species can suppress signals from less abundant ones. Typically, this can be done by adding one or more sample preparation steps prior to MS analysis to remove unwanted species, such as salts, or to induce enzymatic digestion. Although sample preparation is important to improve the detection sensitivity, it should be noted that every additional step in the sample treatment might cause the loss of analytes. In addition, efficient sample preparation requires a profound knowledge about the target molecules and the biological sample.

1.4.3.1.1 Immunoprecipitation

Immunoprecipitation (IP) is a purification method used to isolate a target analyte out of a complex sample matrix, *e.g.,* CSF or blood, using antibodies specific for the particular peptide or protein of interest (Fig. 17).

In this method, a primary antibody designed to target the antigen is immobilized on small (1-4 µm diameter), spherical magnetic beads, pre-coated with a secondary antibody from a different species. The remaining unbound antibody is removed in multiple washing steps. Next, the sample containing the target analyte is incubated with the antibody-bead complex, where the antigen binds to the primary antibody. During several washing steps, separation of the analyte of interest from the rest of the proteins in the sample matrix occurs due to the presence of a magnet retaining the beads. In a final step, the analyte is eluted from the antibody-bead complex.

IP is a sample preparation step preceding further analysis using, *e.g.*, MS. It is used to enrich the target analytes out of a solution containing many other proteins, that are at much higher concentration than the analyte of interest; at the same time, the sample complexity is drastically reduced.

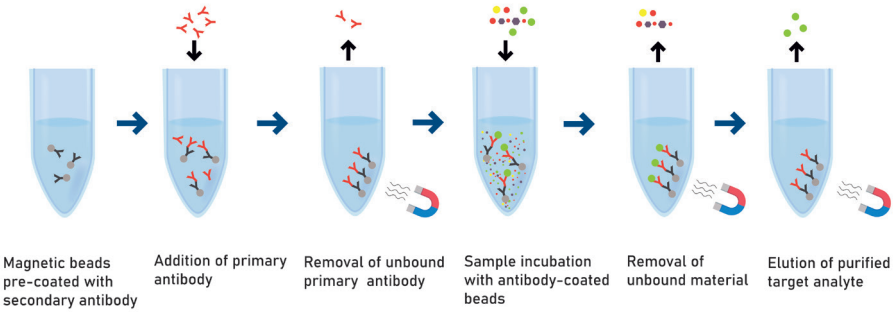

Fig. 17. Immunoprecipitation procedure.

1.4.3.1.2 Protein digestion

Prior to MS analysis, proteins are often broken down into peptides, in order to increase detection sensitivity and solubility. The most used protease for protein digestion is trypsin, due to its high proteolytic activity and stability. In addition, it frequently produces peptides of suitable size for MS analysis. Trypsin cleaves peptides at the carboxyl side of arginine and lysine residues, except when either is followed by a proline. Different proteases can also be mixed, *e.g.*, trypsin with Lys-C, for a more efficient digestion on the C-terminal side of lysine. There are other proteases that can be used when trypsin is unsuitable, one of them is Asp-N that cleaves peptide bonds at the amino terminal side of preferentially aspartic, but also glutamic acid residues. Protease induced digestion can be followed by sample purification using, *e.g.*, solid phase extraction (SPE).

1.4.3.1.3 Solid phase extraction

SPE is an extraction technique used for compound concentration and purification by removing sample matrix such as salts, which might interfere with the MS analysis. The compounds can be retained by the sorbent in different ways, *e.g.*, using reversed phase, where the analytes of interest are purified according to their hydrophobicity. Here, the liquid phase is more or less polar (*e.g.*, water or methanol, respectively), while the stationary phase is more hydrophobic consisting of either silica-based sorbents with, *e.g.*, C_{18} functional groups (traditional SPE) or hydrophilic-lipophilic balanced (HLB) particles (*e.g.*, Oasis HLB). The HLB sorbent is made of a co-polymer (combining a balanced amount of hydrophilic and lipophilic monomers) and has higher recovery for polar analytes than the traditional silica-based sorbents. An additional advantage of HLB-based SPE is that the sorbent beds do not dry out.

The components are separated using a four-stepwise elution using vacuum, as shown in Fig. 18: 1) conditioning with *e.g.*, methanol and subsequent equilibration of the surface with water; 2) loading, where all apart from the most hydrophilic analytes in the sample interact with the more hydrophobic sorbent, while the solvent and other very hydrophilic substances pass through the cartridge; 3) washing with water to remove further hydrophilic interferences; 4) elution of all analytes with methanol.

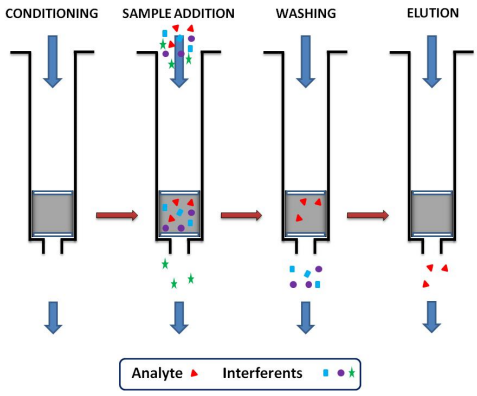

Fig. 18. Stages of solid phase extraction (courtesy of Al-Karawi, Dheyaa Hussein).

1.4.3.2 Liquid chromatography

Liquid chromatography (LC) provides a separation of the sample compounds and can be used prior to MS analysis, in order to reduce complexity of the sample mixture. Samples are injected and carried by the mobile phase at a steady rate under a high pressure through the system. When the sample passes through the column, the sample compounds will interact according to their physicochemical properties with the stationary phase of the column and a separation takes place. In the case of reversed phase LC, the stationary phase is made of a hydrophobic solid adsorbent material, such as porous silica particles with hydrophobic carbon chains attached, that has a stronger affinity for hydrophobic compounds (Fig. 19). Thus, the most hydrophilic molecules will be eluted first as they interact with the stationary phase with the least affinity. Increasing the concentration of organic solvent (*i.e.*, acetonitrile or methanol) in the mobile phase reduces stationary phase-molecular hydrophobic interactions and enables the hydrophobic molecules to elute from the column.

In high-performance LC (HPLC), the size of the column particles is smaller and they are more uniform compared with the earlier standard LC. HPLC operates at high pressure (up to 400 bar), creating more constant flow rates resulting in more reproducible results with higher resolution (narrow, better separated peaks) in a shorter time of analysis. Even higher pressure (over 1000 bar) can be achieved using ultra-high-performance LC (UHPLC) that contains even smaller particles in the column (less than 2 µm).

An HPLC can be operated at different rates depending on the purpose of the experiment: common flows for protein analyses are nanoflow (nanoliters per minute) or microflow (microliters per minute). Nanoflow offers high sensitivity and it is mostly used for explorative purposes, while microflow is less sensitive but more robust and faster, and thus suitable for high-throughput targeted assays.

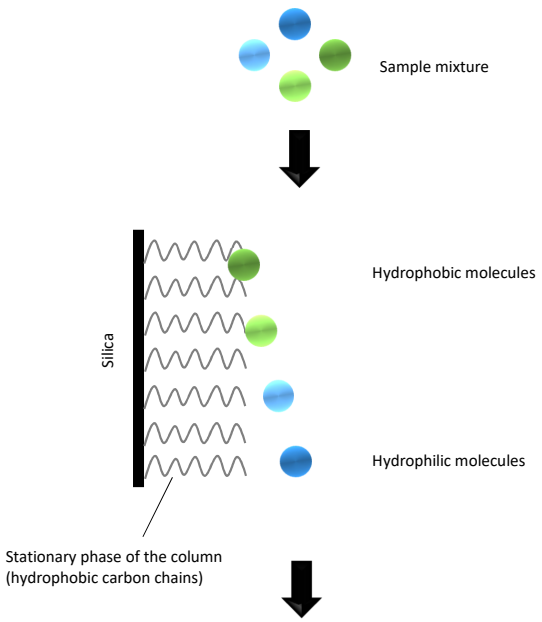

Fig. 19. Reverse phase liquid chromatography. The molecules that are more hydrophobic (green) bind stronger to the hydrophobic stationary phase, while hydrophilic molecules (blue) bind weaker and elute earlier.

1.4.3.3 Mass spectrometry

A mass spectrometer consists of three major parts: an ion source, a mass analyser and a detector.

1.4.3.3.1 Electrospray ionisation source

An ion source transfers molecules into gas phase ions. For example, it can be an interface between the liquid chromatograph and a mass spectrometer, converting the liquid-phase to the gas-phase required in the mass spectrometer. Non-destructive ionisation methods are important to analyse intact biomolecules without significant sample degradation. One of the most commonly used soft ionisation processes is electrospray ionisation (ESI) (Fig. 20).

Here, the sample, dissolved in a polar, volatile solvent, flows to a needle at the end of the capillary. High voltage is applied between the needle and the nozzle causing the liquid to form a conical shape called a Taylor cone. The strong electric field leads to the formation of charged droplets. Further, the capillary needle is heated and surrounded by a warm flow of nitrogen gas facilitating desolvation and droplet shrinkage. In addition, the nozzle consists of a heated transfer tube, which further assists the desolvation, resulting in the formation of single ions in gas-phase. However, the exact mechanism for gas-phase ion production is still not fully understood.

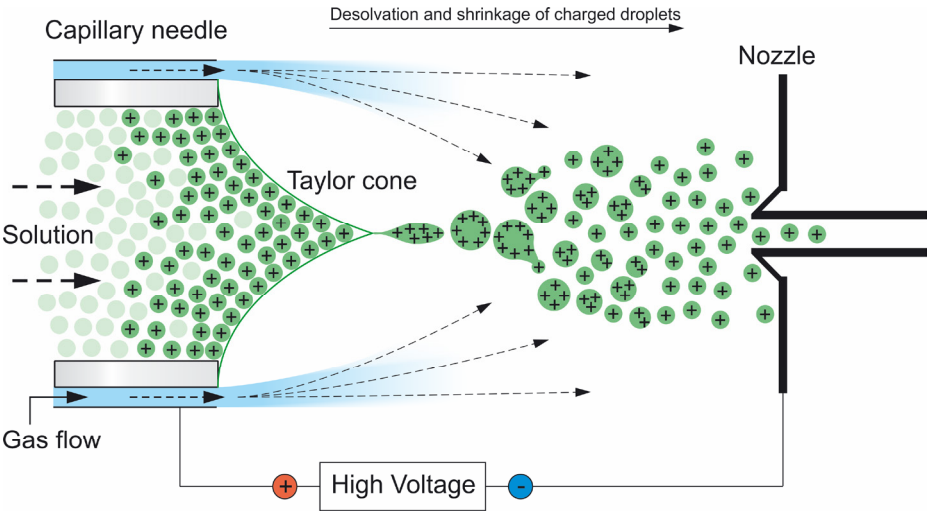

Fig. 20. Schematic of an electrospray ionisation source (courtesy of Ann and Gunnar Brinkmalm).

1.4.3.3.2 Mass analysers

Separation of ions (according to their mass-to-charge ratio, *m/z*) can be achieved in a mass analyser, such as a quadrupole or an orbitrap.

The quadrupole (Fig. 23 A) consists of four rods with hyperbolic surfaces, electrically connected in pairs of opposite potentials. Ions of interest are selected by applying a combination of potentials (radiofrequency and direct current) to the rods matching the desired *m/z*. Ions with matching *m/z* will have a stable trajectory between the rods and pass through, while ions of other *m/z* are filtered away. When acting as a filter, the quadrupole provides high capacity and sensitivity, but comparatively low resolution and mass accuracy.

The orbitrap (Fig. 23 C) consists of a central inner electrode and an outer electrode. The outer electrode is split in two, separated by an insulating material. A voltage is applied between the central and outer electrodes producing an electric field. Ions trapped in this field will revolve around the central electrode in an orbital motion and at the same time oscillate along the axis. The frequency of the back and forth oscillations depends on the ions' *m/z* and the ions induce an electric image current in one of the outer electrodes that act as detector. Thus, the orbitrap serves as both mass analyser and detector. The orbitrap provides very good resolution and mass accuracy, but lower capacity and sensitivity compared with a quadrupole.

1.4.3.3.3 Detectors

In the image-current detection used in the orbitrap, the current induced in the outer electrodes in the orbitrap is converted to a frequency spectrum using Fourier transformation, a mathematical operation that transfers signals from the time domain to the frequency domain (Fig. 21). Mass spectra are then obtained through a simple relationship between frequency and *m/z* (Fig. 21).

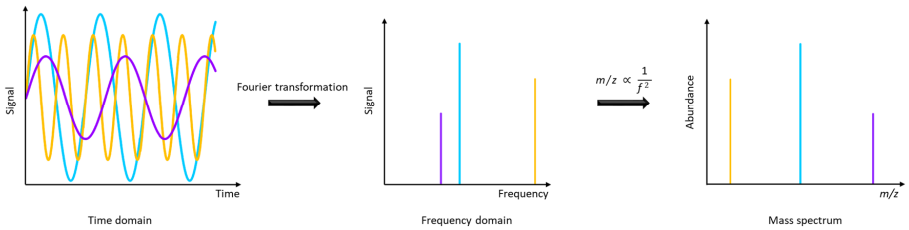

Fig. 21. Schematic of the Fourier transformation (courtesy of Gunnar Brinkmalm).

1.4.3.3.4 Q Exactive hybrid instrument

Several types of mass analysers can be combined to form a hybrid instrument, *e.g.*, the Q Exactive (Thermo Fisher Scientific), which has both a quadrupole and an orbitrap (Fig. 22). Hybrid instruments combine the strengths of the individual analysers. Here, the quadrupole plays a mass filtering role with high capacity, while the orbitrap functions as both a mass analyser and detector providing high-resolution measurements with high mass accuracy.

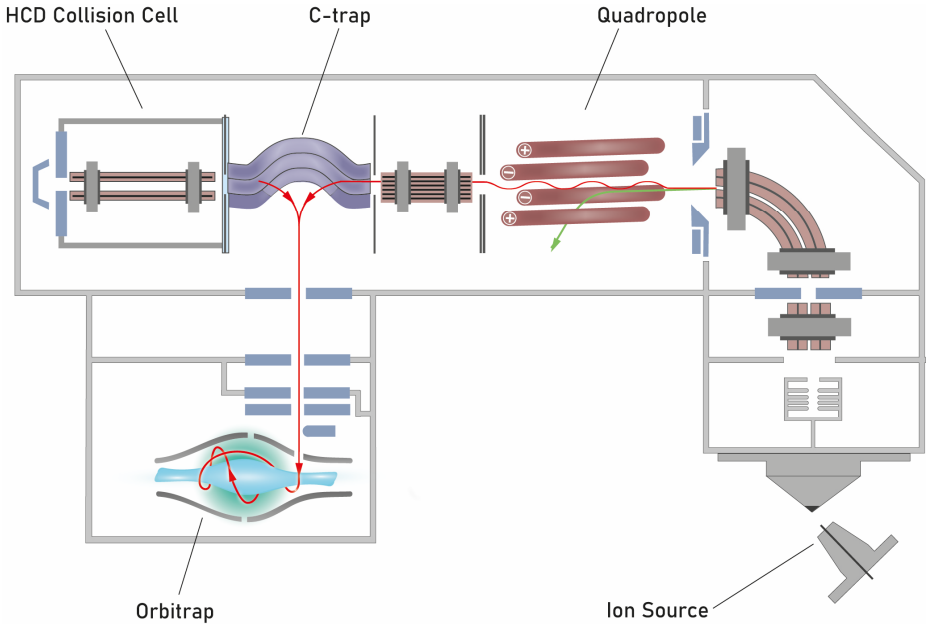

Fig. 22. Schematic of the Q Exactive hybrid quadrupole-orbitrap instrument.

A mass spectrometer can be operated using several acquisition (scan) modes. A "full scan" provides a mass spectrum of all analytes. In the tandem MS (MS/MS) scan mode, an ion (precursor ion) is selected for fragmentation and then the product ions are analysed. When acquiring a full scan in the Q Exactive, all ions pass through the quadrupole, are collected in the C-trap and then injected to the orbitrap for *m/z* separation and detection. For MS/MS, ions are first selected in the quadrupole mass filter and only selected ions travel through. They are then accumulated in the C-trap and further injected into the "higher-energy collisional dissociation" (HCD) cell, where they are subjected to collisions with nitrogen gas molecules. Next, produced fragment ions are ejected from the HCD cell, collected in the C-trap and injected to the orbitrap for analysis and detection.

An explorative proteomic analysis is often performed using so-called data-dependent acquisition. Here, the mass spectrometer generates a full scan mass spectrum and next acquires several MS/MS spectra of the ions with highest intensity. This procedure is then repeated throughout the whole acquisition. The information from both full scans and MS/MS scans are then combined and used to identify fragments by performing searches against protein databases.

For quantitative analysis, a targeted approach is commonly used. Here, a number of compounds are preselected for fragmentation and only the selected ions are measured. One type of targeted approach is parallel reaction monitoring (PRM), which is used with the Q Exactive.

1.4.3.4 Parallel reaction monitoring

PRM is a mass spectrometric method that can be performed on certain hybrid instruments, such as the Q Exactive. Here, a precursor ion is selected and fragmented after which the product ions are monitored in parallel. The quadrupole is used to isolate a precursor ion (Fig. 23 A), which is then fragmented in the HCD cell (Fig. 23 B), and the resulting product ions are transferred to the orbitrap, where a fragment ion mass spectrum is recorded (Fig. 23 C).

Stable isotope-labelled peptides can be used as internal standards (IS) for MS-based quantification. They are typically synthetic peptides with incorporated stable isotopes, *e.g.*, ^{13}C and/or ^{15}N. Sample peptides and labelled peptides have identical chemical properties, but differ in mass. Since these peptides are chemically equivalent, they will be affected in the same way in the HPLC separation and in the ionisation.

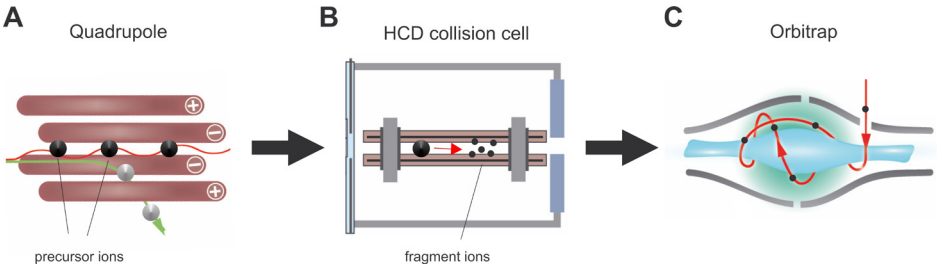

Fig. 23. Schematic of the parallel reaction monitoring.

2 AIM

2.1 Overall aim

The main aims are to identify and quantify ECM proteins, and to characterise their proteolytic processing in human body fluids in relation to various inflicted brain injuries and neurodegenerative disorders.

2.2 Specific aims

Paper I: to investigate if brevican, neurocan, TNC and TNR in ventricular CSF and serum are associated with functional outcome and longitudinal changes following TBI; and to compare the levels of ECM proteins in TBI patients with healthy controls in serum and a non-TBI group (iNPH) in CSF using various ELISAs.

Paper II: to evaluate protein fragment patterns of brevican and neurocan in ventricular CSF of TBI and iNPH patients using tryptic peptides in an MS-based panel; to investigate ADAMTS-derived peptides in CSF; and to study ADAMTS-like enzymatic activity in CSF in relation to TBI and iNPH using a quenched fluorescent substrate.

Paper III: to study the dynamics of various MMPs in ventricular CSF of TBI and iNPH patients in relation to clinical outcome and longitudinal changes following brain injury using fluorescent immunoassays.

Paper IV: to evaluate lumbar and ventricular CSF levels of brevican, neurocan, MMPs and TIMP-1 in iNPH patients in relation to shunt surgery using an MS-based panel and fluorescent or electrochemiluminescent immunoassays.

Paper V: to quantify brevican and neurocan proteolytic peptides in lumbar CSF of patients with AD and VaD in comparison with healthy controls using an MS-based panel.

Paper VI: to quantify brevican, neurocan, TNC and TNR in lumbar CSF of patients with AD compared with healthy controls using various ELISAs.

Paper VII: to evaluate the effects of cranial irradiation in SCLC patients on brevican and neurocan levels in lumbar CSF using ELISAs.

3 MATERIALS

3.1 Ethical approval

All the work included in this thesis was conducted according to the Declaration of Helsinki, the formal statement of ethical principles for medical research involving human material, developed by the World Medical Association. Additionally, sample collections were performed according to the ethical permissions approved by the regional ethical committees. The TBI cohort (**papers I-III**) received ethical approval from the Regional Ethical Board in Stockholm (#2005/1526/31/2), while the iNPH cohort (**papers I-IV**) was approved by the Regional Ethical Board in Gothenburg (154-05). In addition, serum control samples from healthy individuals (**paper I**) were obtained in accordance with the Regional Ethical Board in Gothenburg (823-14). The CSF samples collected from healthy controls as well as AD and/or VaD patients were approved by the Regional Ethical Board in Gothenburg (091-99/T 479-11 and S496-99) (**paper V**) or the Regional Ethical Board in Lund (695/2008) (**paper VI**). For the RIBI-based study (**paper VII**), the use of CSF samples was approved by the Regional Ethical Board in Gothenburg (194-07).

Before any experimental work was undertaken, the ethical risk within each research project was considered by comparing the beneficial effects of the work with the potential risk of harm. Voluntary written informed consents were obtained from participants or, if incapable, from their proxy, prior to the inclusion in the study. The consumption of biological material was kept as low as possible. The samples used for method development or validation purposes were left-over materials from clinical routine care (the Clinical Neurochemistry Laboratory at the Sahlgrenska University Hospital, Mölndal, Sweden), that remained after all planned analyses were performed. These samples were de-identified and cannot be traced back to the individual.

3.2 Cohorts

Table 8. Overview of the patient cohorts showing: number of patients (type of the body fluid).
Ctrl = control; LCSF = lumbar CSF; VCSF = ventricular CSF

Paper	Ctrl	TBI	iNPH	AD	VaD	RIBI
I	9 (serum)	42 (VCSF) 40 (serum)	38 (VCSF)			
II		42 (VCSF)	37 (VCSF)			
III		33 (VCSF)	38 (VCSF)			
IV			31 (VCSF) 31 (LCSF)			
V	I: 33 (LCSF) II: 12 (LCSF)			I: 32 (LCSF) II: 5 (LCSF)	I: 10 (LCSF) II: 14 (LCSF)	
VI	50 (LCSF)			42 (LCSF)		
VII	9 (LCSF)					11 (LCSF)

The control participants included in the various studies were from different cohorts. In **paper I**, healthy controls were recruited by advertisement, primary for the purposes to study sleep deprivation [307]. In **paper V**, the control group consisted of healthy individuals with no subjective symptoms of cognitive dysfunction and, for cohort 1, also cognitively stable MCI patients. **Paper VI** included clinically diagnosed healthy controls. In **paper VII**, CSF samples from healthy controls were collected at the time of preparation for spinal anaesthesia prior to knee surgery.

The TBI cohort (**papers I-III**) included patients suffering from acute brain trauma and requiring neuro-critical care as well as ICP monitoring. They were recruited at the Karolinska University Hospital, Stockholm, Sweden. The cohort included follow-up measurements (up to 14 days after TBI) of both ventricular CSF and serum samples. Functional outcome was defined by the GOS [28], assessed one year after brain injury.

The iNPH cohort (**papers I-IV**) included iNPH patients recruited and diagnosed according to international guidelines [59] at the Hydrocephalus Unit at the Sahlgrenska University Hospital, Gothenburg, Sweden. Severity of the disorder was staged using iNPH scale [72] before and four months after shunt surgery. Lumbar and/or ventricular CSF samples were collected.

The AD patients were recruited at the following Swedish Memory Clinics: in Falköping (**paper V** cohort I), at the Sahlgrenska University Hospital in Mölndal (**paper V** cohort II) and at the Skåne University Hospital in Malmö (**paper VI**). All AD patients met the diagnostic criteria of dementia [308] and of probable AD as defined by NINCDS-ADRDA [102].

The VaD cohort (**paper V**) included patients recruited at the Swedish Memory Clinic in Falköping (cohort I) and at the Sahlgrenska University Hospital in Mölndal (cohort II). They fulfilled the diagnostic criteria of dementia [308] together with the requirements for VaD by NINDS-AIREN [154] or, more specifically, for SSVD established by Erkinjuntti [309].

The RIBI cohort (**paper VII**) included histologically confirmed SCLC, who were eligible for PCI at the Sahlgrenska University Hospital, Gothenburg, Sweden. The cohort included follow-up measurements (three and 12 months after PCI). Three patients were diagnosed with brain metastases at follow-up.

3.3 Sample collection

Lumbar CSF was collected according to standardised procedures [5], where CSF was sampled through a lumbar puncture procedure between the L3/L4 or L4/L5 vertebral interspace (Fig. 1). Ventricular CSF was collected via an EVD procedure, through the insertion of a catheter into the ventricular system of the brain (Fig. 2). For both types of CSF, insoluble material was removed by centrifugation at 2,000 × g at +4 °C for 10-15 min. Following that, the supernatant was aliquoted into polypropylene tubes and stored at -80 °C pending analysis.

Blood was collected through arterial lines. Serum was obtained by centrifugation at 2,500 × g at +4 °C for 10 min to pellet down the clotting factors. The resulting supernatant was aliquoted in polypropylene tubes and stored at -80 °C pending analysis.

4 EXPERIMENTAL DESIGN

4.1 ELISAs targeting ECM proteins

Sandwich ELISA was used in **papers I**, **VI** and **VII** to quantify various ECM proteins in human body fluids.

Commercially available sandwich ELISA kits (RayBiotech, Norcross, GA, USA) were utilised to measure concentrations of brevican, neurocan, TNC and TNR in CSF and serum (however, TNR was not detectable in serum) (Table 9). The analyses were performed according to the instructions from the manufacturer. Epitope mapping was not performed by the company, but the binding site for the brevican detection antibody was examined using IP-MS and determined to be between aa 85 - 274 (Fig. 24). Unfortunately, it was not possible to investigate the epitope binding of the capture brevican antibody, as it was precoated to the assay plate and separate purchase was not possible.

In addition, an in-house developed ELISA based on commercially available antibodies (US Biological Life Sciences, Salem, MA, USA) was used for the quantification of brevican in CSF (see **paper I** for detailed description). Also in this case the brevican epitopes recognised by the antibodies used in the in-house ELISA were unknown, and therefore the binding sites for both capture and detection antibodies were examined using IP-MS. The MS-based results from CSF revealed that when using the capture antibody, only peptides from the C-terminal part of the brevican (spanning aa 718-841) are detected, while for the detection antibody only peptides from the N-terminal part (spanning aa 23-429) are observed (Fig. 24). These antibodies were also used in the analysis of brevican fragment patterns (sections 4.5 and 5.1; **paper II** and **paper V**). In brief, for the in-house ELISA, 96-well strip microplates were coated with monoclonal mouse antibody against human brevican in carbonate buffer overnight at +4 °C. After washing with phosphate-buffered saline/Tween 20-based buffer (PBS-T), wells were blocked with bovine serum albumin (BSA) in PBS-T solution for one hour. As a calibrator, recombinant brevican full-length standard was used. Following the serial dilutions, calibrators were further diluted 1:2 in BSA-PBS-T on the plate to a final concentration range of 0.08-5 ng/mL. CSF samples and quality controls were diluted 1:8 in BSA-PBS-T. Thus, the dilution of samples was 1:4 compared with the calibrators (Table 9). After washing, samples and calibrators were incubated on a plate for one hour, and then the plate was washed again. For the detection biotinylated monoclonal mouse anti-human brevican antibody was added to the wells and incubated for two hours. After additional washes, the plate was incubated with enhanced streptavidin-HRP for 30 min. Following further washes, the plate was incubated with TMB substrate in darkness for 30 min. The reaction was stopped by the addition of sulphuric acid and the absorbance was read in a Sunrise microplate absorbance reader (Tecan, Männedorf, Switzerland) at 450 nm with 650 nm as reference wavelength. A four-parameter logistic regression was used for standard curve-fitting analysis.

Further, another in-house ELISA assay targeting brevican, which uses in-house produced monoclonal mouse antibodies (synthetic peptide used for immunisation: aa 879 - 895, for both capture and detection antibodies), was established in CSF. The development of the assay involved the analysis of best antibody pairs, antibody dilutions, standard peptide dilutions, use of different detergents, tests of stability and parallelism. However, this assay requires much more CSF volume than the other in-house and commercially available brevican ELISAs. It is a big disadvantage of the assay, if the sample volume is a limitation. Thus, this assay was not utilised in the studies. However, the in-house produced antibodies were used in the analysis of brevican fragment patterns (sections 4.5 and 5.1; **paper II**).

Table 9. Summary of ELISAs used in the studies.

	Brevican (commercial assay)	Brevican (in-house assay)	Neurocan	TNC	TNR
Capture antibody	Monoclonal mouse IgG anti-brevican (immunogen: aa 23-911)	Monoclonal mouse IgG anti-brevican (immunogen: aa 23-911)	Polyclonal sheep IgG anti-neurocan (immunogen: aa 23-1321)	Monoclonal rat IgG anti-TNC (immunogen: aa 186-625)	Polyclonal goat IgG anti-TNR (immunogen: aa 34-1358)
Detection antibody	Polyclonal sheep IgG anti-brevican (immunogen: aa 23-911)	Monoclonal mouse IgG anti-brevican (immunogen: aa 23-911)	Polyclonal sheep IgG anti-neurocan (immunogen: aa 23-1321)	Polyclonal goat IgG anti-TNC (immunogen: aa 186-625)	Polyclonal goat IgG anti-TNR (immunogen: aa 34-1358)
Calibrator	Recombinant brevican protein (aa 23-911) 0.041-10 ng/mL	Recombinant brevican protein (aa 23-911) 0.08-5 ng/mL	Recombinant neurocan protein (aa 23-1321) 0.41-40 ng/mL	Recombinant TNC protein (aa 23-625) 2.5-600 pg/mL	Recombinant TNR protein (aa 34-1358) 0.2-50 ng/mL
CSF dilution	1:400	1:4	1:10	1:2	1:2
Serum dilution	1:2	Not detectable	1:2	1:500	Not detectable
Paper	**I** (CSF) **VI** (CSF) **VII** (CSF)	**I** (CSF)	**I** (CSF, serum) **VI** (CSF) **VII** (CSF)	**I** (CSF, serum) **VI** (CSF)	**I** (CSF) **VI** (CSF)

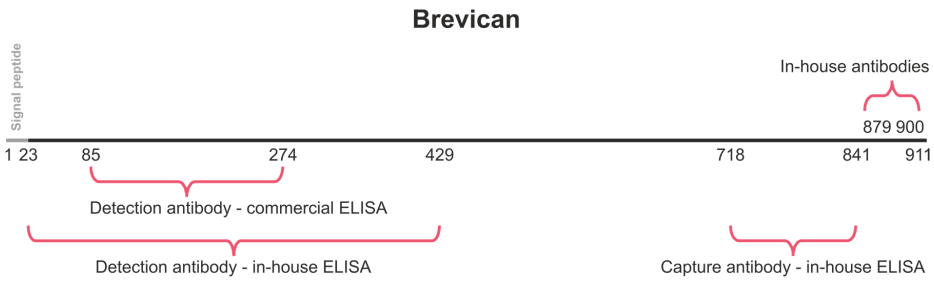

Fig. 24. Binding sites of the brevican-targeting antibodies.

4.2 Fluorescent immunoassays targeting MMPs

This method was used in **paper III** and **paper IV** to quantify various MMPs simultaneously within a single CSF sample. Here, commercially available Milliplex MAP Human MMP magnetic bead panels (EMD Millipore Corp., Billerica, MA, USA) were applied (Table 10).

Table 10. Investigated MMPs in **paper III** and **paper IV**.

MMP PANEL	Paper III	Paper IV
I: HMMP1MAG-55K	MMP-3, -12, -13	
II: HMMP2MAG-55K	MMP-1, -2, -7, -9, -10	MMP-1, -2, -9, -10

MMP-7 was excluded from the MMP panel I in **paper IV** due to its high variability in the previous study (**paper III**).

The analyses were performed according to the instructions from the manufacturer. The antibody information is proprietary by the company. In brief, calibrators and CSF samples, diluted 1:2 in PBS-T-based assay buffer, were incubated with a mixture of antibody-coated magnetic beads on the pre-washed 96-well plate for two hours. Next, washing procedure was performed with the PBS-T-based buffer using an automated magnetic plate washer. Then, a cocktail of biotinylated detection antibodies was added to the wells and incubated for one hour, followed by the addition of PE-conjugated streptavidin for 30 min. After subsequent washes of the plate, the beads were briefly resuspended on a plate shaker using delivery medium. The fluorescent intensities were read using a fluorescence imager (Luminex MAGPIX xMAP 200, Luminex Corp., Austin, TX, USA). A five-parameter logistic regression was used for standard curve-fitting analysis.

4.3 ECL immunoassay targeting TIMP-1

This method was used in **paper IV** to quantify TIMP-1 in human CSF. Here, a commercially available singleplex was applied (MSD Multi-Array, Meso Scale Discovery, Rockville, MD, USA).

The analyses were performed according to the instructions from the manufacturer. The 96-well plate was precoated with mouse monoclonal capture antibody raised against the whole TIMP-1 protein. CSF samples, 1:36 diluted in PBS-T-based buffer, and calibrators (a full-length recombinant TIMP-1 protein) were all further diluted 1:2 in PBS-T-based buffer on a plate, and incubated for two hours. After subsequent washes with PBS-T, the plate was incubated for another two hours with sulfo-tag-labelled polyclonal goat detection antibody also raised against whole TIMP-1 protein. Following another washing step, the samples were dispensed with Tris-based buffer immediately prior to reading with a QUICKPLEX SQ 120 reader (Meso Scale Discovery, Rockville, MD, USA). A four-parameter logistic regression was used for standard curve-fitting analysis.

4.4 ADAMTS-like enzymatic activity

The FRET method was used in **paper II** to identify ADAMTS-like enzymatic activity in CSF. The synthetic quenched FRET peptide (Bachem, Bubendorf, Switzerland) contained a brevican sequence with the ADAMTS cleavage site at ^{400}E/S^{401} and five amino acids before and after the cleavage site (Fig. 25). The FRET peptide incorporates the donor (2-aminobenzoyl (Abz)) at one end and the acceptor (2,4-dinitrophenyl (Dnp) coupled to the ε-NH_2 of a lysine) on the other end of the peptide.

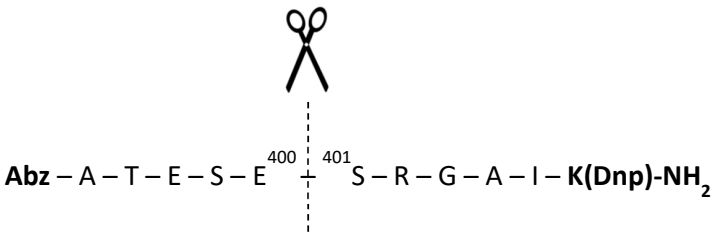

Fig. 25. FRET brevican peptide containing the ADAMTS cleavage site and Abz/Dnp donor/acceptor pair.

The detailed assay description can be found in **paper II**. In brief, in each well of a black 96-well microplate the quenched FRET peptide and 1:2 prediluted CSF were mixed in equal proportions. In addition, the following controls were separately placed on the plate: assay buffer or 1:2 diluted quenched FRET peptide, or 1:4 diluted CSF quality control sample. On top of the surface of all the samples, mineral oil was added to prevent evaporation. The developing fluorescence was recorded overnight at 37 °C on a Spectramax Gemini XPS microplate reader (Molecular Devices, San Jose, CA, USA) using excitation wavelength of 320 nm and emission wavelength of 420 nm. The slope values of quenched FRET peptide and CSF quality control sample were subtracted from the slope values of the study samples.

4.5 Explorative MS-based analyses of brevican

Explorative MS-based analyses were performed to identify ADAMTS-derived brevican peptides in CSF (**paper II**) and to evaluate the brevican fragment pattern in CSF (**papers II** and **paper V**).

In both approaches, IP was used to purify brevican, either from CSF or from recombinant brevican standard solution (R&D, Minneapolis, MN, USA). This was followed by either Asp-N or trypsin digestion, or no enzymatic digestion. Such prepared samples were then analysed by reversed phase nanoflow LC-MS using a Dionex 3000 LC system coupled to a Q Exactive hybrid quadrupole-orbitrap high resolution mass spectrometer with ESI (both Thermo Fisher Scientific). See **paper II** and **paper V** for details.

Briefly, N- or C- terminal anti-brevican antibodies (US Biological Life Science, Salem, MA, USA), or C-terminally directed in-house anti-brevican antibodies were all separately incubated with magnetic beads for one hour. The remaining unbound antibody was removed by washing with PBS-based buffer. To each antibody-conjugated bead suspensions, either CSF pool or recombinant full-length brevican standard (R&D, Minneapolis, MN, USA) were added and incubated for one hour. A KingFisher magnetic particle processor (Thermo Fisher Scientific) was used to perform several washing steps and subsequently elute the brevican from the beads. The collected eluate was dried down in a vacuum centrifuge.

Samples intended for evaluation of endogenous brevican fragments were stored at -20 °C pending LC-MS analysis, while samples intended to study digested brevican peptides were reconstituted in ammonium bicarbonate solution, followed by reduction with dithiothreitol at 60 °C and alkylation with iodoacetamide in darkness at room temperature. Next, the samples were digested with either Asp-N or trypsin overnight at 37 °C. Digestion was stopped with formic acid and the digests were dried down in a vacuum centrifuge, and stored at -20 °C pending analysis.

Both digested and non-digested samples were reconstituted in a formic acid/acetonitrile-based solution and loaded on a trap column. The separation was performed by reversed phase nanoflow LC with a linear gradient. The mass spectrometer was operated in data dependent mode, acquiring both full mass spectra (MS) and tandem mass spectra (MS/MS). Database searches of the LC-MS/MS spectra were performed using Mascot Distiller and Mascot search engine (Matrix Science) against a custom-made database containing the sequences of the ECM proteins of interest.

Table 11. Summary of explorative analyses of brevican

Paper	Antibody	CSF	Brevican standard	Digestion	To study
II	N-terminal	965 µL	-	Asp-N	ADAMTS-derived brevican peptides
II	In-house	965 µL	-	-	endogenous C-terminal part of brevican
V	N-/C-terminal	965 µL	or 400 ng	-/trypsin	fragment patterns of brevican

4.6 MS-based brevican/neurocan panel

This panel was developed to quantify several brevican and neurocan peptides simultaneously in a single CSF sample (**papers II, IV** and **V**). The detailed description of the panel together with the validation can be found in **paper V**.

Briefly, 20 isotope-labelled tryptic peptides, nine brevican (Fig. 26) and 11 neurocan (Fig. 27), labelled with both ^{13}C and ^{15}N at the C-terminal arginine or lysine (JPT Peptide Technologies, Berlin, Germany) were used as IS for MS-based quantification. The IS mixture of all 20 peptides was spiked into either 25 µL (**paper II**) or 100 µL (**paper IV and paper V**) of CSF, followed by reduction with dithiothreitol at 60 °C and alkylation with iodoacetamide in darkness at room temperature. Next, samples were digested with trypsin/Lys-C mix overnight at 37 °C and the reaction was stopped with trifluoroacetic acid. Sample clean-up was performed using SPE with Oasis HLB 96-well plates. The collected eluate was dried down in a vacuum centrifuge. The samples were reconstituted in ammonium bicarbonate prior to LC-MS analysis. The separation was performed by reversed phase microflow LC with an adjusted, broken gradient using a Vanquish UHPLC (Thermo Fisher Scientific). PRM MS analysis was performed using a Q Exactive hybrid quadrupole-orbitrap high resolution mass spectrometer with ESI (Thermo Fisher Scientific), operated as described previously [208]. Skyline software [310] was used to measure the areas of endogenous and IS peptides, and to calculate CSF concentrations of tryptic peptides by multiplying the endogenous-to-IS ratios of the summed fragment peak areas by the known concentration of the corresponding IS.

Method development involved the adjustment of LC gradient, optimisation of collision energies for each peptide and verification of peptide transitions.

Validation of the panel showed overall good dilution linearity of the IS peptides when spiked into CSF, and stability of the majority of the peptides in CSF at different temperature conditions and storage periods, and up to five freeze-thaw cycles.

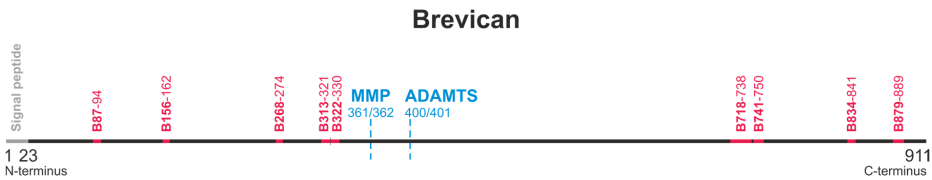

Fig. 26. The brevican peptides measured in the MS-based panel along the protein core.

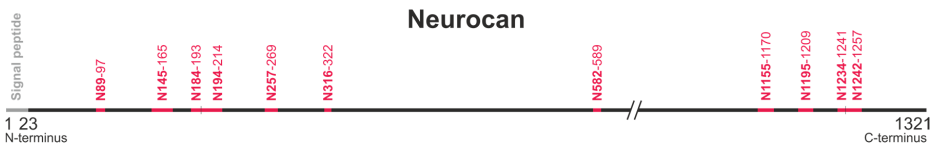

Fig. 27. The neurocan peptides measured in the MS-based panel along the protein core.

Table 12. The amino acid position and sequence of the brevican and neurocan peptides used in the MS-based panel.

Name	Position	Sequence
B87	87-94	EAEVLVAR
B156	156-162	GVVFLYR
B268	268-274	LTLEEAR
B313	313-321	YPIVTPSQR
B322	322-330	CGGGLPGVK
B718	718-738	MYGAHLASISTPEEQDFINNR
B741	741-750	EYQWIGLNDR
B834	834-841	YEVDTVLR
B879	879-889	ALHPEEDPEGR
N89	89-97	QDLPILVAK
N145	145-165	GIEDEQDLVPLEVTGVVFHYR
N184	184-193	LSSAIIAAPR
N194	194-214	HLQAAFEDGFDNCDAGWLSDR
N257	257-269	ELGGEVFYVGPAR
N316	316-322	YPIQTPR
N582	582-589	APVLELEK
N1155	1155-1170	DFQWTDNTGLQFENWR
N1195	1195-1209	WNDVPCNYNLPYVCK
N1234	1234-1241	YNVHATVR
N1242	1242-1257	YQCNEGFAQHHVATIR

Underlined C (C) indicates carbamidomethylation on cysteine.
The name of the peptides refers to the first letter of the protein (B for brevican, N for neurocan) followed by first amino acid position of the peptide.

4.7 Statistical analyses

The Kolmogorov-Smirnov test was used to determine normality of the data. If the original data was skewed and did not follow the assumption of normality for a parametric statistical test, the data was logarithmically transformed to conform to normality.

The differences between the two independent groups were investigated using Mann-Whitney U test. To accommodate more than two groups, Kruskal-Wallis test followed by Dunn's multiple comparison post-hoc test were applied. These tests or Chi-square test were used to evaluate if the independent study groups were age- or gender-matched, respectively.

Analysis of covariance was used to examine the differences between the two independent groups, taking into account the influence of age (set as covariate).

Friedman test followed by Dunn's multiple comparison post-hoc test were used to test for differences between multiple dependent study groups.

Linear mixed effects model was used to analyse the differences between the longitudinal measurements. In the model, the measured analyte was set as dependent variable, time point as fixed factor, individuals as random factors and age/gender as covariates. The Akaike information criterion (AIC) was used to evaluate the overall model fit, where lower AIC value indicated a better-fit model.

The receiver operating characteristic curve analysis was used to display the capacity of measured analyte to separate the two independent groups at the point that maximised the Youden's index (sensitivity + specificity-1). Areas under the curve (AUC) together with sensitivities and specificities were obtained as measures of performance for the tests.

The effect size measurements between the two independent groups were performed either by using Cohen's d (η) or by AUC, while effect size between the time points in longitudinal measures was tested by partial eta squared (η_p^2).

Correlations between non-normally distributed data were investigated using Spearman's rho (Spearman's rank correlation coefficient).

All tests were two-sided and the probability of $p \leq 0.05$ was considered statistically significant, unless the p-value was adjusted using Bonferroni correction for multiple comparisons.

Statistical analyses were performed using GraphPad Prism (GraphPad Software, Inc., San Diego, CA, USA) and SPSS software (IBM Corp., Armonk, NY, USA).

5 RESULTS AND DISCUSSION

5.1 Characterisation of brevican fragment patterns in CSF

In the explorative IP-MS analysis of CSF, I used two different brevican antibodies (US Biological Life Sciences, Salem, MA, USA), one targeting the N-terminal part (detected peptides cover aa 23 - 429) and another directed to the C-terminal part (detected peptides cover aa 718 - 841) (Fig. 28 A). Full-length brevican standard was used as a positive control and IP-MS analysis resulted in the detection of peptides along the whole brevican sequence (detected peptides cover aa 23 - 892), using either N- or C-terminal brevican antibodies (Fig. 28 B). This indicates the presence of at least two separate brevican sets in CSF, one including the N-terminal part and one the C-terminal part of the protein. The observation that the most C-terminal peptide (aa 879 - 889) included in the MS-based panel was seen in IP-MS analysis of full-length brevican standard, but not in CSF, reveals the presence of a third brevican set in CSF, the most C-terminal part of brevican. An additional IP-MS analysis using C-terminally directed in-house produced antibodies indeed revealed the presence of endogenous fragments in CSF at the very C-terminal end of brevican (aa 879 - 900) (Fig. 28 A). Thus, there is a cleavage that occurs between aa 841 and 879. The three observed brevican sets in CSF indicate the presence of at least two endogenous cleavage sites.

There are three separate sets of endogenous brevican fragments, representing three distinct parts of the protein, in human CSF.

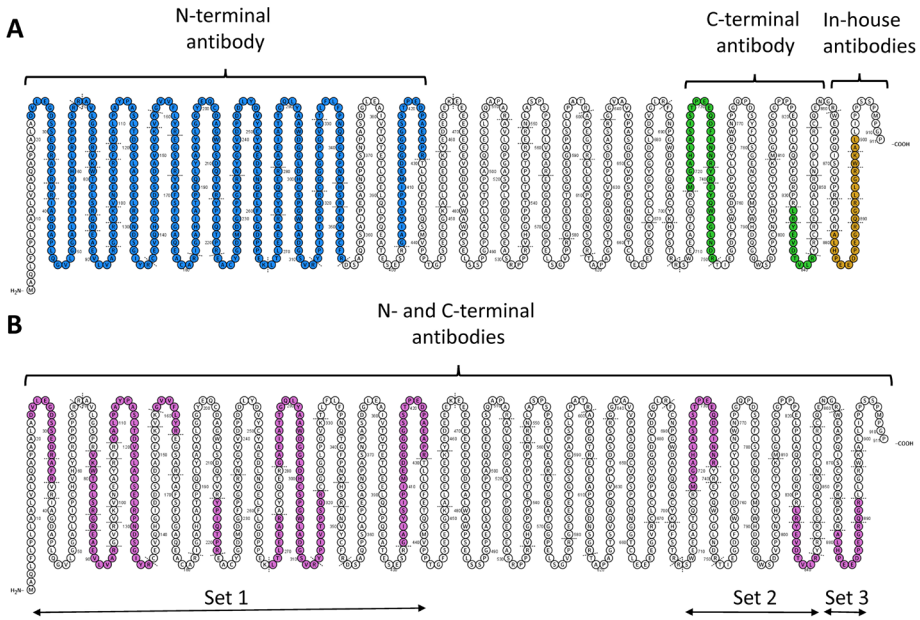

Fig. 28. Brevican peptides detected in IP-MS analysis of CSF (A) and full-length recombinant brevican standard (B) using two commercial brevican antibodies (N- and C-terminal) and two clones of in-house brevican antibodies.

5.2 ECM proteins in TBI and iNPH

5.2.1 CSF levels of brevican in TBI and iNPH

One of the most important findings of this thesis is that brevican can serve as a potential CSF biomarker for clinical outcome prediction following TBI. The results from **paper I** and **paper II** showed that the concentrations of CSF brevican are either significantly increased or showing a trend to be increased in unfavourable outcome following TBI (Fig. 29). Interestingly, the CSF brevican analysed by an in-house ELISA (**paper I**) and the two C-terminal brevican peptides measured by an MS-based panel (**paper II**) demonstrated comparable capacity for TBI outcome prediction as previously established brain injury markers, *i.e.*, NFL, S100B and NSE.

Brevican - a novel CSF marker for outcome prediction after TBI.

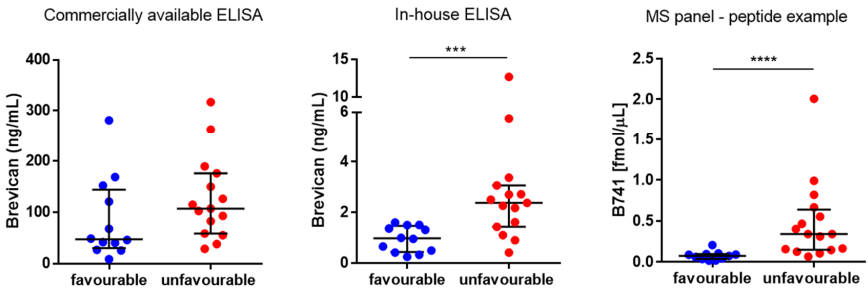

Fig. 29. CSF brevican levels between favourable and unfavourable outcomes of TBI patients.

Since brevican production is known to be increased following brain injury, its levels in CSF are likely to be elevated as CSF reflects biochemical changes in the brain. Although this assumption clarifies the observed raise of brevican in CSF for the unfavourable outcomes, it does not explain the even higher levels of brevican in iNPH patients who were included in the studies as a contrast group to TBI, due to inability of collecting ventricular CSF from healthy controls (Fig. 30).

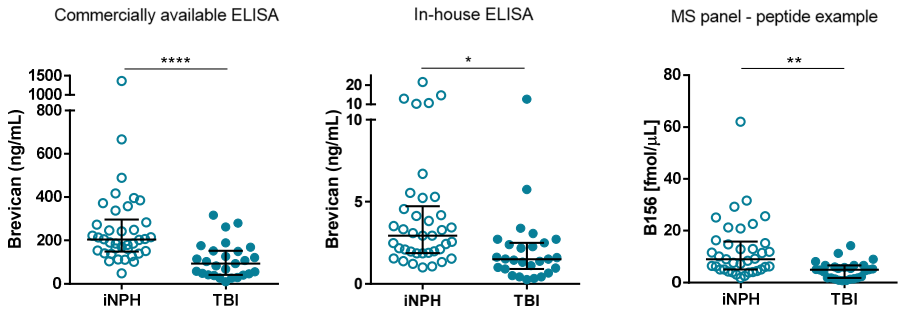

Fig. 30. CSF brevican levels for the iNPH and TBI (time point 1) groups.

There are several possible explanations for the observed discrepancy. First, iNPH does not necessary reflect homeostatic levels in healthy individuals as iNPH has shown increased GFAP levels in CSF [75, 76]. Thus, iNPH pathology involves astroglial activation, which in turn releases ECM proteins [183]. It cannot be ruled out that iNPH might reflect even more severe ECM pathology than TBI. Thus, TBI patients with favourable outcome could closer represent healthy individuals. In addition, it cannot be excluded that preanalytical factors might contribute to the observed contradiction, since the CSF iNPH and TBI samples were collected at different centers. A difference in sample handling might cause the possible bias. Finally, the lower CSF levels of ECM proteins in the TBI group, when compared with iNPH patients might be due to their increased proteolytic degradation, with potential aim to restore brain plasticity and stimulate axonal growth. This statement is supported by the results included in this thesis, where ADAMTS-like enzymatic activity (**paper II**) as well as the majority of MMP concentrations (**paper III**) are both higher in CSF in the TBI group compared with the iNPH group (Fig. 31).

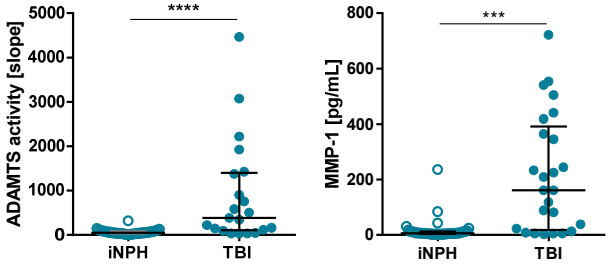

Fig. 31. CSF ADAMTS-like enzymatic activity and CSF MMP levels (example) for the iNPH and TBI (time point 1) groups.

In longitudinal data, the brevican concentrations are either significantly decreased or showed a trend to be decreased following TBI. This is likely an effect of clearance mechanisms triggered after elevated levels of brevican due to brain injury (Fig. 32).

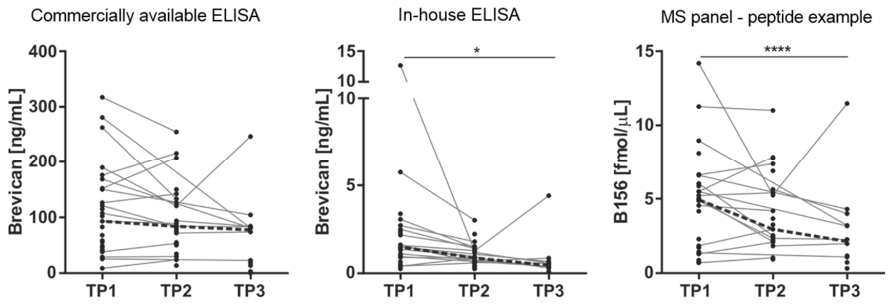

Fig. 32. CSF brevican longitudinal changes following TBI. TP =time point.

In **paper I**, the measurements of brevican in CSF showed slightly different dynamics between the commercially available and the in-house ELISAs. Moreover, the two assays moderately correlated with each other (rho=0.66) and showed differential association with other ECM proteins (Table 13). For instance, brevican levels measured by the in-house assay correlated to tenascins to a much stronger degree than brevican measured by the commercially available assay. However, the commercial assay showed a higher correlation with CSF neurocan levels compared with the in-house ELISA. Altogether, the two assays seem to detect different fragments of brevican, possibly related to distinct biological processes.

Table 13. Correlations of CSF brevican concentrations measured using two different ELISAs (commercial and in-house) with CSF concentrations of the other ECM proteins.

Spearman's rho	neurocan	TNC	TNR
Commercial assay	0.69****	0.52**	0.45*
In-house assay	0.34	0.87****	0.61****

The observed differences in CSF brevican dynamics between the two ELISAs (**paper I**) led to the further investigation of brevican proteolytic processing in TBI and iNPH (**paper II**), where an in-house developed MS-based panel was used, detecting nine brevican tryptic peptides (Fig. 33) (in addition to 11 neurocan tryptic peptides). The name of the peptides refers to the first letter of the protein (B for brevican) followed by the first amino acid position of the peptide.

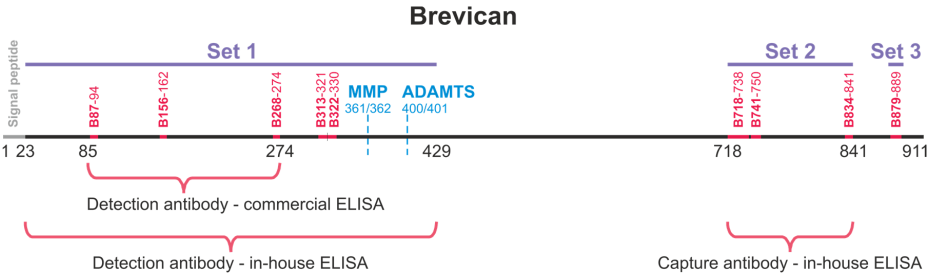

Fig. 33. Set 1 includes N-terminal brevican fragments in CSF recognised by detection antibodies from in-house ELISA (aa 23 - 429) and commercial ELISA (aa 85 - 274). Set 2 includes C-terminal brevican fragments detected by the capture antibody from in-house ELISA (aa 718 - 841). Set 3 includes the most C-terminal part, around aa 879. The brevican peptides measured in the MS-based panel are marked in red. The MMP and ADAMTS cleavage sites are marked in blue.

In **paper II**, the two C-terminal peptides in set 2 (B741, aa 741 - 750; and B834, aa 834 - 841) as well as the most C-terminal fragment/set 3 (B879, aa 879 - 889) showed different dynamics in TBI and iNPH compared with the N-terminal brevican set (Table 14). A possible explanation is that various brevican fragments reflect different pathological processes in TBI.

Table 14. The differences in CSF dynamics between the three brevican sets in TBI in relation to outcome, the contrast group (iNPH) and repeated observations. Arrows indicate increase, decrease or no change of CSF brevican peptide levels.

	CSF levels		
	Set 1	Set 2	Set 3
unfavourable outcome (compared with favourable)	↔	↑	↔
TBI (compared with iNPH)	↓	↔	↓
TP3 (compared with TP1)	↓	↔	↔

Based on the relative abundances (peak areas) of the tryptic peptides, the N-terminal peptides (set 1) and the most C-terminal peptide (set 3) are the most abundant in CSF. Interestingly, the CSF levels of B741 and B834 tryptic peptides (set 2) are lower for an unknown reason. As CSF levels of set 2 are distinctly lower in the favourable outcome group (Fig. 34), it cannot be excluded that this part of the protein is much less prone to exude into the CSF in healthy individuals, while it is more easily secreted into CSF under pathological conditions that are present in both the iNPH and the TBI groups. As opposed to the other brevican fragments, the two C-terminal peptides (set 2) correlated with CSF S100B concentrations indicating that they might be potential indicators for astroglial damage - a common pathology for iNPH and TBI. This possibly explains the equal CSF levels of B741 and B834 between these two groups. Another explanation might be that brevican set 2 is not vulnerable to proteolytic degradation by ADAMTS or MMP enzymes.

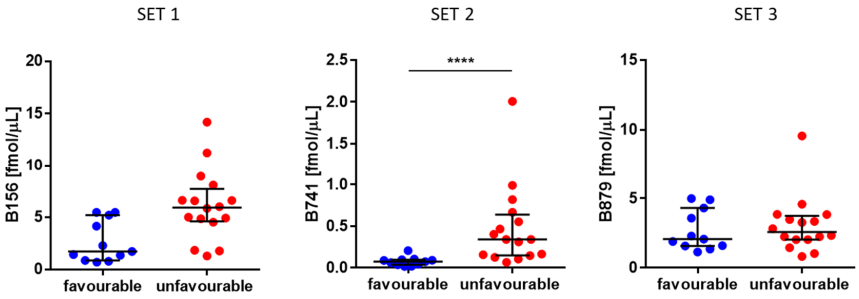

Fig. 34. CSF brevican peptide levels from the three different protein fragment sets in relation to outcome following TBI.

5.2.2 CSF and serum levels of neurocan in TBI and iNPH

Neurocan levels were studied in human body fluids using either the commercially available ELISA (unknown epitope, section 4.1) or an in-house developed MS-based panel that measures 11 neurocan tryptic peptides (section 4.6).

In contrast to brevican, neither CSF nor serum neurocan levels showed any significant discrepancy between the two outcomes following TBI (**paper I** and **paper II**) (Fig. 35).

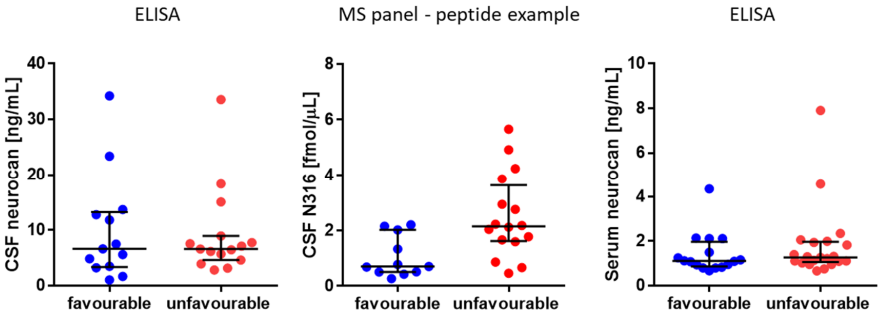

Fig. 35. CSF and serum neurocan levels for the two outcomes following TBI.

CSF neurocan levels measured by ELISA were significantly elevated in the iNPH group compared with TBI (**paper I**), while the neurocan peptides showed less conclusive results, but with a tendency to be higher in the contrast group (**paper II**) (Fig. 36).

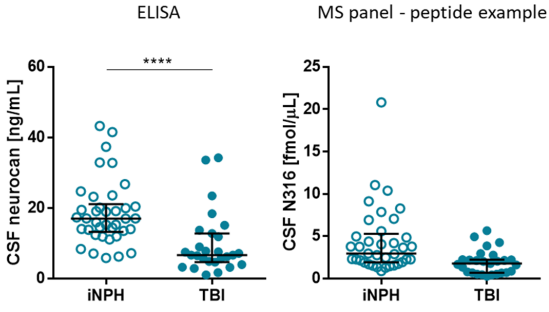

Fig. 36. CSF neurocan levels for the iNPH and TBI (time point 1) groups.

To study neurocan levels in serum, healthy controls were used as a comparison group to TBI. Here, neurocan levels were significantly decreased in TBI compared with the control group (Fig. 37). Similarly to brevican, the lower levels of neurocan in the TBI group might be explained by the more extensive degradation by ADAMTS/MMPs enzymes.

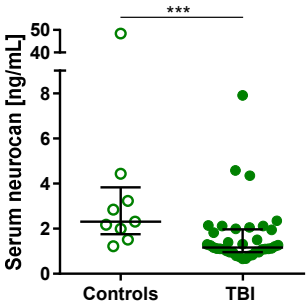

Fig. 37. Serum neurocan levels for healthy controls and TBI (time point 1).

The CSF and serum concentrations of neurocan were either significantly decreased or unchanged following brain injury (**paper I** and **paper II**) (Fig. 38).

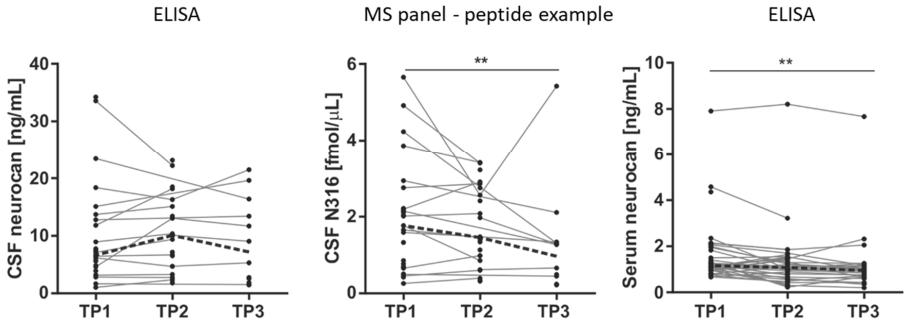

Fig. 38. CSF and serum neurocan longitudinal changes following TBI. TP =time point.

In contrast to brevican, all neurocan peptides showed similar dynamics following TBI and they highly correlated with each other (**paper II**), indicating that there is no evident disease related proteolytic processing of neurocan.

As CSF brevican and neurocan concentrations only moderately correlate with each other (**paper I** and **paper II**), it is possible that neurocan reflects different pathological processes than brevican.

5.2.3 CSF and serum levels of tenascins in TBI and iNPH

The results from **paper I** showed that CSF TNC and TNR concentrations were significantly increased in unfavourable outcome following TBI (Fig. 39). The prediction value was similar to currently known biomarkers of brain injury, *i.e.*, NFL, NSE and S100B.

Tenascins - novel CSF markers for outcome prediction after TBI.

However, there were no differences in serum TNC concentrations in relation to TBI outcome (Fig. 39).

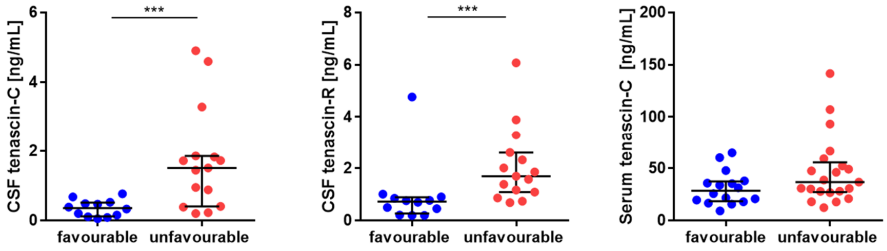

Fig. 39. CSF and serum tenascin concentrations for the two TBI outcomes.

CSF TNC and TNR concentrations did not differ between the TBI (time point 1) and the iNPH groups. However, serum TNC concentrations were higher in TBI than in healthy controls (Fig. 40), which could be explained by release of TNC from peripheral tissues, including muscle, to serum.

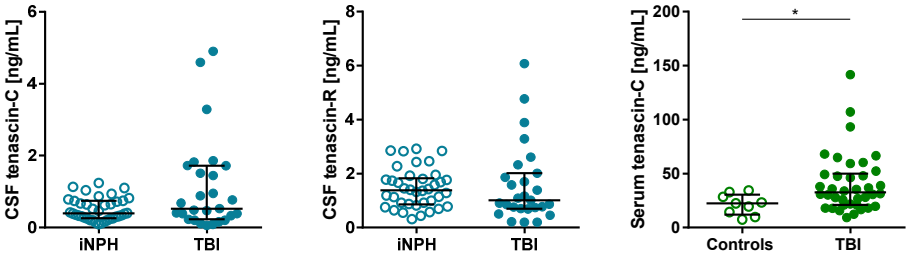

Fig. 40. CSF and serum tenascin concentrations for the TBI (time point 1) and iNPH or control groups.

Although CSF TNC concentrations did not differ between the longitudinal data following TBI, the CSF TNR concentrations showed a gradual decrease (Fig. 41).

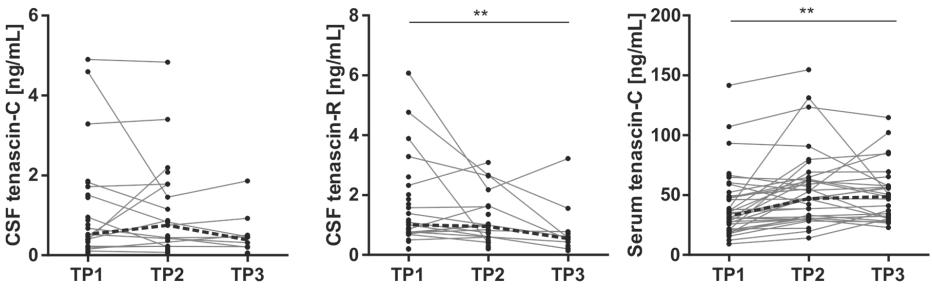

Fig. 41. CSF and serum tenascin longitudinal changes following TBI. TP =time point.

TNC is not CNS-specific as opposed to brevican, neurocan and TNR.

The commonly seen decrease of ECM proteins following TBI can be explained by clearance mechanisms after an injury-induced initial increase. However, serum TNC shows opposite dynamics - its levels increase with time after a brain injury (Fig. 41). This might be explained by the origin of this analyte in the periphery rather than the CNS, as opposed to CNS-specific brevican, neurocan and TNR. One can speculate that injury to the muscles during TBI could cause a release of TNC from the muscles to the blood, which possibly explains the increased concentrations of TNC in serum. This is supported by higher TNC concentrations in serum compared with CSF and by a lack of correlation between these body fluids for TNC.

5.2.4 CSF levels of MMPs in TBI and iNPH

Paper III describes a variable pattern of changes in CSF concentrations of several MMPs in relation to TBI (see Table 15 for summary), which indicates that specific MMPs might serve different roles in TBI pathophysiology.

Individual MMPs show different dynamics in TBI.

Table 15. The differences in CSF dynamics between the MMPs in TBI in relation to outcome, the contrast group (iNPH) and repeated observations. Arrows indicate increase, decrease or no change of CSF MMP levels.

	MMP-1	MMP-2	MMP-3	MMP-9	MMP-10	MMP-12
unfavourable (vs favourable)	↔	↑	↔	↔	↑	↔
TBI (vs iNPH)	↑	↔	↑	↔	↑	↔
TP3 (vs TP1)	↓	↔	↓	↔	↓	↔

Increased CSF concentrations of MMP-2 and -10 are associated with unfavourable TBI outcome (Fig. 42), to a similar degree as currently known biomarkers of brain injury, *i.e.*, NSE and S100B. Analogous, but not significant, a trend was observed for MMP-1 and -3.

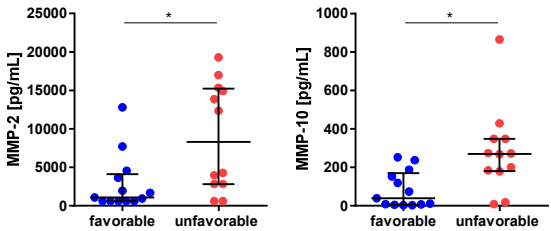

MMP-2 and MMP-10 are novel CSF markers for outcome prediction after TBI.

Fig. 42. CSF MMP levels for the two TBI outcomes.

CSF concentrations of MMP-1, -3 and -10 were increased in the TBI group compared with the iNPH group (Fig. 43), which may reflect axonal recovery and/or neuroplasticity after brain injury, while the rest of the studied MMPs (MMP-2, -9 and -12) did not differ between the two groups. This does not exclude that a change might have been detected in relation to a healthy control group.

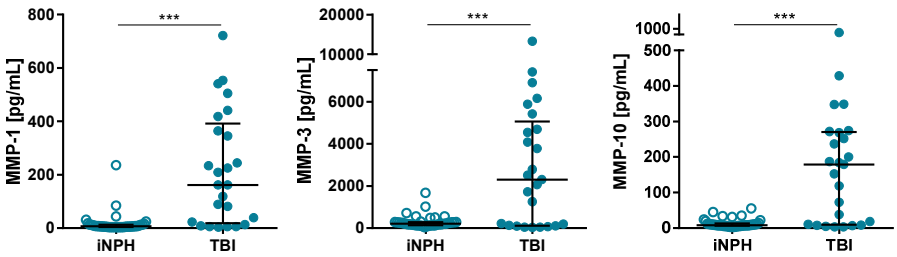

Fig. 43. CSF MMP levels for the iNPH and TBI (time point 1) groups.

CSF concentrations of MMP-1, -3 and -10 decreased with time after trauma (Fig. 44), likely due to clearance mechanisms after an injury-induced initial increase.

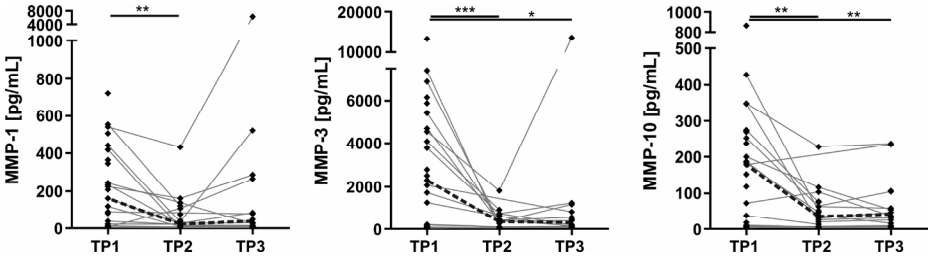

Fig. 44. CSF MMP longitudinal changes following TBI. TP =time point.

The apparent significant correlations between the MMP-1, -2, -3 and -10 (Fig. 45) indicate that they might be regulated in similar ways and/or exhibit related functions. Interestingly, these correlations are higher in TBI than in iNPH. Thus, this MMP group might measure similar physiological and/or pathological processes more specific to TBI.

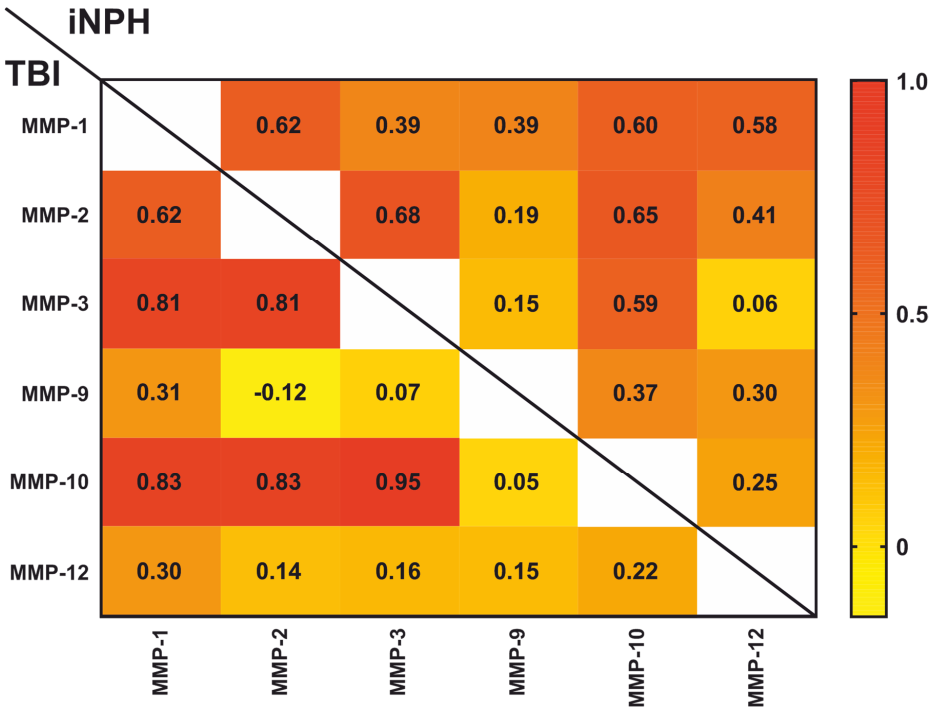

Fig. 45. Correlation matrix between CSF MMP concentrations in the TBI and iNPH groups.

5.2.5 ECM proteins in relation to shunt surgery in iNPH

Brevican and neurocan are not influenced by CSF origin.

The levels of the CNS-specific brevican and neurocan did not differ between lumbar and ventricular sources of CSF (Fig. 46). The majority of MMPs and TIMP-1 were elevated in lumbar CSF compared with ventricular CSF (Fig. 46), which could be explained by their diffusion from periphery to CSF along the spinal channel, as these proteins are widely expressed in multiple tissues. Interestingly, MMP-9 showed the opposite dynamics - its levels were decreased in lumbar CSF (Fig. 46). This observation is difficult to explain based on the current knowledge. However, since CSF MMP-9 levels did not correlate with CSF levels of other ECM proteins, this protease might reflect different pathological changes in iNPH.

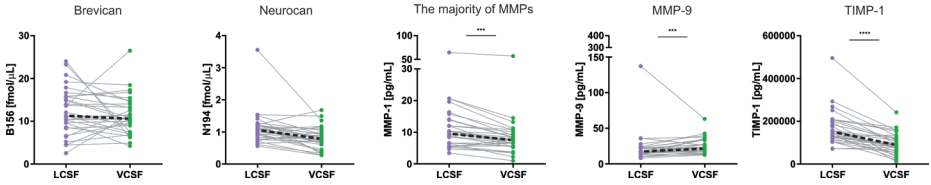

Fig. 46. Examples of brevican/neurocan peptides, MMP and TIMP-1 changes between pre-operative lumbar CSF (LCSF) and ventricular CSF (VCSF).

CSF ECM protein concentrations might reflect improved CSF dynamics following shunt surgery.

There was a general trend of CSF ECM protein levels to increase following shunt surgery, which could be explained by restitution CSF dynamics after the treatment procedure. This was seen in both sources of CSF, although the treatment-induced changes of MMPs/TIMP-1 were more evident in ventricular CSF (Fig. 47), possibly due to the contribution of their peripheral origin to lumbar CSF levels.

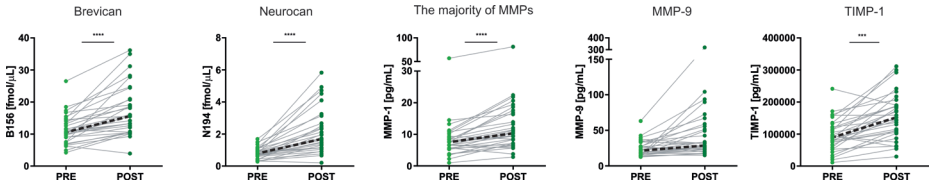

Fig. 47. Examples of brevican/neurocan peptides, MMP and TIMP-1 changes between preoperative (PRE) and postoperative (POST) ventricular CSF.

The CSF levels of brevican and neurocan peptides were increased in iNPH patients who suffered from cardiovascular comorbidities compared with those who did not exhibit such complications (Fig. 48). Thus, CSF brevican and neurocan peptide concentrations might serve as novel indicators for cardiovascular pathologies in iNPH.

CSF brevican and neurocan peptide concentrations are potential novel indicators for cardiovascular related CNS pathology in iNPH.

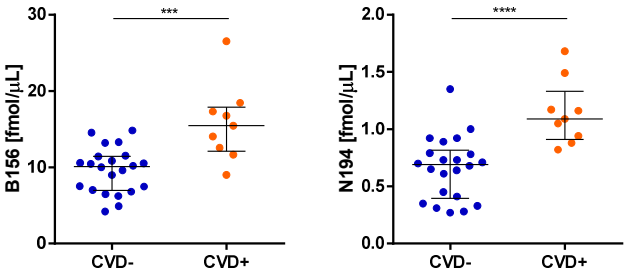

Fig. 48. Examples of ventricular preoperative CSF concentrations of brevican/neurocan peptides for patients who did (CVD+) or did not (CVD-) suffer from cardiovascular comorbidities.
CVD = cardiovascular disease

There was no association between the CSF ECM protein levels and the clinical improvement after shunt surgery. Thus, these proteins cannot serve as the outcome predictors following the treatment.

5.3 ECM proteins in AD and VaD

In **paper V**, brevican and neurocan proteolytic peptides were quantified in human CSF using an MS-based panel. The study involved two independent cohorts that both included AD and VaD patients, as well as healthy controls. Both cohorts showed similar results.

Several CSF brevican and neurocan peptide concentrations were decreased in the VaD group as compared with both AD patients and with healthy individuals (Fig. 48 shows examples of the peptide concentrations). The results could indicate an enhanced degradation of these two proteoglycans in VaD, which could be explained by increased CSF levels of MMPs, enzymes degrading proteoglycans, in VaD patients [159].

CSF brevican and neurocan peptide concentrations are potential novel diagnostic biomarkers to differentiate VaD from AD.

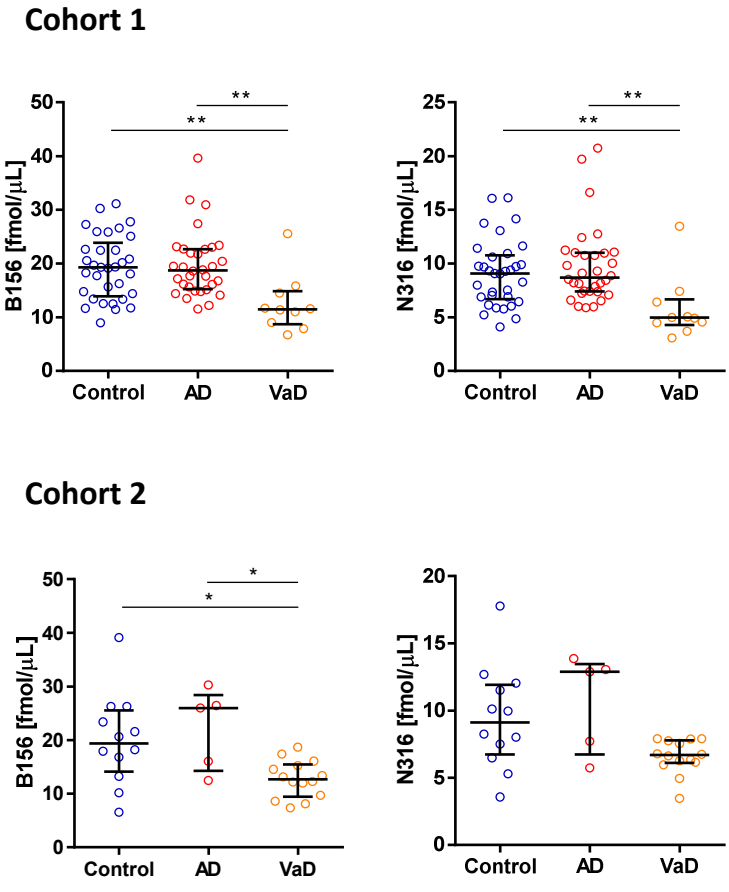

Fig. 48. Examples of CSF concentrations of brevican (B156) and neurocan (N316) peptides in both cohorts between the control, AD and VaD groups.

All the brevican and neurocan peptides correlated with each other in both control and AD groups (Fig. 49 A-B). However, in the VaD group (Fig. 49 C), the correlations between brevican fragments were much weaker, especially between the N-terminal and C-terminal part of the protein. In addition, neurocan peptides showed weaker correlations between each other in the VaD group, to a similar degree along the whole core protein. The weaker correlations among brevican or neurocan peptides in VaD compared with the AD/control groups indicate that the proteolytic processing of these proteoglycans is dysregulated in VaD and seems to be specific to this disease. Possibly, this results from an imbalance between the synthesis and degradation of different brevican/neurocan parts in VaD.

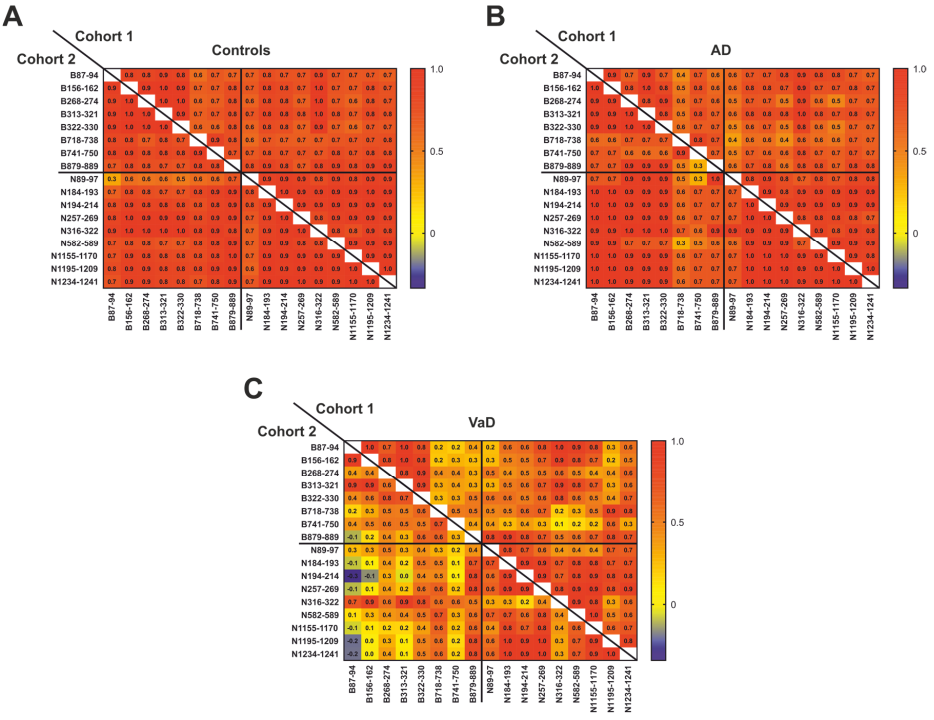

Fig. 49. Correlation matrices between CSF concentrations of brevican and neurocan peptides in the control (A), AD (B) and VaD (C) groups in both cohorts.

The CSF concentrations of brevican and neurocan peptides did not differ between AD patients and the control group (Fig. 48). Similarly, no differences were observed for these groups using a different methodology - commercially available ELISAs and a different cohort (**paper VI**) (Fig. 50).

In addition to brevican and neurocan, CSF concentrations of TNC and TNR were also not altered between the control and AD groups (Fig. 50).

Brevican, neurocan, TNC and TNR levels in CSF do not reflect AD -pathology.

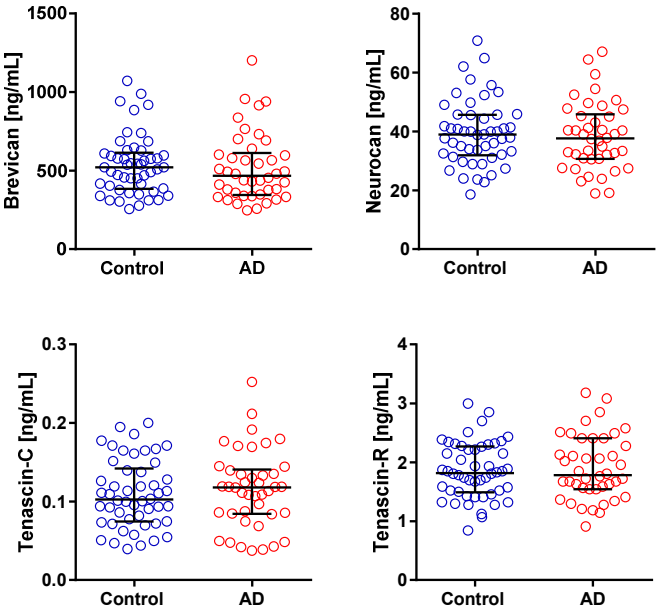

Fig. 50. CSF ECM protein concentrations for the control and AD groups.

Furthermore, CSF TNC and TNR concentrations were slightly higher in women than in men in the AD group (Fig. 51), but not in the control group. Since tenascins are involved in inflammatory processes [223], these results might reveal a sexual dimorphism in the CNS immunity during AD.

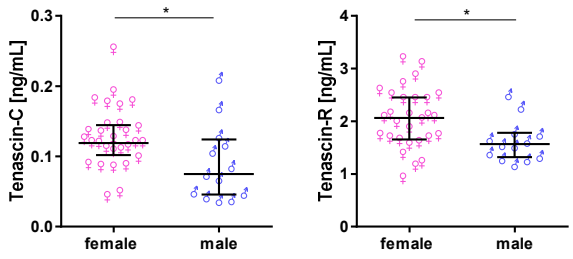

Fig. 51. CSF concentrations of tenascins for females and males in the AD group.

5.4 ECM proteins in RIBI

In **paper VII**, CSF brevican and neurocan concentrations showed a progressive decline over time following cranial radiotherapy in patients without brain metastases (Fig. 52). The lack of differences in longitudinal measures of patients with brain metastases indicates that the changes seen in patients without brain metastases reflect radiation effects, rather than tumour-induced damage. In support of this, there was no difference in the concentrations of ECM proteins between healthy controls and SCLC patients before cranial radiotherapy.

Brevican and neurocan progressive decline in CSF may represent long-term structural remodelling of the ECM after cranial radiotherapy.

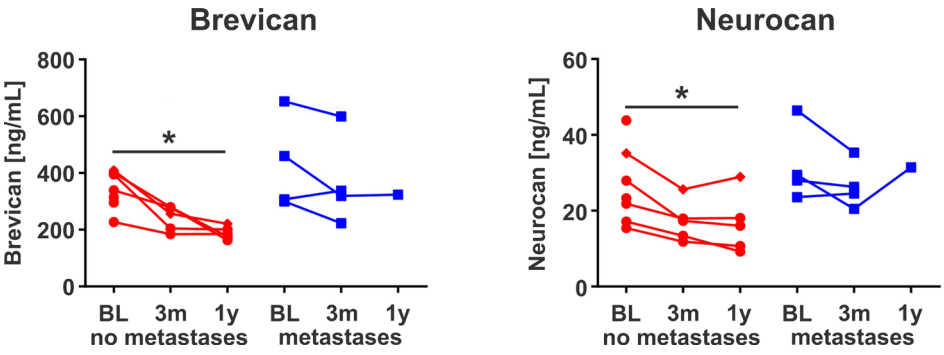

Fig. 52. Longitudinal changes of CSF brevican and neurocan after cranial radiotherapy given to SCLC patients.

This progressive decline of brevican and neurocan over the time of one year might represent a long-term structural remodelling of the brain ECM after cranial radiotherapy. It could be further explained by the upregulation of MMPs, that degrade proteoglycans, in the brain following cranial radiotherapy [311].

There was a strong correlation between the progressive decline of brevican and sAPPα (rho=0.92, $p<0.001$). The increase of both of these proteins in the brain has previously been established to be linked with an improved hippocampal-dependent learning [312, 313] and hippocampus is severely injured by irradiation [314, 315]. Thus, the observed correlation might be related to memory dysfunction in patients after cranial radiotherapy.

5.5 Summary

Table 16. Summary of the results.

Fluid	Analyte	HC	TBI	iNPH	AD	VaD	RIBI
CSF	**Brevican**	↔ vs AD ↑ vs VaD ↔ vs SCLC	↓ vs iNPH ↑ unfavourable ↓ post-injury	↑ vs TBI ↔ CSF origin ↑ post-surgery	↔ vs HC ↑ vs VaD	↓ vs HC ↓ vs AD	↓ post-PCI
	Neurocan	↔ vs AD ↑ vs VaD ↔ vs SCLC	↓ vs iNPH ↔ outcome ↓ post-injury	↑ vs TBI ↔ CSF origin ↑ post-surgery	↔ vs HC ↑ vs VaD	↓ vs HC ↓ vs AD	↓ post-PCI
	TNC	↔ vs AD	↔ vs iNPH ↑ unfavourable ↔ post-injury	↔ vs TBI	↔ vs HC ↑ females		
	TNR	↔ vs AD	↔ vs iNPH ↑ unfavourable ↓ post-injury	↔ vs TBI	↔ vs HC ↑ females		
	MMP-1		↑ vs iNPH ↔ outcome ↓ post-injury	↓ vs TBI ↑ lumbar CSF ↑ post-surgery			
	MMP-2		↔ vs iNPH ↑ unfavourable ↔ post-injury	↔ vs TBI ↑ lumbar CSF ↔ post-surgery			
	MMP-3		↑ vs iNPH ↔ outcome ↓ post-injury	↓ vs TBI			
	MMP-9		↔ vs iNPH ↔ outcome ↔ post-injury	↔ vs TBI ↑ ventricular CSF ↔ post-surgery			
	MMP-10		↑ vs iNPH ↑ unfavourable ↓ post-injury	↓ vs TBI ↑ lumbar CSF ↑ post-surgery			
	MMP-12		↔ as to iNPH ↔ outcome ↔ post-injury	↔ vs TBI			
	ADAMTS (activity)		↑ vs iNPH	↓ vs TB			
	TIMP-1			↑ lumbar CSF ↑ shunt-surgery			
Serum	**Neurocan**	↑ vs TBI	↓ vs HC ↔ outcome ↓ post-injury				
	TNC	↓ vs TBI	↑ vs HC ↔ outcome ↑ post-injury				

6 STUDY LIMITATIONS AND STRENGTHS

Evaluation of study limitations and strengths is important to judge the quality and the in-depth understanding of the further research.

CSF analysis was central for all the studies included in this thesis. Although the proximity of CSF to the brain tissue is relevant for exploring CNS pathology, it is important to point out that even though CSF is in close contact with the brain, protein levels in CSF do not necessarily reflect their dynamics in the brain. Thus, based only on CSF analysis, it is difficult to elucidate how the proteins are expressed or regulated in the brain. It is unclear whether a change in protein concentration in CSF is a result of a change in the brain's production and/or leakage from the brain tissue into the CSF. Access to ventricular CSF (**papers I-IV**) collected using the EVD procedure is very rare. It is believed that this type of CSF even closer reflects the pathological changes in the brain than lumbar CSF [3], which is affected by a larger influx of non CNS-specific proteins along the spine. However, it is practically impossible to collect ventricular CSF from healthy controls for ethical reasons. Instead, ventricular CSF collected from iNPH patients was used as a contrast group to TBI in **papers I-III**. It is not an ideal control group as iNPH does not reflect homeostatic levels in healthy individuals, *e.g.*, iNPH pathology involves astroglial activation that can be reflected in CSF by increased GFAP levels [75, 76].

Blood-based biomarkers are more attractive as they are more easily accessible and involve minimal complication risks compared with CSF. However, blood lacks direct contact with the brain and thus contains lower levels of brain-derived proteins and higher levels of CNS-unspecific proteins, making CSF a better source to evaluate CNS pathology. To compare the utility of these body fluids for a specific biomarker, often paired CSF and blood samples are collected at the same time and analysed in similar manner (**paper I**). None of the projects included studies on human brain tissue, which would more directly display brain protein alterations. However, since the aim of the projects presented in this thesis was to identify novel biomarkers for accurate disease diagnosis or outcome prediction, post-mortem brain tissue is not suitable for this type of research.

Due to the acuteness of TBI (**papers I-III**), it was difficult to strictly adhere to a sampling protocol, which resulted in numerous gaps in the follow-up measurements and CSF samples were not collected at the same time interval. More importantly, the longitudinal measurements were only up to 14 days, which is insufficient for long-term evaluation of biomarker dynamics. Such a longer follow-up of brain injury markers showed importance in a previous study, where serum NFL levels were increasing up to 12 days and then decreasing to control levels at 1 year [49]. Furthermore, the majority of the patients in this cohort suffered from severe TBI and thus it was difficult to evaluate the association of studied proteins in relation to trauma severity.

Longitudinal measures in AD studies (**papers V-VI**) are missing and thus, it was not possible to evaluate the dynamics of ECM proteins in the progression of this neurodegenerative disease. Interestingly, CSF neurocan levels have previously been shown to be increased in MCI, but not in AD, when compared with subjective cognitive decline (SCD) [207]. Although this might indicate that ECM changes are already evident at the MCI stage, the return of neurocan levels in the AD group towards the control (SCD) levels is difficult to interpret [207]. In the same study the MCI and AD groups involved different sets of individuals. I believe it would be more interesting to evaluate how the ECM protein levels change across the AD continuum for the same patients.

Another important limitation is small sample size (*e.g.*, n=9 for healthy controls in **paper I** and n=5 for AD patients, second cohort, in **paper V**). In these cases, it was difficult to perform any reliable statistics and effect size analysis is recommended instead, where the capacity of discrimination between the two groups is evaluated. The minimum recommended sample size sufficient to perform the statistical analysis with a meaningful result is 100 [316]. Although the studies included in this thesis involved less than 100 individuals per group, I believe that smaller sample sizes are still acceptable considering the exploratory nature of the studies.

Pre-analytical factors such as sampling, initial processing or storage conditions, might influence sample composition before analysis. To reduce discrepancies in sample treatment, case-control study samples preferably should be collected at the same centres. While this was the case for some of the studies, the others (**papers I-III**) included samples from control/contrast groups that were collected at different centres than the TBI cohort. The future solution for multicentre research projects is to standardise the pre-analytical factors in order to obtain consistent analytical quality.

In addition, it is important that the study populations are age- and gender-matched (which was a strength of **papers IV-VII**), and if they cannot be, for example, iNPH patients were approximately 10 years older than TBI patients (**papers I-III**), an adjustment is required. The fact that some of the ECM proteins correlate with age (*e.g.*, MMP-2, -3, -10 in **paper III**) further emphasizes the need to perform age-adjustment.

Due to the limited sample volume, samples were measured in singlicates or the analysis could not be performed, *e.g.*, brevican could not be analysed in serum (**paper I**).

Low abundance of certain proteins may exclude the possibility to perform desired measurements. Although tenascins showed promising results to differentiate between the TBI outcome groups (**paper I**), their levels in CSF were too low to include tenascins in the in-house developed MS-based panel (**paper II-V**). Brevican was the most studied ECM protein in this thesis both due to its relatively high abundance in CSF and promising outcomes from the studies. However, the limited prior research on brevican (and related ECM proteins), makes it difficult to lay a foundation for detailed understanding of their pathophysiological roles.

A methodological strength of some of the studies presented in this thesis is the ability to measure several analytes simultaneously in a single sample (MS-based panel in **papers II, IV** and **V**, and fluorescent multiplex immunoassays in **papers III-IV**).

All of the studies included well-characterised material with additional biomarker and clinical data, which allowed for performing a series of associations between the different variables to increase the understanding of the pathophysiological roles of the studied proteins.

The involvement of two (**paper V**) or more independent cohorts in a single study is important to demonstrate that the findings are reproducible, adding strength to the conclusions.

7 CONCLUSION AND FUTURE PERSPECTIVES

There are several currently known CSF and serum biomarker candidates for brain tissue injury, such as NFL, NSE and S100B [43-46, 48-51]. NFL and S100B also perform well for clinical outcome prediction following TBI [46-49, 52, 53]. Nevertheless, an improvement of TBI outcome assessments would aid clinicians to further understand the patient's condition and proceed with the most suitable treatment. The current brain injury markers reflect either neuronal or astroglial damage. However, TBI involves multiple complex pathological processes, including ECM remodelling. The development of additional biomarkers would not only improve the accuracy of outcome prediction but could also elucidate different aspects of TBI pathophysiology. Here, it is shown that ECM proteins are promising novel biomarker candidates for TBI outcome prediction and could act as potential targets for therapeutic interventions. However, it is also possible that increased levels of ECM proteins in the human brain or body fluids are side effects of more complex processes in TBI, and therefore targeting them will not necessarily improve the outcome. Thus, further studies are needed to evaluate the role of ECM proteins and their proteolytic processing in the pathophysiology of TBI.

The studies of CSF ECM protein levels in this thesis revealed both surprising and mysterious results on iNPH pathophysiology. More specifically, iNPH might reflect even more severe ECM-related disease stages of the brain than TBI, possibly involving astroglial activation. However, more research is needed to improve the largely unknown function of ECM proteins in iNPH.

Members of the ECM protease families, such as MMPs, can play multiple, different biological roles. However, the complex network of cross-activations between various MMPs together with overlapping substrate recognition impede the full understanding of pathophysiological functions of individual MMPs. Here, it is shown that there is also a large unexplored variability in the dynamic changes among different MMPs in TBI and iNPH, suggesting that individual MMPs have different roles in these pathologies. I believe that a deeper understanding of the diverse MMP functions in different pathologies must be attained to uncover novel targets offering therapeutic opportunities for many diseases. Attention must be given to target specific individual MMPs and to time the therapy correctly, given that the ECM undergoes active remodelling.

The more apparent differentiation of VaD from AD is of a great importance to guide treatment decisions as the clinical care for these diseases differs. The overlap of clinical features between AD and VaD patients, in addition to mixed pathologies, makes the differential diagnosis challenging. Here, brevican and neurocan showed a potential as diagnostic CSF markers to distinguish between AD and VaD patients. These findings need to be replicated in a larger population to further evaluate their applicability.

Although PCI reduces the risk of brain metastasis incidence in SCLC patients, various neurologic side effects can be observed following the therapy [167]. Brevican and neurocan might reflect the long-term ECM remodelling after PCI. Further research is needed to evaluate if CSF brevican/neurocan levels can predict the radiation-mediated side effects and thereby assist in the identification of patients with an increased risk of complications prior to PCI so that the radiation dose, type or localization can be individualized, or if an alternative treatment should be considered.

In summary, the ECM is a dynamic and complex structure that triggers numerous biological activities. A better understanding of how the ECM components function and how they affect disease progression may contribute to improved diagnostics and potentially also to the development of new therapeutic strategies.

8 ACKNOWLEDGEMENTS

I would like to express my deepest gratitude to everybody who offered me help and support during this amazing scientific journey of my life. Without you, this work would not have been possible!

The greatest thank you to **Ulf Andreasson**, my main supervisor, who was extremely supporting over all these years, scientifically, personally and beer-ally ☺ Thank you for believing in me. You were always able to turn my achievements into a greater motivation and my mistakes into an opportunity to learn something new. You taught me how to become an independent and more mature scientist. I will truly miss our Friday meetings, full of stimulating discussions and your valuable advices. One of which, a "Julskinka" story, was a true guide through my PhD. Its moral is to never stop questioning and to not be afraid of having a diverse opinion.

Henrik Zetterberg, my co-supervisor, for sharing your extensive knowledge and innovative ideas. Your unlimited enthusiasm for science fuelled my motivation throughout the years. Thank you for introducing me to many collaborations and for helping me to broaden my future scientific community. You are one of the most inspiring scientists I have met! To sum up, it was GREAT! ☺

Kaj Blennow, my co-supervisor, for your excellent scientific guidance, valuable advice and constructive criticism. Thank you for your patience and important lessons for which I am extremely grateful. I have always felt privileged to be able to introduce myself as a member of Prof. Blennow's team. I was truly lucky to be under your wings and I cannot thank you enough.

Erik Portelius, my co-supervisor, for believing in me and letting me begin my career at the Neurochemistry Laboratory in Mölndal. Thank you for introducing me to MALDI and for all the personal and scientific tips of how to improve academic writing and how to speak with confidence. Along with brevican, thank you for trusting us! I hope we did not let you down ☺

Gunnar Brinkmalm, my mentor, for all your valuable advices and interesting discussions, and for being always available to answer my questions. Words cannnot express how much I appreciated it. It has been a privilege working with you and I will miss it the most! Thank you for all the laughs we had together, cheering me up with the Polish countryballs and for your huge support when my health disappointed me (although my ears will never forgive you for Behemoth…).

Bruno Becker, for contributing to fruitful scientific discussions and teaching me how to see things from different perspectives. In addition, thank you for helping me out in the TREM project.

Former and current proteomic section fellows: **Annika Öhrfelt**. **Ann Brinkmalm-Westman**, **Johan Gobom**, **Josef Pannee**, **Jörg Hanrieder**, **Katarina Tomazin**, **Kina Höglund**, **Kjell Johansson**, **Rahil Dahlén**, and all the highly skilled early career scientists: **Agathe Vrillon**, **Aitana Sogorb**, **Ajay Pradhan**, **Ambra Dreos**, **Andréa Benedet**, **Anniina Snellman**, **Barbara Gomez**, **Claudia Cicognola**, **Elena Camporesi**, **Eleni Gkanatsiou**, **Fani Pujol-Calderón**, **Hlin Kvartsberg**, **Jasmine Chebli**, **Joel Simrén**, **Johanna Nilsson**, **Juan Lantero Rodriguez**, **Junyue Ge**, **Karl Hansson**, **Katie Stringer**, **Laia Montoliu-Gaya**, **Marc Suárez-Calvet**, **Marianne Astrid von Euler Chelpin**, **Michael Schöll**, **Nicholas Ashton**, **Oliver Stange**, **Patrick Wehrli**, **Rakesh Banote**, **Srinivas Koutarapu** (best photographer ever!), **Thomas Karikari**, **Tobias Skillbäck**, **Tuğçe Munise Şatir**, for all work-related and unrelated discussions, and all the fun times we had together! A special thank you to **Simon Sjödin** and **Wojciech Michno**, my lab-brothers who were always there to pick me up when I was falling …after you finish laughing ☺

My co-authors, **Anders Wallin**, **Anna Jeppsson**, **Åsa Sandelius**, **Eric P. Thelin**, **Erik Fernström**, **Faiez Al Nimer**, **Fredrik Piehl**, **Jan Nyman**, **Johan Svensson**, **Marie Kalm, Mats Tullberg**, **Nicholas Cullen**, **Oskar Hansson**, **Per Johansson**, **Petronella Kettunen**, **Pontus Wasling**, **Shorena Janelidze**, for all the help and highly valuable contributions to the papers.

All former and present colleagues at the Clinical Neurochemistry Laboratory, thank you for your warm support. In particular: **Anders Elmgren**, for fixing my back problems by voluntary offering me your adjustable table (on condition that I will put a note on it ``Anders is the best``). **Annika Lekman** and **Staffan Persson**, for bearing our loud Friday meetings and for taking a good care of Ulf when I am not around. **Annika Lindkvist**, **Jennie Larsson**, **Karin Palm**, **Kerstin Andersson, Rita Persson** and **Sofia Rasch** for creating a productive and pleasant atmosphere in ELISA lab. **Ann-Charlotte Hansson**, **Bozena Jakubowicz-Zayer**, **Celia Hök Fröhlander**, **Maria Björkevik** and **Rose-Marie Fishman Grell**, for all the help with administrative and practical matters. **Celia** (again; a multitasker pro!), **Hanane Belhaj**, **Irina Nilsson** and **Ulrika Wallström**, for rummaging through the freezers to find all the hidden samples. **Charlotta Otter**, for keeping the lab up and running. **Emma Sjons** and **Frida Gustavsson**, for helping me aliquoting enormous amounts of BioFinder samples. **Gösta Karlsson**, for being my lab-MacGyver. **Irena Matecko-Burmann** and **Maria Olsson**, for producing recombinant peptides for my project. **Petra Bergström**, **Sandra Roselli** and other colleagues at the main Sahlgrenska, for introducing me to the cell lab. **Marcus Clarin** and **Ulrika Sjöbom**, for being great guides during my first weeks in the lab. **Marcus Nordén**, for being my freezer-hero. **Monica Malmberg** and **Lobna Almasalmeh**, for all your kindness and introduction to immunoassays.

My dearest friends, for all the good time we have together, filled with laughter and unforgettable memories: **Brad Ververs**, **Cyril Zanella**, **Ecehan Iskender**, **Gudný Tómasdóttir**, **Hanna Göthe**, **Katharina Köhn**, **Kati Sundström**, **Mariusz Gawrych**, **Natalia** and **Johen Ermann**, and **Siri Monland**. A special thank you to **Anna Marszałek**, for all the amazing illustrations in this thesis! **Daniel Jusys**, **Özgur Uzun** and **Sofia Wahlin**, for helping me to survive the first months in Sweden. For real, I wouldn't have made it without you! **Daphne Aldridge**, the best dance (and spa) partner ever, together with all the dance crew, for making me believing in myself, and for sharing the positive energy I needed to write this thesis! **Iwona Domańska**, for being there for me when I needed you the most. **Johanna Kaartinen**, for the best psychological evaluations ☺ **Fran Mantovani**, **Leo Bianchi**, **Marina Moreira** and **Sabrina Rossi**, for all your love and immeasurable hospitality. Leo, who told me to be mentioned at least twice, you are my absolute best friend, tamo junto! **Mathias Sauer**, for endowing my life with endless (frequently uncontrolled) laughter and for encouraging me to dream big. I am very lucky to have met you! **Natalia Zawierta**, for being my true loyal friend over many years who never let me do crazy stuff alone! ☺ **Olga Śliwakowska**, always standing by my side for over two decades!

My Swedish family, **Mari**, **Per**, **Emil**, **Jonas**, **Amanda**, for all your warm welcome and support.

My Polish family, including the best brother-in-law ever, **Andrzej**, for warmly welcoming me home, always! My beloved sister, **Dorotka**, for your positive energy and all the inspirational lessons you gave me. My dad, **Jerzy**, for introducing me to science and for always beliving in me. Although I cannot share my satisfaction with you right now, I wanted to acknowledge the most loving person I ever met, my biggest inspiration. My mum, **Krystyna**, for playing two roles of being a mother and a father for so many years, raising me as a strong and independent woman. Without your enormous support, I wouldn't be even close to where I am now.

My sötnos, **Jesper**, for your endless love, patience, understanding and encouragment throughout all these years. Having you in my life completes every part of me. I love you.

Last, but not the least, I would like to thank for all the patients, whom in giving the concent to the studies, made it possible. This work is dedicated to you. Furthermore, I would like to express my gratitude to **Adlerbetska Stipendiestiftelsen**, **Gun och Bertil Stohnes Stiftelse**, **Knut och Alice Wallenbergs Stiftelse**, **Rune och Ulla Amlövs Stiftelse**, **Stiftelsen för Gamla Tjänarinnor** and **Wilhem och Martina Lungrens Stiftelse**, for providing fundings for the projects.

9 BIBLIOGRAPHY

1. Telano LN, Baker S. Physiology, Cerebral Spinal Fluid (CSF). StatPearls. Treasure Island (FL)2020.
2. Engelhardt B, Sorokin L. The blood-brain and the blood-cerebrospinal fluid barriers: function and dysfunction. Semin Immunopathol. 2009;31(4):497-511.
3. Regeniter A, Kuhle J, Mehling M, Moller H, Wurster U, Freidank H, et al. A modern approach to CSF analysis: pathophysiology, clinical application, proof of concept and laboratory reporting. Clin Neurol Neurosurg. 2009;111(4):313-8.
4. Deisenhammer F. SF, Teunissen C., Tumani H. Cerebrospinal fluid in clinical neurology: Springer, Cham; 2015.
5. Vanderstichele H, Bibl M, Engelborghs S, Le Bastard N, Lewczuk P, Molinuevo JL, et al. Standardization of preanalytical aspects of cerebrospinal fluid biomarker testing for Alzheimer's disease diagnosis: a consensus paper from the Alzheimer's Biomarkers Standardization Initiative. Alzheimers Dement. 2012;8(1):65-73.
6. WHO. WHO International Programme on Chemical Safety Biomarkers in Risk Assessment: Validity and Validation 2001 [Available from: http://www.inchem.org/documents/ehc/ehc/ehc222.htm.
7. Zhang F, Chen JY. Data mining methods in Omics-based biomarker discovery. Methods Mol Biol. 2011;719:511-26.
8. Buckley JS, Salpeter SR. A Risk-Benefit Assessment of Dementia Medications: Systematic Review of the Evidence. Drugs Aging. 2015;32(6):453-67.
9. International AsD. World Alzheimer Report 2019: Attitudes to dementia 2019 [Available from: https://www.alz.co.uk/research/world-report-2019.
10. Petersen RC. Mild cognitive impairment as a diagnostic entity. J Intern Med. 2004;256(3):183-94.
11. Petersen RC, Smith GE, Waring SC, Ivnik RJ, Tangalos EG, Kokmen E. Mild cognitive impairment: clinical characterization and outcome. Arch Neurol. 1999;56(3):303-8.
12. Canevelli M, Grande G, Lacorte E, Quarchioni E, Cesari M, Mariani C, et al. Spontaneous Reversion of Mild Cognitive Impairment to Normal Cognition: A Systematic Review of Literature and Meta-Analysis. J Am Med Dir Assoc. 2016;17(10):943-8.
13. Dewan MC, Rattani A, Gupta S, Baticulon RE, Hung YC, Punchak M, et al. Estimating the global incidence of traumatic brain injury. J Neurosurg. 2018:1-18.
14. Acosta JA, Yang JC, Winchell RJ, Simons RK, Fortlage DA, Hollingsworth-Fridlund P, et al. Lethal injuries and time to death in a level I trauma center. J Am Coll Surg. 1998;186(5):528-33.
15. Hyder AA, Wunderlich CA, Puvanachandra P, Gururaj G, Kobusingye OC. The impact of traumatic brain injuries: a global perspective. NeuroRehabilitation. 2007;22(5):341-53.
16. Blennow K, Brody DL, Kochanek PM, Levin H, McKee A, Ribbers GM, et al. Traumatic brain injuries. Nat Rev Dis Primers. 2016;2:16084.
17. Georges A, Booker JG. Traumatic Brain Injury. StatPearls. Treasure Island (FL)2020.
18. Alzheimer's A. 2016 Alzheimer's disease facts and figures. Alzheimers Dement. 2016;12(4):459-509.
19. Gaetz M. The neurophysiology of brain injury. Clin Neurophysiol. 2004;115(1):4-18.
20. Sav A, Rotondo F, Syro LV, Serna CA, Kovacs K. Pituitary pathology in traumatic brain injury: a review. Pituitary. 2019;22(3):201-11.

21. Steiner LA, Andrews PJ. Monitoring the injured brain: ICP and CBF. Br J Anaesth. 2006;97(1):26-38.
22. Corsellis JA, Bruton CJ, Freeman-Browne D. The aftermath of boxing. Psychol Med. 1973;3(3):270-303.
23. Stein TD, Montenigro PH, Alvarez VE, Xia W, Crary JF, Tripodis Y, et al. Beta-amyloid deposition in chronic traumatic encephalopathy. Acta Neuropathol. 2015;130(1):21-34.
24. McKee AC, Gavett BE, Stern RA, Nowinski CJ, Cantu RC, Kowall NW, et al. TDP-43 proteinopathy and motor neuron disease in chronic traumatic encephalopathy. J Neuropathol Exp Neurol. 2010;69(9):918-29.
25. Zeng S, Jiang JX, Xu MH, Xu LS, Shen GJ, Zhang AQ, et al. Prognostic value of apolipoprotein E epsilon4 allele in patients with traumatic brain injury: a meta-analysis and meta-regression. Genet Test Mol Biomarkers. 2014;18(3):202-10.
26. Jordan BD, Relkin NR, Ravdin LD, Jacobs AR, Bennett A, Gandy S. Apolipoprotein E epsilon4 associated with chronic traumatic brain injury in boxing. JAMA. 1997;278(2):136-40.
27. Kutner KC, Erlanger DM, Tsai J, Jordan B, Relkin NR. Lower cognitive performance of older football players possessing apolipoprotein E epsilon4. Neurosurgery. 2000;47(3):651-7; discussion 7-8.
28. Teasdale G, Jennett B. Assessment of coma and impaired consciousness. A practical scale. Lancet. 1974;2(7872):81-4.
29. Management of Concussion/m TBIWG. VA/DoD Clinical Practice Guideline for Management of Concussion/Mild Traumatic Brain Injury. J Rehabil Res Dev. 2009;46(6):CP1-68.
30. Greenspan L, McLellan BA, Greig H. Abbreviated Injury Scale and Injury Severity Score: a scoring chart. J Trauma. 1985;25(1):60-4.
31. Marshall LF, Marshall SB, Klauber MR, Van Berkum Clark M, Eisenberg H, Jane JA, et al. The diagnosis of head injury requires a classification based on computed axial tomography. J Neurotrauma. 1992;9 Suppl 1:S287-92.
32. Maas AI, Hukkelhoven CW, Marshall LF, Steyerberg EW. Prediction of outcome in traumatic brain injury with computed tomographic characteristics: a comparison between the computed tomographic classification and combinations of computed tomographic predictors. Neurosurgery. 2005;57(6):1173-82; discussion -82.
33. Raj R, Siironen J, Skrifvars MB, Hernesniemi J, Kivisaari R. Predicting outcome in traumatic brain injury: development of a novel computerized tomography classification system (Helsinki computerized tomography score). Neurosurgery. 2014;75(6):632-46; discussion 46-7.
34. Nelson DW, Nystrom H, MacCallum RM, Thornquist B, Lilja A, Bellander BM, et al. Extended analysis of early computed tomography scans of traumatic brain injured patients and relations to outcome. J Neurotrauma. 2010;27(1):51-64.
35. Firsching R, Woischneck D, Klein S, Reissberg S, Dohring W, Peters B. Classification of severe head injury based on magnetic resonance imaging. Acta Neurochir (Wien). 2001;143(3):263-71.
36. Haydel MJ, Preston CA, Mills TJ, Luber S, Blaudeau E, DeBlieux PM. Indications for computed tomography in patients with minor head injury. N Engl J Med. 2000;343(2):100-5.
37. Stiell IG, Lesiuk H, Wells GA, McKnight RD, Brison R, Clement C, et al. The Canadian CT Head Rule Study for patients with minor head injury: rationale, objectives, and methodology for phase I (derivation). Ann Emerg Med. 2001;38(2):160-9.
38. Jennett B, Bond M. Assessment of outcome after severe brain damage. Lancet. 1975;1(7905):480-4.
39. Papa L, Robinson G, Oli M, Pineda J, Demery J, Brophy G, et al. Use of biomarkers for diagnosis and management of traumatic brain injury patients. Expert Opin Med Diagn. 2008;2(8):937-45.

40. Franz G, Beer R, Kampfl A, Engelhardt K, Schmutzhard E, Ulmer H, et al. Amyloid beta 1-42 and tau in cerebrospinal fluid after severe traumatic brain injury. Neurology. 2003;60(9):1457-61.
41. Zemlan FP, Jauch EC, Mulchahey JJ, Gabbita SP, Rosenberg WS, Speciale SG, et al. C-tau biomarker of neuronal damage in severe brain injured patients: association with elevated intracranial pressure and clinical outcome. Brain Res. 2002;947(1):131-9.
42. Ost M, Nylen K, Csajbok L, Ohrfelt AO, Tullberg M, Wikkelso C, et al. Initial CSF total tau correlates with 1-year outcome in patients with traumatic brain injury. Neurology. 2006;67(9):1600-4.
43. Zetterberg H, Hietala MA, Jonsson M, Andreasen N, Styrud E, Karlsson I, et al. Neurochemical aftermath of amateur boxing. Arch Neurol. 2006;63(9):1277-80.
44. Neselius S, Brisby H, Theodorsson A, Blennow K, Zetterberg H, Marcusson J. CSF-biomarkers in Olympic boxing: diagnosis and effects of repetitive head trauma. PLoS One. 2012;7(4):e33606.
45. Berger RP, Pierce MC, Wisniewski SR, Adelson PD, Clark RS, Ruppel RA, et al. Neuron-specific enolase and S100B in cerebrospinal fluid after severe traumatic brain injury in infants and children. Pediatrics. 2002;109(2):E31.
46. Goyal A, Failla MD, Niyonkuru C, Amin K, Fabio A, Berger RP, et al. S100b as a prognostic biomarker in outcome prediction for patients with severe traumatic brain injury. J Neurotrauma. 2013;30(11):946-57.
47. Pleines UE, Morganti-Kossmann MC, Rancan M, Joller H, Trentz O, Kossmann T. S-100 beta reflects the extent of injury and outcome, whereas neuronal specific enolase is a better indicator of neuroinflammation in patients with severe traumatic brain injury. J Neurotrauma. 2001;18(5):491-8.
48. Al Nimer F, Thelin E, Nystrom H, Dring AM, Svenningsson A, Piehl F, et al. Comparative Assessment of the Prognostic Value of Biomarkers in Traumatic Brain Injury Reveals an Independent Role for Serum Levels of Neurofilament Light. PLoS One. 2015;10(7):e0132177.
49. Shahim P, Gren M, Liman V, Andreasson U, Norgren N, Tegner Y, et al. Serum neurofilament light protein predicts clinical outcome in traumatic brain injury. Sci Rep. 2016;6:36791.
50. Thelin EP, Jeppsson E, Frostell A, Svensson M, Mondello S, Bellander BM, et al. Utility of neuron-specific enolase in traumatic brain injury; relations to S100B levels, outcome, and extracranial injury severity. Crit Care. 2016;20:285.
51. Vos PE, Jacobs B, Andriessen TM, Lamers KJ, Borm GF, Beems T, et al. GFAP and S100B are biomarkers of traumatic brain injury: an observational cohort study. Neurology. 2010;75(20):1786-93.
52. Thelin EP, Johannesson L, Nelson D, Bellander BM. S100B is an important outcome predictor in traumatic brain injury. J Neurotrauma. 2013;30(7):519-28.
53. Raabe A, Grolms C, Seifert V. Serum markers of brain damage and outcome prediction in patients after severe head injury. Br J Neurosurg. 1999;13(1):56-9.
54. McHugh GS, Engel DC, Butcher I, Steyerberg EW, Lu J, Mushkudiani N, et al. Prognostic value of secondary insults in traumatic brain injury: results from the IMPACT study. J Neurotrauma. 2007;24(2):287-93.
55. Cinalli G, Spennato P, Nastro A, Aliberti F, Trischitta V, Ruggiero C, et al. Hydrocephalus in aqueductal stenosis. Childs Nerv Syst. 2011;27(10):1621-42.
56. Hakim S, Adams RD. The special clinical problem of symptomatic hydrocephalus with normal cerebrospinal fluid pressure. Observations on cerebrospinal fluid hydrodynamics. J Neurol Sci. 1965;2(4):307-27.
57. Oliveira LM, Nitrini R, Roman GC. Normal-pressure hydrocephalus: A critical review. Dement Neuropsychol. 2019;13(2):133-43.

58. Ghosh S, Lippa C. Diagnosis and prognosis in idiopathic normal pressure hydrocephalus. Am J Alzheimers Dis Other Demen. 2014;29(7):583-9.
59. Relkin N, Marmarou A, Klinge P, Bergsneider M, Black PM. Diagnosing idiopathic normal-pressure hydrocephalus. Neurosurgery. 2005;57(3 Suppl):S4-16; discussion ii-v.
60. Jaraj D, Rabiei K, Marlow T, Jensen C, Skoog I, Wikkelso C. Prevalence of idiopathic normal-pressure hydrocephalus. Neurology. 2014;82(16):1449-54.
61. Andersson J, Rosell M, Kockum K, Lilja-Lund O, Soderstrom L, Laurell K. Prevalence of idiopathic normal pressure hydrocephalus: A prospective, population-based study. PLoS One. 2019;14(5):e0217705.
62. Kuriyama N, Miyajima M, Nakajima M, Kurosawa M, Fukushima W, Watanabe Y, et al. Nationwide hospital-based survey of idiopathic normal pressure hydrocephalus in Japan: Epidemiological and clinical characteristics. Brain Behav. 2017;7(3):e00635.
63. Reeves BC, Karimy JK, Kundishora AJ, Mestre H, Cerci HM, Matouk C, et al. Glymphatic System Impairment in Alzheimer's Disease and Idiopathic Normal Pressure Hydrocephalus. Trends Mol Med. 2020;26(3):285-95.
64. Hiraoka K, Meguro K, Mori E. Prevalence of idiopathic normal-pressure hydrocephalus in the elderly population of a Japanese rural community. Neurol Med Chir (Tokyo). 2008;48(5):197-99; discussion 9-200.
65. Israelsson H, Carlberg B, Wikkelso C, Laurell K, Kahlon B, Leijon G, et al. Vascular risk factors in INPH: A prospective case-control study (the INPH-CRasH study). Neurology. 2017;88(6):577-85.
66. Miyamoto J, Imahori Y, Mineura K. Cerebral oxygen metabolism in idiopathic-normal pressure hydrocephalus. Neurol Res. 2007;29(8):830-4.
67. Hamilton R, Patel S, Lee EB, Jackson EM, Lopinto J, Arnold SE, et al. Lack of shunt response in suspected idiopathic normal pressure hydrocephalus with Alzheimer disease pathology. Ann Neurol. 2010;68(4):535-40.
68. McGirr A, Cusimano MD. Familial aggregation of idiopathic normal pressure hydrocephalus: novel familial case and a family study of the NPH triad in an iNPH patient cohort. J Neurol Sci. 2012;321(1-2):82-8.
69. Huovinen J, Kastinen S, Komulainen S, Oinas M, Avellan C, Frantzen J, et al. Familial idiopathic normal pressure hydrocephalus. J Neurol Sci. 2016;368:11-8.
70. Yang Y, Tullberg M, Mehlig K, Rosengren A, Toren K, Zetterberg H, et al. The APOE Genotype in Idiopathic Normal Pressure Hydrocephalus. PLoS One. 2016;11(7):e0158985.
71. Krauss JK, Regel JP, Vach W, Droste DW, Borremans JJ, Mergner T. Vascular risk factors and arteriosclerotic disease in idiopathic normal-pressure hydrocephalus of the elderly. Stroke. 1996;27(1):24-9.
72. Hellstrom P, Klinge P, Tans J, Wikkelso C. A new scale for assessment of severity and outcome in iNPH. Acta Neurol Scand. 2012;126(4):229-37.
73. Picascia M, Zangaglia R, Bernini S, Minafra B, Sinforiani E, Pacchetti C. A review of cognitive impairment and differential diagnosis in idiopathic normal pressure hydrocephalus. Funct Neurol. 2015;30(4):217-28.
74. Jeppsson A, Zetterberg H, Blennow K, Wikkelso C. Idiopathic normal-pressure hydrocephalus: pathophysiology and diagnosis by CSF biomarkers. Neurology. 2013;80(15):1385-92.
75. Tullberg M, Rosengren L, Blomsterwall E, Karlsson JE, Wikkelso C. CSF neurofilament and glial fibrillary acidic protein in normal pressure hydrocephalus. Neurology. 1998;50(4):1122-7.
76. Albrechtsen M, Sorensen PS, Gjerris F, Bock E. High cerebrospinal fluid concentration of glial fibrillary acidic protein (GFAP) in patients with normal pressure hydrocephalus. J Neurol Sci. 1985;70(3):269-74.

77. Klinge P, Hellstrom P, Tans J, Wikkelso C, European i NPHMSG. One-year outcome in the European multicentre study on iNPH. Acta Neurol Scand. 2012;126(3):145-53.
78. Tullberg M, Jensen C, Ekholm S, Wikkelso C. Normal pressure hydrocephalus: vascular white matter changes on MR images must not exclude patients from shunt surgery. AJNR Am J Neuroradiol. 2001;22(9):1665-73.
79. Tullberg M, Hellstrom P, Piechnik SK, Starmark JE, Wikkelso C. Impaired wakefulness is associated with reduced anterior cingulate CBF in patients with normal pressure hydrocephalus. Acta Neurol Scand. 2004;110(5):322-30.
80. Tullberg M, Blennow K, Mansson JE, Fredman P, Tisell M, Wikkelso C. Cerebrospinal fluid markers before and after shunting in patients with secondary and idiopathic normal pressure hydrocephalus. Cerebrospinal Fluid Res. 2008;5:9.
81. Association As. 2020 Alzheimer's disease facts and figures. Alzheimers Dement. 2020.
82. Masters CL, Bateman R, Blennow K, Rowe CC, Sperling RA, Cummings JL. Alzheimer's disease. Nat Rev Dis Primers. 2015;1:15056.
83. Kukull WA, Higdon R, Bowen JD, McCormick WC, Teri L, Schellenberg GD, et al. Dementia and Alzheimer disease incidence: a prospective cohort study. Arch Neurol. 2002;59(11):1737-46.
84. Bekris LM, Yu CE, Bird TD, Tsuang DW. Genetics of Alzheimer disease. J Geriatr Psychiatry Neurol. 2010;23(4):213-27.
85. Alzheimer A, Stelzmann RA, Schnitzlein HN, Murtagh FR. An English translation of Alzheimer's 1907 paper, "Uber eine eigenartige Erkankung der Hirnrinde". Clin Anat. 1995;8(6):429-31.
86. Thal DR, Rub U, Orantes M, Braak H. Phases of A beta-deposition in the human brain and its relevance for the development of AD. Neurology. 2002;58(12):1791-800.
87. Braak H, Braak E. Neuropathological stageing of Alzheimer-related changes. Acta Neuropathol. 1991;82(4):239-59.
88. Blennow K, Bogdanovic N, Alafuzoff I, Ekman R, Davidsson P. Synaptic pathology in Alzheimer's disease: relation to severity of dementia, but not to senile plaques, neurofibrillary tangles, or the ApoE4 allele. J Neural Transm (Vienna). 1996;103(5):603-18.
89. Hardy JA, Higgins GA. Alzheimer's disease: the amyloid cascade hypothesis. Science. 1992;256(5054):184-5.
90. Wisniewski KE, Wisniewski HM, Wen GY. Occurrence of neuropathological changes and dementia of Alzheimer's disease in Down's syndrome. Ann Neurol. 1985;17(3):278-82.
91. Reitz C. Alzheimer's disease and the amyloid cascade hypothesis: a critical review. Int J Alzheimers Dis. 2012;2012:369808.
92. Akiyama H, Barger S, Barnum S, Bradt B, Bauer J, Cole GM, et al. Inflammation and Alzheimer's disease. Neurobiol Aging. 2000;21(3):383-421.
93. Markesbery WR. Oxidative stress hypothesis in Alzheimer's disease. Free Radic Biol Med. 1997;23(1):134-47.
94. Blennow K, de Leon MJ, Zetterberg H. Alzheimer's disease. Lancet. 2006;368(9533):387-403.
95. Poirier J, Davignon J, Bouthillier D, Kogan S, Bertrand P, Gauthier S. Apolipoprotein E polymorphism and Alzheimer's disease. Lancet. 1993;342(8873):697-9.
96. Corder EH, Saunders AM, Strittmatter WJ, Schmechel DE, Gaskell PC, Small GW, et al. Gene dose of apolipoprotein E type 4 allele and the risk of Alzheimer's disease in late onset families. Science. 1993;261(5123):921-3.
97. Holtzman DM, Herz J, Bu G. Apolipoprotein E and apolipoprotein E receptors: normal biology and roles in Alzheimer disease. Cold Spring Harb Perspect Med. 2012;2(3):a006312.

98. Bu G. Apolipoprotein E and its receptors in Alzheimer's disease: pathways, pathogenesis and therapy. Nat Rev Neurosci. 2009;10(5):333-44.
99. Liu CC, Liu CC, Kanekiyo T, Xu H, Bu G. Apolipoprotein E and Alzheimer disease: risk, mechanisms and therapy. Nat Rev Neurol. 2013;9(2):106-18.
100. Farrer LA, Cupples LA, Haines JL, Hyman B, Kukull WA, Mayeux R, et al. Effects of age, sex, and ethnicity on the association between apolipoprotein E genotype and Alzheimer disease. A meta-analysis. APOE and Alzheimer Disease Meta Analysis Consortium. JAMA. 1997;278(16):1349-56.
101. Norton S, Matthews FE, Barnes DE, Yaffe K, Brayne C. Potential for primary prevention of Alzheimer's disease: an analysis of population-based data. Lancet Neurol. 2014;13(8):788-94.
102. McKhann G, Drachman D, Folstein M, Katzman R, Price D, Stadlan EM. Clinical diagnosis of Alzheimer's disease: report of the NINCDS-ADRDA Work Group under the auspices of Department of Health and Human Services Task Force on Alzheimer's Disease. Neurology. 1984;34(7):939-44.
103. Dubois B, Feldman HH, Jacova C, Dekosky ST, Barberger-Gateau P, Cummings J, et al. Research criteria for the diagnosis of Alzheimer's disease: revising the NINCDS-ADRDA criteria. Lancet Neurol. 2007;6(8):734-46.
104. Dubois B, Feldman HH, Jacova C, Hampel H, Molinuevo JL, Blennow K, et al. Advancing research diagnostic criteria for Alzheimer's disease: the IWG-2 criteria. Lancet Neurol. 2014;13(6):614-29.
105. Jack CR, Jr., Bennett DA, Blennow K, Carrillo MC, Feldman HH, Frisoni GB, et al. A/T/N: An unbiased descriptive classification scheme for Alzheimer disease biomarkers. Neurology. 2016;87(5):539-47.
106. Jack CR, Jr., Bennett DA, Blennow K, Carrillo MC, Dunn B, Haeberlein SB, et al. NIA-AA Research Framework: Toward a biological definition of Alzheimer's disease. Alzheimers Dement. 2018;14(4):535-62.
107. Folstein MF, Folstein SE, McHugh PR. "Mini-mental state". A practical method for grading the cognitive state of patients for the clinician. J Psychiatr Res. 1975;12(3):189-98.
108. Monsch AU, Foldi NS, Ermini-Funfschilling DE, Berres M, Taylor KI, Seifritz E, et al. Improving the diagnostic accuracy of the Mini-Mental State Examination. Acta Neurol Scand. 1995;92(2):145-50.
109. Olsson B, Lautner R, Andreasson U, Ohrfelt A, Portelius E, Bjerke M, et al. CSF and blood biomarkers for the diagnosis of Alzheimer's disease: a systematic review and meta-analysis. Lancet Neurol. 2016;15(7):673-84.
110. Andreasen N, Hesse C, Davidsson P, Minthon L, Wallin A, Winblad B, et al. Cerebrospinal fluid beta-amyloid(1-42) in Alzheimer disease: differences between early- and late-onset Alzheimer disease and stability during the course of disease. Arch Neurol. 1999;56(6):673-80.
111. Baldeiras I, Santana I, Leitao MJ, Gens H, Pascoal R, Tabuas-Pereira M, et al. Addition of the Abeta42/40 ratio to the cerebrospinal fluid biomarker profile increases the predictive value for underlying Alzheimer's disease dementia in mild cognitive impairment. Alzheimers Res Ther. 2018;10(1):33.
112. Blennow K, Zetterberg H. Biomarkers for Alzheimer's disease: current status and prospects for the future. J Intern Med. 2018;284(6):643-63.
113. Janelidze S, Zetterberg H, Mattsson N, Palmqvist S, Vanderstichele H, Lindberg O, et al. CSF Abeta42/Abeta40 and Abeta42/Abeta38 ratios: better diagnostic markers of Alzheimer disease. Ann Clin Transl Neurol. 2016;3(3):154-65.
114. Lewczuk P, Esselmann H, Otto M, Maler JM, Henkel AW, Henkel MK, et al. Neurochemical diagnosis of Alzheimer's dementia by CSF Abeta42, Abeta42/Abeta40 ratio and total tau. Neurobiol Aging. 2004;25(3):273-81.

115. Wiltfang J, Esselmann H, Bibl M, Hull M, Hampel H, Kessler H, et al. Amyloid beta peptide ratio 42/40 but not A beta 42 correlates with phospho-Tau in patients with low- and high-CSF A beta 40 load. J Neurochem. 2007;101(4):1053-9.
116. Hansson O, Zetterberg H, Buchhave P, Andreasson U, Londos E, Minthon L, et al. Prediction of Alzheimer's disease using the CSF Abeta42/Abeta40 ratio in patients with mild cognitive impairment. Dement Geriatr Cogn Disord. 2007;23(5):316-20.
117. Blennow K, Hampel H. CSF markers for incipient Alzheimer's disease. Lancet Neurol. 2003;2(10):605-13.
118. Grundke-Iqbal I, Iqbal K, Tung YC, Quinlan M, Wisniewski HM, Binder LI. Abnormal phosphorylation of the microtubule-associated protein tau (tau) in Alzheimer cytoskeletal pathology. Proc Natl Acad Sci U S A. 1986;83(13):4913-7.
119. Hampel H, Buerger K, Zinkowski R, Teipel SJ, Goernitz A, Andreasen N, et al. Measurement of phosphorylated tau epitopes in the differential diagnosis of Alzheimer disease: a comparative cerebrospinal fluid study. Arch Gen Psychiatry. 2004;61(1):95-102.
120. Wellington H, Paterson RW, Portelius E, Tornqvist U, Magdalinou N, Fox NC, et al. Increased CSF neurogranin concentration is specific to Alzheimer disease. Neurology. 2016;86(9):829-35.
121. Ovod V, Ramsey KN, Mawuenyega KG, Bollinger JG, Hicks T, Schneider T, et al. Amyloid beta concentrations and stable isotope labeling kinetics of human plasma specific to central nervous system amyloidosis. Alzheimers Dement. 2017;13(8):841-9.
122. Nakamura A, Kaneko N, Villemagne VL, Kato T, Doecke J, Dore V, et al. High performance plasma amyloid-beta biomarkers for Alzheimer's disease. Nature. 2018;554(7691):249-54.
123. Janelidze S, Stomrud E, Palmqvist S, Zetterberg H, van Westen D, Jeromin A, et al. Plasma beta-amyloid in Alzheimer's disease and vascular disease. Sci Rep. 2016;6:26801.
124. Tatebe H, Kasai T, Ohmichi T, Kishi Y, Kakeya T, Waragai M, et al. Quantification of plasma phosphorylated tau to use as a biomarker for brain Alzheimer pathology: pilot case-control studies including patients with Alzheimer's disease and down syndrome. Mol Neurodegener. 2017;12(1):63.
125. Karikari TK, Pascoal TA, Ashton NJ, Janelidze S, Benedet AL, Rodriguez JL, et al. Blood phosphorylated tau 181 as a biomarker for Alzheimer's disease: a diagnostic performance and prediction modelling study using data from four prospective cohorts. Lancet Neurol. 2020;19(5):422-33.
126. Janelidze S, Mattsson N, Palmqvist S, Smith R, Beach TG, Serrano GE, et al. Plasma P-tau181 in Alzheimer's disease: relationship to other biomarkers, differential diagnosis, neuropathology and longitudinal progression to Alzheimer's dementia. Nat Med. 2020;26(3):379-86.
127. Ferrer I. Cognitive impairment of vascular origin: neuropathology of cognitive impairment of vascular origin. J Neurol Sci. 2010;299(1-2):139-49.
128. O'Brien JT, Thomas A. Vascular dementia. Lancet. 2015;386(10004):1698-706.
129. Writing Group M, Mozaffarian D, Benjamin EJ, Go AS, Arnett DK, Blaha MJ, et al. Heart Disease and Stroke Statistics-2016 Update: A Report From the American Heart Association. Circulation. 2016;133(4):e38-360.
130. Jorm AF, Jolley D. The incidence of dementia: a meta-analysis. Neurology. 1998;51(3):728-33.
131. Kua EH, Ho E, Tan HH, Tsoi C, Thng C, Mahendran R. The natural history of dementia. Psychogeriatrics. 2014;14(3):196-201.
132. Roman G. Vascular dementia: a historical background. Int Psychogeriatr. 2003;15 Suppl 1:11-3.
133. Hachinski VC, Lassen NA, Marshall J. Multi-infarct dementia. A cause of mental deterioration in the elderly. Lancet. 1974;2(7874):207-10.

134. Kalaria RN, Erkinjuntti T. Small vessel disease and subcortical vascular dementia. J Clin Neurol. 2006;2(1):1-11.
135. Sachdev P, Kalaria R, O'Brien J, Skoog I, Alladi S, Black SE, et al. Diagnostic criteria for vascular cognitive disorders: a VASCOG statement. Alzheimer Dis Assoc Disord. 2014;28(3):206-18.
136. Bowler JV, Hachinski V. Vascular cognitive impairment: a new approach to vascular dementia. Baillieres Clin Neurol. 1995;4(2):357-76.
137. Hu X, De Silva TM, Chen J, Faraci FM. Cerebral Vascular Disease and Neurovascular Injury in Ischemic Stroke. Circ Res. 2017;120(3):449-71.
138. Fisher CM. Lacunar strokes and infarcts: a review. Neurology. 1982;32(8):871-6.
139. Iadecola C. The pathobiology of vascular dementia. Neuron. 2013;80(4):844-66.
140. Benjamin P, Lawrence AJ, Lambert C, Patel B, Chung AW, MacKinnon AD, et al. Strategic lacunes and their relationship to cognitive impairment in cerebral small vessel disease. Neuroimage Clin. 2014;4:828-37.
141. Staekenborg SS, van Straaten EC, van der Flier WM, Lane R, Barkhof F, Scheltens P. Small vessel versus large vessel vascular dementia: risk factors and MRI findings. J Neurol. 2008;255(11):1644-51; discussion 813-4.
142. Jellinger KA, Attems J. Is there pure vascular dementia in old age? J Neurol Sci. 2010;299(1-2):150-4.
143. Chabriat H, Joutel A, Dichgans M, Tournier-Lasserve E, Bousser MG. Cadasil. Lancet Neurol. 2009;8(7):643-53.
144. Chabriat H, Levy C, Taillia H, Iba-Zizen MT, Vahedi K, Joutel A, et al. Patterns of MRI lesions in CADASIL. Neurology. 1998;51(2):452-7.
145. Ikram MA, Bersano A, Manso-Calderon R, Jia JP, Schmidt H, Middleton L, et al. Genetics of vascular dementia - review from the ICVD working group. BMC Med. 2017;15(1):48.
146. Kimura S, Saito H, Minami M, Togashi H, Nakamura N, Nemoto M, et al. Pathogenesis of vascular dementia in stroke-prone spontaneously hypertensive rats. Toxicology. 2000;153(1-3):167-78.
147. Strachan MW, Reynolds RM, Marioni RE, Price JF. Cognitive function, dementia and type 2 diabetes mellitus in the elderly. Nat Rev Endocrinol. 2011;7(2):108-14.
148. Chui HC, Victoroff JI, Margolin D, Jagust W, Shankle R, Katzman R. Criteria for the diagnosis of ischemic vascular dementia proposed by the State of California Alzheimer's Disease Diagnostic and Treatment Centers. Neurology. 1992;42(3 Pt 1):473-80.
149. Lees R, Selvarajah J, Fenton C, Pendlebury ST, Langhorne P, Stott DJ, et al. Test accuracy of cognitive screening tests for diagnosis of dementia and multidomain cognitive impairment in stroke. Stroke. 2014;45(10):3008-18.
150. Ylikoski R, Jokinen H, Andersen P, Salonen O, Madureira S, Ferro J, et al. Comparison of the Alzheimer's Disease Assessment Scale Cognitive Subscale and the Vascular Dementia Assessment Scale in differentiating elderly individuals with different degrees of white matter changes. The LADIS Study. Dement Geriatr Cogn Disord. 2007;24(2):73-81.
151. Lyketsos CG, Lopez O, Jones B, Fitzpatrick AL, Breitner J, DeKosky S. Prevalence of neuropsychiatric symptoms in dementia and mild cognitive impairment: results from the cardiovascular health study. JAMA. 2002;288(12):1475-83.
152. Gupta M, Dasgupta A, Khwaja GA, Chowdhury D, Patidar Y, Batra A. Behavioural and psychological symptoms in poststroke vascular cognitive impairment. Behav Neurol. 2014;2014:430128.
153. Grinberg LT, Heinsen H. Toward a pathological definition of vascular dementia. J Neurol Sci. 2010;299(1-2):136-8.
154. Roman GC, Tatemichi TK, Erkinjuntti T, Cummings JL, Masdeu JC, Garcia JH, et al. Vascular dementia: diagnostic criteria for research studies. Report of the NINDS-AIREN International Workshop. Neurology. 1993;43(2):250-60.

155. Association AP. DSM-IV. Diagnosic and statistical manual of mental disorders. Washington, DC: American Psychiatric Association. 1994.
156. Organization WH. The ICD-10 classification of mental and behavioural disorders. Diagnostic criteria for research Geneva: World Health Organization. 1993.
157. Looi JC, Sachdev PS. Differentiation of vascular dementia from AD on neuropsychological tests. Neurology. 1999;53(4):670-8.
158. Nation DA, Sweeney MD, Montagne A, Sagare AP, D'Orazio LM, Pachicano M, et al. Blood-brain barrier breakdown is an early biomarker of human cognitive dysfunction. Nat Med. 2019;25(2):270-6.
159. Bjerke M, Zetterberg H, Edman A, Blennow K, Wallin A, Andreasson U. Cerebrospinal fluid matrix metalloproteinases and tissue inhibitor of metalloproteinases in combination with subcortical and cortical biomarkers in vascular dementia and Alzheimer's disease. J Alzheimers Dis. 2011;27(3):665-76.
160. Fredman P, Wallin A, Blennow K, Davidsson P, Gottfries CG, Svennerholm L. Sulfatide as a biochemical marker in cerebrospinal fluid of patients with vascular dementia. Acta Neurol Scand. 1992;85(2):103-6.
161. Zetterberg H, Rohrer JD, Schott JM. Cerebrospinal fluid in the dementias. Handb Clin Neurol. 2017;146:85-97.
162. Erkinjuntti T, Roman G, Gauthier S, Feldman H, Rockwood K. Emerging therapies for vascular dementia and vascular cognitive impairment. Stroke. 2004;35(4):1010-7.
163. Chabriat H, Bousser MG. Vascular dementia: potential of antiplatelet agents in prevention. Eur Neurol. 2006;55(2):61-9.
164. Siegel RL, Miller KD, Jemal A. Cancer Statistics, 2017. CA Cancer J Clin. 2017;67(1):7-30.
165. Nugent JL, Bunn PA, Jr., Matthews MJ, Ihde DC, Cohen MH, Gazdar A, et al. CNS metastases in small cell bronchogenic carcinoma: increasing frequency and changing pattern with lengthening survival. Cancer. 1979;44(5):1885-93.
166. Hirsch FR, Paulson OB, Hansen HH, Vraa-Jensen J. Intracranial metastases in small cell carcinoma of the lung: correlation of clinical and autopsy findings. Cancer. 1982;50(11):2433-7.
167. Greene-Schloesser D, Robbins ME, Peiffer AM, Shaw EG, Wheeler KT, Chan MD. Radiation-induced brain injury: A review. Front Oncol. 2012;2:73.
168. Shaw EG, Robbins ME. The management of radiation-induced brain injury. Cancer Treat Res. 2006;128:7-22.
169. Kurita H, Kawahara N, Asai A, Ueki K, Shin M, Kirino T. Radiation-induced apoptosis of oligodendrocytes in the adult rat brain. Neurol Res. 2001;23(8):869-74.
170. Tsuruda JS, Kortman KE, Bradley WG, Wheeler DC, Van Dalsem W, Bradley TP. Radiation effects on cerebral white matter: MR evaluation. AJR Am J Roentgenol. 1987;149(1):165-71.
171. Lee WH, Warrington JP, Sonntag WE, Lee YW. Irradiation alters MMP-2/TIMP-2 system and collagen type IV degradation in brain. Int J Radiat Oncol Biol Phys. 2012;82(5):1559-66.
172. Hwang SY, Jung JS, Kim TH, Lim SJ, Oh ES, Kim JY, et al. Ionizing radiation induces astrocyte gliosis through microglia activation. Neurobiol Dis. 2006;21(3):457-67.
173. Moore ED, Kooshki M, Metheny-Barlow LJ, Gallagher PE, Robbins ME. Angiotensin-(1-7) prevents radiation-induced inflammation in rat primary astrocytes through regulation of MAP kinase signaling. Free Radic Biol Med. 2013;65:1060-8.
174. Calvo W, Hopewell JW, Reinhold HS, Yeung TK. Time- and dose-related changes in the white matter of the rat brain after single doses of X rays. Br J Radiol. 1988;61(731):1043-52.
175. Lassen U, Kristjansen PE, Hansen HH. Brain metastases in small-cell lung cancer. Ann Oncol. 1995;6(9):941-4.

176. Kalm M, Abel E, Wasling P, Nyman J, Hietala MA, Bremell D, et al. Neurochemical evidence of potential neurotoxicity after prophylactic cranial irradiation. Int J Radiat Oncol Biol Phys. 2014;89(3):607-14.
177. Dityatev A, Schachner M. Extracellular matrix molecules and synaptic plasticity. Nat Rev Neurosci. 2003;4(6):456-68.
178. John N, Krugel H, Frischknecht R, Smalla KH, Schultz C, Kreutz MR, et al. Brevican-containing perineuronal nets of extracellular matrix in dissociated hippocampal primary cultures. Mol Cell Neurosci. 2006;31(4):774-84.
179. Cui H, Freeman C, Jacobson GA, Small DH. Proteoglycans in the central nervous system: role in development, neural repair, and Alzheimer's disease. IUBMB Life. 2013;65(2):108-20.
180. Yamaguchi Y. Lecticans: organizers of the brain extracellular matrix. Cell Mol Life Sci. 2000;57(2):276-89.
181. Yamada H, Watanabe K, Shimonaka M, Yamaguchi Y. Molecular cloning of brevican, a novel brain proteoglycan of the aggrecan/versican family. J Biol Chem. 1994;269(13):10119-26.
182. Dzyubenko E, Gottschling C, Faissner A. Neuron-Glia Interactions in Neural Plasticity: Contributions of Neural Extracellular Matrix and Perineuronal Nets. Neural Plast. 2016;2016:5214961.
183. Siebert JR, Conta Steencken A, Osterhout DJ. Chondroitin sulfate proteoglycans in the nervous system: inhibitors to repair. Biomed Res Int. 2014;2014:845323.
184. Haas CA, Rauch U, Thon N, Merten T, Deller T. Entorhinal cortex lesion in adult rats induces the expression of the neuronal chondroitin sulfate proteoglycan neurocan in reactive astrocytes. J Neurosci. 1999;19(22):9953-63.
185. Frischknecht R, Seidenbecher CI. Brevican: a key proteoglycan in the perisynaptic extracellular matrix of the brain. Int J Biochem Cell Biol. 2012;44(7):1051-4.
186. Zhou XH, Brakebusch C, Matthies H, Oohashi T, Hirsch E, Moser M, et al. Neurocan is dispensable for brain development. Mol Cell Biol. 2001;21(17):5970-8.
187. Rauvala H, Paveliev M, Kuja-Panula J, Kulesskaya N. Inhibition and enhancement of neural regeneration by chondroitin sulfate proteoglycans. Neural Regen Res. 2017;12(5):687-91.
188. Ajmo JM, Bailey LA, Howell MD, Cortez LK, Pennypacker KR, Mehta HN, et al. Abnormal post-translational and extracellular processing of brevican in plaque-bearing mice over-expressing APPsw. J Neurochem. 2010;113(3):784-95.
189. Stanton H, Melrose J, Little CB, Fosang AJ. Proteoglycan degradation by the ADAMTS family of proteinases. Biochim Biophys Acta. 2011;1812(12):1616-29.
190. Rauch U, Feng K, Zhou XH. Neurocan: a brain chondroitin sulfate proteoglycan. Cell Mol Life Sci. 2001;58(12-13):1842-56.
191. Seidenbecher CI, Smalla KH, Fischer N, Gundelfinger ED, Kreutz MR. Brevican isoforms associate with neural membranes. J Neurochem. 2002;83(3):738-46.
192. Nakamura H, Fujii Y, Inoki I, Sugimoto K, Tanzawa K, Matsuki H, et al. Brevican is degraded by matrix metalloproteinases and aggrecanase-1 (ADAMTS4) at different sites. J Biol Chem. 2000;275(49):38885-90.
193. Gottschall PE, Howell MD. ADAMTS expression and function in central nervous system injury and disorders. Matrix Biol. 2015;44-46:70-6.
194. Rauch U, Gao P, Janetzko A, Flaccus A, Hilgenberg L, Tekotte H, et al. Isolation and characterization of developmentally regulated chondroitin sulfate and chondroitin/keratan sulfate proteoglycans of brain identified with monoclonal antibodies. J Biol Chem. 1991;266(22):14785-801.

195. Matsui F, Watanabe E, Oohira A. Immunological identification of two proteoglycan fragments derived from neurocan, a brain-specific chondroitin sulfate proteoglycan. Neurochem Int. 1994;25(5):425-31.
196. Fontanil T, Mohamedi Y, Moncada-Pazos A, Cobo T, Vega JA, Cobo JL, et al. Neurocan is a New Substrate for the ADAMTS12 Metalloprotease: Potential Implications in Neuropathies. Cell Physiol Biochem. 2019;52(5):1003-16.
197. Turk BE, Huang LL, Piro ET, Cantley LC. Determination of protease cleavage site motifs using mixture-based oriented peptide libraries. Nat Biotechnol. 2001;19(7):661-7.
198. Brakebusch C, Seidenbecher CI, Asztely F, Rauch U, Matthies H, Meyer H, et al. Brevican-deficient mice display impaired hippocampal CA1 long-term potentiation but show no obvious deficits in learning and memory. Mol Cell Biol. 2002;22(21):7417-27.
199. Thon N, Haas CA, Rauch U, Merten T, Fassler R, Frotscher M, et al. The chondroitin sulphate proteoglycan brevican is upregulated by astrocytes after entorhinal cortex lesions in adult rats. Eur J Neurosci. 2000;12(7):2547-58.
200. Jones LL, Margolis RU, Tuszynski MH. The chondroitin sulfate proteoglycans neurocan, brevican, phosphacan, and versican are differentially regulated following spinal cord injury. Exp Neurol. 2003;182(2):399-411.
201. Jaworski DM, Kelly GM, Hockfield S. Intracranial injury acutely induces the expression of the secreted isoform of the CNS-specific hyaluronan-binding protein BEHAB/brevican. Exp Neurol. 1999;157(2):327-37.
202. Morawski M, Bruckner G, Jager C, Seeger G, Matthews RT, Arendt T. Involvement of perineuronal and perisynaptic extracellular matrix in Alzheimer's disease neuropathology. Brain Pathol. 2012;22(4):547-61.
203. Howell MD, Bailey LA, Cozart MA, Gannon BM, Gottschall PE. Hippocampal administration of chondroitinase ABC increases plaque-adjacent synaptic marker and diminishes amyloid burden in aged APPswe/PS1dE9 mice. Acta Neuropathol Commun. 2015;3:54.
204. Lendvai D, Morawski M, Negyessy L, Gati G, Jager C, Baksa G, et al. Neurochemical mapping of the human hippocampus reveals perisynaptic matrix around functional synapses in Alzheimer's disease. Acta Neuropathol. 2013;125(2):215-29.
205. Vegh MJ, Heldring CM, Kamphuis W, Hijazi S, Timmerman AJ, Li KW, et al. Reducing hippocampal extracellular matrix reverses early memory deficits in a mouse model of Alzheimer's disease. Acta Neuropathol Commun. 2014;2:76.
206. Jonesco DS, Karsdal MA, Henriksen K. The CNS-specific proteoglycan, brevican, and its ADAMTS4-cleaved fragment show differential serological levels in Alzheimer's disease, other types of dementia and non-demented controls: A cross-sectional study. PLoS One. 2020;15(6):e0234632.
207. Duits FH, Brinkmalm G, Teunissen CE, Brinkmalm A, Scheltens P, Van der Flier WM, et al. Synaptic proteins in CSF as potential novel biomarkers for prognosis in prodromal Alzheimer's disease. Alzheimers Res Ther. 2018;10(1):5.
208. Brinkmalm G, Sjodin S, Simonsen AH, Hasselbalch SG, Zetterberg H, Brinkmalm A, et al. A Parallel Reaction Monitoring Mass Spectrometric Method for Analysis of Potential CSF Biomarkers for Alzheimer's Disease. Proteomics Clin Appl. 2018;12(1).
209. Milev P, Chiba A, Haring M, Rauvala H, Schachner M, Ranscht B, et al. High affinity binding and overlapping localization of neurocan and phosphacan/protein-tyrosine phosphatase-zeta/beta with tenascin-R, amphoterin, and the heparin-binding growth-associated molecule. J Biol Chem. 1998;273(12):6998-7005.
210. Grumet M, Milev P, Sakurai T, Karthikeyan L, Bourdon M, Margolis RK, et al. Interactions with tenascin and differential effects on cell adhesion of neurocan and phosphacan, two major chondroitin sulfate proteoglycans of nervous tissue. J Biol Chem. 1994;269(16):12142-6.

211. Roll L, Faissner A. Tenascins in CNS lesions. Semin Cell Dev Biol. 2019;89:118-24.
212. Chiquet-Ehrismann R, Tucker RP. Tenascins and the importance of adhesion modulation. Cold Spring Harb Perspect Biol. 2011;3(5).
213. Human Protein Atlas [Available from: www.proteinatlas.org.
214. Hsia HC, Schwarzbauer JE. Meet the tenascins: multifunctional and mysterious. J Biol Chem. 2005;280(29):26641-4.
215. Reinhard J, Roll L, Faissner A. Tenascins in Retinal and Optic Nerve Neurodegeneration. Front Integr Neurosci. 2017;11:30.
216. Milev P, Fischer D, Haring M, Schulthess T, Margolis RK, Chiquet-Ehrismann R, et al. The fibrinogen-like globe of tenascin-C mediates its interactions with neurocan and phosphacan/protein-tyrosine phosphatase-zeta/beta. J Biol Chem. 1997;272(24):15501-9.
217. Carnemolla B, Borsi L, Bannikov G, Troyanovsky S, Zardi L. Comparison of human tenascin expression in normal, simian-virus-40-transformed and tumor-derived cell lines. Eur J Biochem. 1992;205(2):561-7.
218. Woodworth A, Pesheva P, Fiete D, Baenziger JU. Neuronal-specific synthesis and glycosylation of tenascin-R. J Biol Chem. 2004;279(11):10413-21.
219. Jones FS, Jones PL. The tenascin family of ECM glycoproteins: structure, function, and regulation during embryonic development and tissue remodeling. Dev Dyn. 2000;218(2):235-59.
220. Gotz B, Scholze A, Clement A, Joester A, Schutte K, Wigger F, et al. Tenascin-C contains distinct adhesive, anti-adhesive, and neurite outgrowth promoting sites for neurons. J Cell Biol. 1996;132(4):681-99.
221. Loers G, Schachner M. Recognition molecules and neural repair. J Neurochem. 2007;101(4):865-82.
222. Yuan W, Zhang W, Yang X, Zhou L, Hanghua Z, Xu K. Clinical significance and prognosis of serum tenascin-C in patients with sepsis. BMC Anesthesiol. 2018;18(1):170.
223. Jakovcevski I, Miljkovic D, Schachner M, Andjus PR. Tenascins and inflammation in disorders of the nervous system. Amino Acids. 2013;44(4):1115-27.
224. Saga Y, Yagi T, Ikawa Y, Sakakura T, Aizawa S. Mice develop normally without tenascin. Genes Dev. 1992;6(10):1821-31.
225. Forsberg E, Hirsch E, Frohlich L, Meyer M, Ekblom P, Aszodi A, et al. Skin wounds and severed nerves heal normally in mice lacking tenascin-C. Proc Natl Acad Sci U S A. 1996;93(13):6594-9.
226. Garcion E, Faissner A, ffrench-Constant C. Knockout mice reveal a contribution of the extracellular matrix molecule tenascin-C to neural precursor proliferation and migration. Development. 2001;128(13):2485-96.
227. Freitag S, Schachner M, Morellini F. Behavioral alterations in mice deficient for the extracellular matrix glycoprotein tenascin-R. Behav Brain Res. 2003;145(1-2):189-207.
228. Montag-Sallaz M, Montag D. Severe cognitive and motor coordination deficits in tenascin-R-deficient mice. Genes Brain Behav. 2003;2(1):20-31.
229. Laywell ED, Dorries U, Bartsch U, Faissner A, Schachner M, Steindler DA. Enhanced expression of the developmentally regulated extracellular matrix molecule tenascin following adult brain injury. Proc Natl Acad Sci U S A. 1992;89(7):2634-8.
230. Deller T, Haas CA, Naumann T, Joester A, Faissner A, Frotscher M. Up-regulation of astrocyte-derived tenascin-C correlates with neurite outgrowth in the rat dentate gyrus after unilateral entorhinal cortex lesion. Neuroscience. 1997;81(3):829-46.
231. Deckner M, Lindholm T, Cullheim S, Risling M. Differential expression of tenascin-C, tenascin-R, tenascin/J1, and tenascin-X in spinal cord scar tissue and in the olfactory system. Exp Neurol. 2000;166(2):350-62.

232. Brodkey JA, Laywell ED, O'Brien TF, Faissner A, Stefansson K, Dorries HU, et al. Focal brain injury and upregulation of a developmentally regulated extracellular matrix protein. J Neurosurg. 1995;82(1):106-12.
233. Hausmann R, Betz P. Course of glial immunoreactivity for vimentin, tenascin and alpha1-antichymotrypsin after traumatic injury to human brain. Int J Legal Med. 2001;114(6):338-42.
234. Zhao YY, Lou L, Yang KC, Wang HB, Xu Y, Lu G, et al. Correlation of tenascin-C concentrations in serum with outcome of traumatic brain injury in humans. Clin Chim Acta. 2017;472:46-50.
235. Suzuki H, Kanamaru K, Shiba M, Fujimoto M, Kawakita F, Imanaka-Yoshida K, et al. Tenascin-C is a possible mediator between initial brain injury and vasospasm-related and -unrelated delayed cerebral ischemia after aneurysmal subarachnoid hemorrhage. Acta Neurochir Suppl. 2015;120:117-21.
236. Apostolova I, Irintchev A, Schachner M. Tenascin-R restricts posttraumatic remodeling of motoneuron innervation and functional recovery after spinal cord injury in adult mice. J Neurosci. 2006;26(30):7849-59.
237. Xie K, Liu Y, Hao W, Walter S, Penke B, Hartmann T, et al. Tenascin-C deficiency ameliorates Alzheimer's disease-related pathology in mice. Neurobiol Aging. 2013;34(10):2389-98.
238. Mi Z, Halfter W, Abrahamson EE, Klunk WE, Mathis CA, Mufson EJ, et al. Tenascin-C Is Associated with Cored Amyloid-beta Plaques in Alzheimer Disease and Pathology Burdened Cognitively Normal Elderly. J Neuropathol Exp Neurol. 2016;75(9):868-76.
239. Serrano-Pozo A, Frosch MP, Masliah E, Hyman BT. Neuropathological alterations in Alzheimer disease. Cold Spring Harb Perspect Med. 2011;1(1):a006189.
240. Donovan LE, Higginbotham L, Dammer EB, Gearing M, Rees HD, Xia Q, et al. Analysis of a membrane-enriched proteome from postmortem human brain tissue in Alzheimer's disease. Proteomics Clin Appl. 2012;6(3-4):201-11.
241. Beggah AT, Dours-Zimmermann MT, Barras FM, Brosius A, Zimmermann DR, Zurn AD. Lesion-induced differential expression and cell association of Neurocan, Brevican, Versican V1 and V2 in the mouse dorsal root entry zone. Neuroscience. 2005;133(3):749-62.
242. Asher RA, Morgenstern DA, Fidler PS, Adcock KH, Oohira A, Braistead JE, et al. Neurocan is upregulated in injured brain and in cytokine-treated astrocytes. J Neurosci. 2000;20(7):2427-38.
243. Yi JH, Katagiri Y, Susarla B, Figge D, Symes AJ, Geller HM. Alterations in sulfated chondroitin glycosaminoglycans following controlled cortical impact injury in mice. J Comp Neurol. 2012;520(15):3295-313.
244. Dobbertin A, Rhodes KE, Garwood J, Properzi F, Heck N, Rogers JH, et al. Regulation of RPTPbeta/phosphacan expression and glycosaminoglycan epitopes in injured brain and cytokine-treated glia. Mol Cell Neurosci. 2003;24(4):951-71.
245. Fawcett JW, Oohashi T, Pizzorusso T. The roles of perineuronal nets and the perinodal extracellular matrix in neuronal function. Nat Rev Neurosci. 2019;20(8):451-65.
246. Schmidt S, Arendt T, Morawski M, Sonntag M. Neurocan Contributes to Perineuronal Net Development. Neuroscience. 2020;442:69-86.
247. Rogers SL, Rankin-Gee E, Risbud RM, Porter BE, Marsh ED. Normal Development of the Perineuronal Net in Humans; In Patients with and without Epilepsy. Neuroscience. 2018;384:350-60.
248. Irintchev A, Rollenhagen A, Troncoso E, Kiss JZ, Schachner M. Structural and functional aberrations in the cerebral cortex of tenascin-C deficient mice. Cereb Cortex. 2005;15(7):950-62.

249. Morawski M, Dityatev A, Hartlage-Rubsamen M, Blosa M, Holzer M, Flach K, et al. Tenascin-R promotes assembly of the extracellular matrix of perineuronal nets via clustering of aggrecan. Philos Trans R Soc Lond B Biol Sci. 2014;369(1654):20140046.
250. Geissler M, Gottschling C, Aguado A, Rauch U, Wetzel CH, Hatt H, et al. Primary hippocampal neurons, which lack four crucial extracellular matrix molecules, display abnormalities of synaptic structure and function and severe deficits in perineuronal net formation. J Neurosci. 2013;33(18):7742-55.
251. Jansen S, Gottschling C, Faissner A, Manahan-Vaughan D. Intrinsic cellular and molecular properties of in vivo hippocampal synaptic plasticity are altered in the absence of key synaptic matrix molecules. Hippocampus. 2017;27(8):920-33.
252. Gottschling C, Wegrzyn D, Denecke B, Faissner A. Elimination of the four extracellular matrix molecules tenascin-C, tenascin-R, brevican and neurocan alters the ratio of excitatory and inhibitory synapses. Sci Rep. 2019;9(1):13939.
253. Golgi C. On the structure of the nerve cells of the spinal ganglia. 1898. J Microsc. 1989;155(Pt 1):9-14.
254. Anlar B, Gunel-Ozcan A. Tenascin-R: role in the central nervous system. Int J Biochem Cell Biol. 2012;44(9):1385-9.
255. Morawski M, Bruckner MK, Riederer P, Bruckner G, Arendt T. Perineuronal nets potentially protect against oxidative stress. Exp Neurol. 2004;188(2):309-15.
256. Miyata S, Nishimura Y, Nakashima T. Perineuronal nets protect against amyloid beta-protein neurotoxicity in cultured cortical neurons. Brain Res. 2007;1150:200-6.
257. Bruckner G, Hausen D, Hartig W, Drlicek M, Arendt T, Brauer K. Cortical areas abundant in extracellular matrix chondroitin sulphate proteoglycans are less affected by cytoskeletal changes in Alzheimer's disease. Neuroscience. 1999;92(3):791-805.
258. Cox TR, Erler JT. Remodeling and homeostasis of the extracellular matrix: implications for fibrotic diseases and cancer. Dis Model Mech. 2011;4(2):165-78.
259. Rocks N, Paulissen G, El Hour M, Quesada F, Crahay C, Gueders M, et al. Emerging roles of ADAM and ADAMTS metalloproteinases in cancer. Biochimie. 2008;90(2):369-79.
260. Raeeszadeh-Sarmazdeh M, Do LD, Hritz BG. Metalloproteinases and Their Inhibitors: Potential for the Development of New Therapeutics. Cells. 2020;9(5).
261. Murphy G, Nagase H. Progress in matrix metalloproteinase research. Mol Aspects Med. 2008;29(5):290-308.
262. Bonnans C, Chou J, Werb Z. Remodelling the extracellular matrix in development and disease. Nat Rev Mol Cell Biol. 2014;15(12):786-801.
263. Rempe RG, Hartz AMS, Bauer B. Matrix metalloproteinases in the brain and blood-brain barrier: Versatile breakers and makers. J Cereb Blood Flow Metab. 2016;36(9):1481-507.
264. Nelson KK, Melendez JA. Mitochondrial redox control of matrix metalloproteinases. Free Radic Biol Med. 2004;37(6):768-84.
265. Eckhard U, Huesgen PF, Schilling O, Bellac CL, Butler GS, Cox JH, et al. Active site specificity profiling of the matrix metalloproteinase family: Proteomic identification of 4300 cleavage sites by nine MMPs explored with structural and synthetic peptide cleavage analyses. Matrix Biol. 2016;49:37-60.
266. Matsumoto S, Kobayashi T, Katoh M, Saito S, Ikeda Y, Kobori M, et al. Expression and localization of matrix metalloproteinase-12 in the aorta of cholesterol-fed rabbits: relationship to lesion development. Am J Pathol. 1998;153(1):109-19.
267. Muir EM, Adcock KH, Morgenstern DA, Clayton R, von Stillfried N, Rhodes K, et al. Matrix metalloproteases and their inhibitors are produced by overlapping populations of activated astrocytes. Brain Res Mol Brain Res. 2002;100(1-2):103-17.
268. Siri A, Knauper V, Veirana N, Caocci F, Murphy G, Zardi L. Different susceptibility of small and large human tenascin-C isoforms to degradation by matrix metalloproteinases. J Biol Chem. 1995;270(15):8650-4.

269. Imai K, Kusakabe M, Sakakura T, Nakanishi I, Okada Y. Susceptibility of tenascin to degradation by matrix metalloproteinases and serine proteinases. FEBS Lett. 1994;352(2):216-8.
270. Grossetete M, Phelps J, Arko L, Yonas H, Rosenberg GA. Elevation of matrix metalloproteinases 3 and 9 in cerebrospinal fluid and blood in patients with severe traumatic brain injury. Neurosurgery. 2009;65(4):702-8.
271. Zheng K, Li C, Shan X, Liu H, Fan W, Wang Z, et al. Matrix metalloproteinases and their tissue inhibitors in serum and cerebrospinal fluid of patients with moderate and severe traumatic brain injury. Neurol India. 2013;61(6):606-9.
272. Liu CL, Chen CC, Lee HC, Cho DY. Matrix metalloproteinase-9 in the ventricular cerebrospinal fluid correlated with the prognosis of traumatic brain injury. Turk Neurosurg. 2014;24(3):363-8.
273. Vilalta A, Sahuquillo J, Rosell A, Poca MA, Riveiro M, Montaner J. Moderate and severe traumatic brain injury induce early overexpression of systemic and brain gelatinases. Intensive Care Med. 2008;34(8):1384-92.
274. Backstrom JR, Lim GP, Cullen MJ, Tokes ZA. Matrix metalloproteinase-9 (MMP-9) is synthesized in neurons of the human hippocampus and is capable of degrading the amyloid-beta peptide (1-40). J Neurosci. 1996;16(24):7910-9.
275. Yan P, Hu X, Song H, Yin K, Bateman RJ, Cirrito JR, et al. Matrix metalloproteinase-9 degrades amyloid-beta fibrils in vitro and compact plaques in situ. J Biol Chem. 2006;281(34):24566-74.
276. Mizoguchi H, Takuma K, Fukuzaki E, Ibi D, Someya E, Akazawa KH, et al. Matrix metalloprotease-9 inhibition improves amyloid beta-mediated cognitive impairment and neurotoxicity in mice. J Pharmacol Exp Ther. 2009;331(1):14-22.
277. Beroun A, Mitra S, Michaluk P, Pijet B, Stefaniuk M, Kaczmarek L. MMPs in learning and memory and neuropsychiatric disorders. Cell Mol Life Sci. 2019;76(16):3207-28.
278. Adair JC, Charlie J, Dencoff JE, Kaye JA, Quinn JF, Camicioli RM, et al. Measurement of gelatinase B (MMP-9) in the cerebrospinal fluid of patients with vascular dementia and Alzheimer disease. Stroke. 2004;35(6):e159-62.
279. Lemarchant S, Wojciechowski S, Vivien D, Koistinaho J. ADAMTS-4 in central nervous system pathologies. J Neurosci Res. 2017;95(9):1703-11.
280. Mohamedi Y, Fontanil T, Cobo T, Cal S, Obaya AJ. New Insights into ADAMTS Metalloproteases in the Central Nervous System. Biomolecules. 2020;10(3).
281. Gurses MS, Ural MN, Gulec MA, Akyol O, Akyol S. Pathophysiological Function of ADAMTS Enzymes on Molecular Mechanism of Alzheimer's Disease. Aging Dis. 2016;7(4):479-90.
282. Cua RC, Lau LW, Keough MB, Midha R, Apte SS, Yong VW. Overcoming neurite-inhibitory chondroitin sulfate proteoglycans in the astrocyte matrix. Glia. 2013;61(6):972-84.
283. Miguel RF, Pollak A, Lubec G. Metalloproteinase ADAMTS-1 but not ADAMTS-5 is manifold overexpressed in neurodegenerative disorders as Down syndrome, Alzheimer's and Pick's disease. Brain Res Mol Brain Res. 2005;133(1):1-5.
284. Nakada M, Miyamori H, Kita D, Takahashi T, Yamashita J, Sato H, et al. Human glioblastomas overexpress ADAMTS-5 that degrades brevican. Acta Neuropathol. 2005;110(3):239-46.
285. Tauchi R, Imagama S, Natori T, Ohgomori T, Muramoto A, Shinjo R, et al. The endogenous proteoglycan-degrading enzyme ADAMTS-4 promotes functional recovery after spinal cord injury. J Neuroinflammation. 2012;9:53.
286. Zhen EY, Brittain IJ, Laska DA, Mitchell PG, Sumer EU, Karsdal MA, et al. Characterization of metalloprotease cleavage products of human articular cartilage. Arthritis Rheum. 2008;58(8):2420-31.

287. Brew K, Dinakarpandian D, Nagase H. Tissue inhibitors of metalloproteinases: evolution, structure and function. Biochim Biophys Acta. 2000;1477(1-2):267-83.
288. de Bruyn M, Vandooren J, Ugarte-Berzal E, Arijs I, Vermeire S, Opdenakker G. The molecular biology of matrix metalloproteinases and tissue inhibitors of metalloproteinases in inflammatory bowel diseases. Crit Rev Biochem Mol Biol. 2016;51(5):295-358.
289. Ahmed SH, Clark LL, Pennington WR, Webb CS, Bonnema DD, Leonardi AH, et al. Matrix metalloproteinases/tissue inhibitors of metalloproteinases: relationship between changes in proteolytic determinants of matrix composition and structural, functional, and clinical manifestations of hypertensive heart disease. Circulation. 2006;113(17):2089-96.
290. Niebroj-Dobosz I, Janik P, Sokolowska B, Kwiecinski H. Matrix metalloproteinases and their tissue inhibitors in serum and cerebrospinal fluid of patients with amyotrophic lateral sclerosis. Eur J Neurol. 2010;17(2):226-31.
291. Brew K, Nagase H. The tissue inhibitors of metalloproteinases (TIMPs): an ancient family with structural and functional diversity. Biochim Biophys Acta. 2010;1803(1):55-71.
292. Troeberg L, Fushimi K, Scilabra SD, Nakamura H, Dive V, Thogersen IB, et al. The C-terminal domains of ADAMTS-4 and ADAMTS-5 promote association with N-TIMP-3. Matrix Biol. 2009;28(8):463-9.
293. Shi WZ, Ju JY, Xiao HJ, Xue F, Wu J, Pan MM, et al. Dynamics of MMP9, MMP2 and TIMP1 in a rat model of brain injury combined with traumatic heterotopic ossification. Mol Med Rep. 2017;15(4):2129-35.
294. Lorente L, Martin MM, Lopez P, Ramos L, Blanquer J, Caceres JJ, et al. Association between serum tissue inhibitor of matrix metalloproteinase-1 levels and mortality in patients with severe brain trauma injury. PLoS One. 2014;9(4):e94370.
295. Brkic M, Balusu S, Libert C, Vandenbroucke RE. Friends or Foes: Matrix Metalloproteinases and Their Multifaceted Roles in Neurodegenerative Diseases. Mediators Inflamm. 2015;2015:620581.
296. Lorenzl S, Albers DS, Relkin N, Ngyuen T, Hilgenberg SL, Chirichigno J, et al. Increased plasma levels of matrix metalloproteinase-9 in patients with Alzheimer's disease. Neurochem Int. 2003;43(3):191-6.
297. Morita-Fujimura Y, Fujimura M, Gasche Y, Copin JC, Chan PH. Overexpression of copper and zinc superoxide dismutase in transgenic mice prevents the induction and activation of matrix metalloproteinases after cold injury-induced brain trauma. J Cereb Blood Flow Metab. 2000;20(1):130-8.
298. Shigemori Y, Katayama Y, Mori T, Maeda T, Kawamata T. Matrix metalloproteinase-9 is associated with blood-brain barrier opening and brain edema formation after cortical contusion in rats. Acta Neurochir Suppl. 2006;96:130-3.
299. Vecil GG, Larsen PH, Corley SM, Herx LM, Besson A, Goodyer CG, et al. Interleukin-1 is a key regulator of matrix metalloproteinase-9 expression in human neurons in culture and following mouse brain trauma in vivo. J Neurosci Res. 2000;61(2):212-24.
300. Wang X, Jung J, Asahi M, Chwang W, Russo L, Moskowitz MA, et al. Effects of matrix metalloproteinase-9 gene knock-out on morphological and motor outcomes after traumatic brain injury. J Neurosci. 2000;20(18):7037-42.
301. Lin Y, Pan Y, Wang M, Huang X, Yin Y, Wang Y, et al. Blood-brain barrier permeability is positively correlated with cerebral microvascular perfusion in the early fluid percussion-injured brain of the rat. Lab Invest. 2012;92(11):1623-34.
302. Guilfoyle MR, Carpenter KL, Helmy A, Pickard JD, Menon DK, Hutchinson PJ. Matrix Metalloproteinase Expression in Contusional Traumatic Brain Injury: A Paired Microdialysis Study. J Neurotrauma. 2015;32(20):1553-9.
303. Vilalta A, Sahuquillo J, Poca MA, De Los Rios J, Cuadrado E, Ortega-Aznar A, et al. Brain contusions induce a strong local overexpression of MMP-9. Results of a pilot study. Acta Neurochir Suppl. 2008;102:415-9.

304. Stomrud E, Bjorkqvist M, Janciauskiene S, Minthon L, Hansson O. Alterations of matrix metalloproteinases in the healthy elderly with increased risk of prodromal Alzheimer's disease. Alzheimers Res Ther. 2010;2(3):20.
305. Horstmann S, Budig L, Gardner H, Koziol J, Deuschle M, Schilling C, et al. Matrix metalloproteinases in peripheral blood and cerebrospinal fluid in patients with Alzheimer's disease. Int Psychogeriatr. 2010;22(6):966-72.
306. Soares HD, Potter WZ, Pickering E, Kuhn M, Immermann FW, Shera DM, et al. Plasma biomarkers associated with the apolipoprotein E genotype and Alzheimer disease. Arch Neurol. 2012;69(10):1310-7.
307. Olsson M, Arlig J, Hedner J, Blennow K, Zetterberg H. Sleep deprivation and cerebrospinal fluid biomarkers for Alzheimer's disease. Sleep. 2018;41(5).
308. Runeson BS, Rich CL. Diagnostic and statistical manual of mental disorders, 3rd ed. (DSM-III), adaptive functioning in young Swedish suicides. Ann Clin Psychiatry. 1994;6(3):181-3.
309. Erkinjuntti T, Inzitari D, Pantoni L, Wallin A, Scheltens P, Rockwood K, et al. Research criteria for subcortical vascular dementia in clinical trials. J Neural Transm Suppl. 2000;59:23-30.
310. MacLean B, Tomazela DM, Shulman N, Chambers M, Finney GL, Frewen B, et al. Skyline: an open source document editor for creating and analyzing targeted proteomics experiments. Bioinformatics. 2010;26(7):966-8.
311. Lee YW, Cho HJ, Lee WH, Sonntag WE. Whole brain radiation-induced cognitive impairment: pathophysiological mechanisms and therapeutic targets. Biomol Ther (Seoul). 2012;20(4):357-70.
312. Xiong M, Jones OD, Peppercorn K, Ohline SM, Tate WP, Abraham WC. Secreted amyloid precursor protein-alpha can restore novel object location memory and hippocampal LTP in aged rats. Neurobiol Learn Mem. 2017;138:291-9.
313. Saroja SR, Sase A, Kircher SG, Wan J, Berger J, Hoger H, et al. Hippocampal proteoglycans brevican and versican are linked to spatial memory of Sprague-Dawley rats in the morris water maze. J Neurochem. 2014;130(6):797-804.
314. Makale MT, McDonald CR, Hattangadi-Gluth JA, Kesari S. Mechanisms of radiotherapy-associated cognitive disability in patients with brain tumours. Nat Rev Neurol. 2017;13(1):52-64.
315. Fike JR, Rosi S, Limoli CL. Neural precursor cells and central nervous system radiation sensitivity. Semin Radiat Oncol. 2009;19(2):122-32.
316. Brysbaert M. How Many Participants Do We Have to Include in Properly Powered Experiments? A Tutorial of Power Analysis with Reference Tables. J Cogn. 2019;2(1):16.